Design considerations for a Seismograph Network for Oaxaca State, Mexico with telemetery of data by radio link to Mexico City.

by

R.B. Hayman

Seismological Service of Canada

Internal Report # 78-5

Division of Seismology and

Geothermal Studies.

Earth Physics Branch

Department of Energy, Mines and Resources

Ottawa - April 1977

1. Introduction

This report was prepared following a visit to the Instituto de Investigaciones Matematicas Aplicados y en Sistemas (IIMAS), Universidad National Antonoma de Mexico (UNAM) by the author in February 1978. The report discusses some of the design considerations in establishing a seismograph network in Oaxaca State in southern Mexico with telemetry of data by radio link to IIMAS in Mexico City. At IIMAS the telemetered data would be processed on-line by the RESMAC seismological network data processor which is based on an PDP11-40 minicomputer system and has been described by Lomnitz (1976) and in a previous internal report by Hayman (77-9). Consequently, the body of the report relates mainly to problems of data transmission from the remote seismograph sites to Mexico City. Much of the material presented herein was discussed with the staff at IIMAS during the visit.

A paper published by Ohtake, Matumoto and Latham predicting a magnitude $7\frac{1}{2}$ earthquake in Oaxaca State has focussed attention on the seismic risk of the area. Burk and colleagues (news release, April 1978) have since suggested that because of the continued quiescence in the area a magnitude 8 event can now be expected.

Much of Oaxaca State is wild mountainous country but there is also a farming area in the region of the state capital of Oaxaca. Acapulco is just off the eastern edge of the area. The topography is unusual since a broad valley, separates two ranges of high mountains; the coastal range and the volcanic zone near Mexico City. This terrain presents unusual opportunities for radio telemetry of seismic data.

Introduction (continued)

This report does not contain proposals for the exact network layout since first-hand knowledge of the terrain is essential in preparing a detailed design. Instead, members of the staff at UNAM have been given references (for example, Bullington, 1957 'Radio Propagation Fundamentals') which will enable them to estimate the reliability of a particular radio link. An example of such an estimate is included in the report. A map showing one possible network configuration is shown in fig. 1. The corresponding equipment block diagram is shown in fig. 2.

2. Radio Network

The distances involved in the proposed Oaxaca network are large, with the longest link being 270 km. It is only the fairly unusual topography which exists in Mexico that permits such long path lengths to be considered. A minimum requirement for the larger paths is that free space propagation conditions exist (neglecting atmospheric affects). Thus potential paths should include generous Fresnel Zone clearance at both antenna sites and along the path. This appears feasible. Atmospheric effects including diffraction, multipathing and channelling will cause fading but the effects of these can be reduced by ensuring generous midpath clearance (3 or 4 times Fresnel Zone) and a generous fade margin. Calculations show the proposed network to be a reasonable proposition, but it must be recognized that a particular link cannot be considered fully proven until it has been in operation through one annual cycle. This extended evaluation period is considered more desirable than adding more repeaters into the initial design. In the worst case more repeaters may have to be added (and other stations moved) during the evaluation period.

2.1 Frequency Band

Two options exist, the 132-174 MHZ VHF band and the 450-470 MHZ UHF band. In all but remote rural areas the VHF band is congested and subject to interference, particularly if frequency usage is not carefully controlled. The SISMEX network suffers from this problem on radio links within about 50 km of Mexico City. There is little can be done if this type of interference is a problem. Highly selective RF cavity filters can be used if the problem is on an adjacent frequency but these are bulky items in the VHF band.

Currently, the UHF band is not as heavily used as the VHF band and so there is less likelihood of interference problems. There are however, other factors.

Since at 450 MHZ the antenna aperture is one third of that at 150 MHZ there will be an inherent 9.5dB 'loss' if geometrically similar antennas are used. This can be compensated for by using higher gain antennas or by increasing the transmitter power. The latter solution is not attractive if the system is to be powered by primary storage batteries recharged by solar panels. An advantage of UHF systems is that it is easier to satisfy the generous Fresnel clearance zone requirements because of the shorter wavelength.

One option would be to use the UHF band for the links from Oaxaca to Mexico City and the VHF band in the remote rural areas.

A further consideration is the desirability of using the same equipment throughout the network in order to maximise the ease of network maintenance and to keep the spares inventory to a minimum.

On balance, it is considered best to avoid the uncertainties of man-made interference and to deal instead with more controlable factors in the UHF band.

2.2 Frequency Plan

At repeater locations the transmit frequency must be separated by a minimum of 5MHZ from the receiver frequency to prevent the transmitter from desensitising the receiver. A further requirement is that sufficient physical separation exists between the transmit and receive antennas.

There also exists the possibility of interference due to intermodulation distortion

in the receivers. Careful choice of the RF frequencies will prevent problems from 3rd order intermodulation products. For example, the following group of five frequencies is free from interfering 3rd order intermodulation products, where FO is the first channel and ΔF is the channel separation.

Channel	Frequency
1	FO
2	FO + ΔF
3	FO + $4\Delta F$
4	FO + $9\Delta F$
5	FO + $12\Delta F$

At sites where more than two RF frequencies are received careful choice of frequency with the aid of the table above will avoid problems from intermodulation distortion. The possibility of interference can be reduced further by avoiding the use of channels separated by the legal minimum (25KHZ). If possible a minimum of 100KHZ spacing between channels should be used (ΔF = 100KHz). This would include consideration of other licenced users in the vicinity of any one link.

Careful frequency planning may also permit the use of a given frequency more than once provided appropriate attention is paid to possible interference problems. Calculations on path loss can be made for possible interfering paths in much the same manner as desired paths except that the fade margin uncertainty should be given the opposite sign.

2.3 Path Loss Calculations

Path loss calculations are not included as part of this report. References have been left with IIMAS which permit required transmitter power, antenna gain and expected operational margin to be estimated. Path profiles should be drawn for all paths and for each path the expected performance should be estimated.

A quick look at many paths suggests that free space propagation conditions are an essential part of the scheme for the network to operate. Thus the key effort in the calculations will be devoted to ensuring that there is clearance to 3 to 4 times the Fresnel ellipsoid (horizontal as well as vertical clearance).

The most effective method of increasing the fade margin is to increase the antenna gain at both ends of the link rather than to increase the transmitter power, which would require larger power supplies. An example of the type of antenna which might be used is a 15 element yagi which has a gain of 13.5dB. If even more gain is required these units can be stacked and interconnected by a matching transformer. In this manner two units will yield an additional 3dB and four units 6dB, etc.

3. Data encoding schemes

There are two basic schemes to be considered in methods of encoding the data and modulating the radio link; analogue and digital.

3.1 Analog telemetry

In this scheme the amplified filtered seismometer signal is used to drive a voltage controlled oscillator. This produces a sinusoidal audio carrier on which the instantaneous frequency is proportional to the ground velocity. The audio frequency is then used to modulate a VHF/UHF transmitter. In many existing applications, the transmitters have been constructed by modification of circuit boards originally designed for use in personal "walkie-talkie" radios (e.g. USGS scheme as used in California and Nicaragua. Lamont also uses a similar scheme.) In its simplest form involving only a single link with no repeaters and no multiplexing this approach typically has a dynamic range approaching 60dB (at Yellowknife array the figure is 56dB).

A particular attraction of this method is the ease of multiplexing since this can be done by simply adding the various audio sub-carriers and using the composite signal to modulate a transmitter. Each sub-carrier is allocated a separate band of frequencies. At the receiving end frequency selective bandpass filters are used to separate the various channels. This scheme has been used to multiplex up to nine channels of data onto one RF carrier. There are of course, trade-offs. As the number of channels and/or number of repeaters increases the dynamic range of each channel decreases and the amount of cross-talk increases. The degree of degradation is

influenced by the following factors:

a. The spectral purity of the generated sinusoidal sub-carriers. A distorted sine wave has harmonics which may interfere with the fundamental of a higher frequency sub-carrier.

b. Any distortion in the adder circuit. This is not likely.

c. Distortion in the transmitter modulation process. This can be severe particularly in transmitters which have automatic level control and bandwidth limiters. Since there are FCC requirements in walkie-talkie radios care is needed when these are used.

d. The RF carrier to noise ratio at the receiver input terminals. At low received signal levels random noise will appear in the demodulated seismic output.

e. Distortion and non-linearity in the receiver.

f. The sharpness of the bandpass filters used to separate the multiplexed channels.

g. The linearity of the sub-carrier demodulator. This is less important.

It should be noted that distortion in the RF modulation-demodulation is a key specification if optimum performance is to be obtained. Any system which includes a summed set of sinusoids and is subject to distortion will have all the usual distortion products which include harmonics of the fundamental and many intermodulation products (e.g. $F_1 + F_2 - F_3 = F_4$, $2F_1 - F_2 = F_3$). The difference between radios which are good for multiplex use and those which are not can probably be linked directly to the harmonic distortion specification.

3.2 Digital-Telemetry

In this scheme data are quantised at the remote location into a binary bit stream and transmitted as a binary signal by land line or radio link. Most schemes have used a modem to adapt the digital signals to frequency shift keyed signals which are acceptable to the telephone companies. Digital schemes offer the promise of re-shaping and re-timing the signals when appropriate so that the original signal fidelity can be preserved through a large number of repeaters. However, digital signals are more complex to multiplex since the signals require time slice multiplexing rather than simply adding the signals as in an analog system. Conceptually the digital scheme is no more complicated, but in practice it requires a higher degree of sophistication at repeater and multiplex sites.

3.3 The recommended encoding scheme

In the intest of expediency I suggest that the analog scheme is most appropriate for use at the present time and will lead to usable data in the shortest time frame. The technology has been proved and all of the equipment can be bought off-the-shelf.

As a longer term proposition I believe the analogue radio network could be upgraded to operate in the digital mode as better methods of modulating and multiplexing digital signals are developed. In an orderly scheme of development, experimental digital technology could be tried and proved on a selected radio link. After a period of evaluation the whole network could gradually be upgraded to digital operation whilst remaining fully operational at all times. However, it should be noted that the transmission of digital data may require more bandwidth from the transmission channel depending on the sampling rate, data format and encoding scheme employed.

4. Remote Station Configuration

In order to consider the remote station configuration in more detail it is necessary to make a few assumptions. It is safe to assume that the total remote electronics package can be contained in a volume of about 10cm x 10cm x 10cm. Secondly, it can be shown that the RF power levels at the transmitter output will be between 200mW and 2W according to the frequency band and the path loss.

At a low power level, primary storage batteries can be used, although they do represent a continuing expense since they must be renewed at least annually. Because of greatly increased interest in the USA due to the 'energy crisis', the price of solar panels is on a downward trend, since price is closely tied to production volume. Large volume users are now paying about $15. per peak watt of solar power (as measured in midday sun). Solar power also has the attraction of a one time capital cost and thereafter negligible operating expense.

Another desirable feature of a remote station location is that the amount of on-site work should be kept to a minimum. In the early stages of the establishment of a more or less permanent network a distinct advantage would be ease of movement to a better site as operational experience is accumulated.

4.1 Solar Power System

The scheme proposed below has been based on a 1 watt RF output since this

will be satisfactory for most locations. In order to obtain 1 watt RF output from transmitters, approximately 4 watts input will be required from the power system at 12 volts dc. The Solar Panels are used to charge a 12 volt battery and a simple regulator prevents the batteries from over-charging. The exact power levels will depend on the efficiency of the transmitter. The figures above are based on an efficiency of 33% (RF output/DC input).

Discussions with several manufacturers suggest that a solar array of about 25 watts peak power at 100mW/cm^2 and 28^{o}C would provide the necessary power. The panels would be inclined at about 45^o to the horizontal. The battery capacity would be something between 90 and 180 ampere-hours. There is evidently a trade off between the size of the battery and the size of the solar array. Low self-discharge sealed lead-calcium batteries appear to be favoured for this type of application. The typical surface area of a suitable solar array would be 2000cm^2.

Most companies operating in this field have computer programs which will optimise a design and match it to their products. This is usually available free of charge to prospective customers.

4.2 Remote site physical layout

One possible design for the remote stations follows directly from the following considerations:

4.2.1 The civil engineering works should be kept to a minimum.

4.2.2 All equipment should be mounted on a single structure: except of course, the seismometer.

4.2.3 Whilst burying the equipment has been used successfully elsewhere, it requires a hole to be dug, and an equipment case to be buried in it. It has the advantage of a stable temperature but subjects equipment to a higher humidity and to the possibility of flooding in a thunderstorm. Equipment must be dug up before it can be moved.

4.2.4 The antenna mast should always be high enough to ensure Fresnel zone clearance in the vicinity of the antenna.

4.2.5 A common design should be used for all locations.

4.2.6 It should be possible to climb the mast to service the antenna and solar panels.

4.2.7 All equipment should be .303 calibre bullet proof (except the solar panels. Bullet proof panels are available, but it is cheaper to replace broken panels, unless there is a recurring problem).

4.2.8 Equipment should be protected from the direct heat of the sun.

4.2.9 All equipment cases should be locked.

4.2.10 Storage batteries should be in a separate vented container.

4.2.11 Space should be provided for additional radio equipment in case the site is also a repeater.

4.2.12 It is desirable (though not essential) to use low cost conduit between the seismometer and the mast to contain the seismometer cable and to provide a good ground connection.

4.3 Remote Site: recommended scheme

A scheme which meets these requirements is sketched in figure 3. Triangular steel tower as used for TV antennas is used for the mast. The electronics, equipment case, solar panel and antenna are all bolted securely to the mast. A lightweight steel panel, insulated with styrofoam on the underside is used to protect the electronics package from direct solar radiation and provide additional protection from rain. Conduit is used to contain solar panel cables, antenna cable and seismometer cables. Steel enclosures of 12 gage construction would be dented but not pierced by rifle fire. The site would require only a small concrete base for the tower. Guy wires would be used to steady the tower.

5. Repeater Station Configuration

In the simplest repeater configuration the received composite audio signal is simply retransmitted. However, because the incremental cost is low it will usually be expedient to include a local seismometer. The local VCO output is added to the received tone(s) and the new composite signal is retransmitted. Of course, at some sites there will be more than one receiver which will in turn require a multi-channel adder circuit.

If an attempt is made to standardise on a single design which can be used economically at all sites then a choice must be made as to the number of additional receivers for which space, power, multiplex facilities etc. are to be provided for.

A review of the proposed network for Oaxaca State and for other networks suggests that a reasonable compromise would be to provide facilities for up to two receivers and a VCO at each site in a standard design. Stations which do not fit into this scheme could be considered special stations. This approach would provide a reasonable degree of flexibility in network design so that configuration changes could be made without extensive hardware changes. In addition there would be a limited amount of redundant equipment at simple stations having only a VCO and transmitter.

As an aid to optimising network performance each input channel on a multiplex adder should be equipped with a calibrated attenuation control which could be used to balance the amplitude of the tones before retransmission. At the

time of initial deployment all potentiometers would be set to the 0dB mark. Subsequently, operational measurements would permit calibrated adjustments of ±6dB to be made as required.

At key repeater sites where a single RF link can carry the entire network data, it may be desirable, at additional cost, to provide a parallel RF link so that each link carries only half the network data. This doubling up can be implemented with varying degrees independence between the two channels, ranging from the use of a completely different routing with additional intermediate repeater sites, to the attachment of a second transmitter to an existing site.

6. Terminal Station Configuration

At the terminal station at UNAM the received composite signal must be de-multiplexed and demodulated into individual channels and then digitally multiplexed, converted to digital format and finally serialised for input to the PDP11-40 computer through one channel of the DH11 multiplexer.

The analog demodulators are commercially available and usually include one complete channel demodulator in a single module. The module usually includes the bandpass filter required to separate a channel from the composite signal.

The digital multiplexer, analog to digital converter and serialiser would be constructed at UNAM according to established RESMAC standards.

Optimum received signal to noise will be obtained if the receiver is mounted near the antenna so that RF cable losses are minimised. At UHF frequencies several decibels of unneccessary attenuation can be quickly accumulated if care is not used in planning the antenna down lead.

7. System Design

7.1 Network Layout

A map of the proposed station locations is shown in figure 1 and a system block diagram in figure 2.

Note that the most distant signal must pass through four repeaters and that the final link from Ajusco to UNAM must carry seven signals.

7.2 An example of RF pathloss calculation

A UHF radio link of 280km length is to be designed using a one watt transmitter and a receiver of .34μV SINAD sensitivity. The link is to have a reliability of 99.99% (8sec/day loss).

		Gain Margin (rel to 1 watt)
Add Receiver sensitivity, 12dB SINAD = .35μV. Convert to decibels below one watt. Assume 50 ohm input impedance = 146dBW	146dBW	146
Add Receiver antenna gain. Try a 5 element Yagi with 9dB gain	+9dB	155
Subtract Receiver cable loss. Calculate by multiplying cable loss in dB/ft by length. Assume 1dB.	-1dB	154
Subtract Path loss. Free space propagation at 150MHZ over 280 km. 3 to 4 times Fresnel Zone clearance	-122dB	32
Add Transmitter antenna gain. Try a 5 element Yagi with 9dB gain	+ 9db	41
Subtract Transmitter cable loss. As RX.	- 1db	40

	brought forward	40
Subtract Loss due to reduced antenna aperture at 450MHZ (Path loss was taken at 150MHZ).	-9.5dB	30.5
Subtract FADE MARGIN. Use Rayleigh distribution, 99.99% or 8sec/day	-38dB	- 7.5

The negative margin indicates that the transmitter power must be 7.5dB above one watt. The actual transmitter power required would be $10^{.75}$ = 5.6 watts. In order to use a 1 watt transmitter more gain is required. Try increasing Tx and Rx gain from 9 to 13.5dB by using 13 element yagis to gain 2 x 4.5dB = 9dB.

Continuing the calculation:

Add Additional gain from 2 13.5 yagis	+ 9dB	1.5

The required transmitter power is now $10^{-.15}$ = 0.7 watts and so one watt transmitter would be satisfactory. Note however, that a figure of 0.35 μV was taken for the receiver sensitivity from typical manufactures specifications. This is the figure for a demodulated signal to noise ratio of 12dB. In practice, this figure is too low to achieve a satisfactory signal quality on the helicorder. A received signal level of 1μV produces acceptable results. This implies a further gain of $20\log_{10}(\frac{1}{.35})$, or 9dB is required. This can be achieved by using pairs of 13 element yagis at each end of the link to gain a further 6dB (nominal, in practice 5dB).

Continuing the calculation:

Subtract Loss due to higher minimum signal strength	- 9dB	-7.5
Add Gain by doubling up on the number of yagis	+ 5dB	-2.5dB

The power required has now increased to 1.7 watts. Bearing in mind all the factors taken into consideration and the fade margin employed, this design could be implemented using a standard 1 watt transmitter and the performance evaluated. Subsequently, if necessary, a further 5dB of gain can be obtained by adding two more yagis at each end. The alternatives would be to reduce the repeater spacing or increase the transmitter power and power supply. Clearly, higher gain antennas are much more cost effective.

7.3 Site Tests

Calculations on path loss should be verified by making signal strength tests using a transmitter, a wattmeter, two yagi antennas, two masts and a calibrated receiver or a signal strength meter. Actual path loss can then be measured and compared with the calculated path loss. However, it should be noted that care must be used since the measured value will not be representative of the median value since it ignores the effect of diurnal and annual variations. Since the diurnal variation is likely to be greater than annual variations, results accurate to ±10dB might be obtained by monitoring the signal throughout a 24 hour period.

7.4 Remote Station VCO centre frequencies

In order to optimise the system performance the VCO centre frequencies should be chosen carefully so that harmonic and intermodulation products are minimised. One approach is to attempt to choose the frequencies so that most of the unwanted products fall outside the transmission bandwidth. As with the RF system design, the most troublesome products are likely to be terms of the form f1 + f2 - f3. A more complete list of harmonic and intermodulation products is given in appendix B.

8. Operational Considerations

8 1 Test equipment

In order to calibrate, maintain and test the network equipment the following special test equipment will be required. In each case one vendor is mentioned, but others certainly exist and should be considered.

Description	Vendor	Model	Cost $
RF Dummy Load 50Ω	Bird	-	10
RF Wattmeter	Bird	43	200
VHF-UHF Signal Generator	Hewlett Packard	8640	6000
FM Deviation Meter	Marconi	TF2304	1200
Digital Multimeter	Dana	2100	300
Frequency counter to 500MHZ	Hewlett Packard	5383A	1000
Distortion Analyser	" "	331A	1200
Low frequency signal generator, 0.01HZ-100K HZ	" "	3310A	1000
Oscilloscope, portable	Teletronix	221	1300
Calibrated RF attenuator	Telonic Instruments	TG950	∿100

8.2 Calibration

As remote stations are installed, an in-situ overall system calibration should be performed with the data received at IIMAS during the calibration sequence being recorded in the normal manner. A small battery operated calibration box can be constructed to generate a range of equivalent ground velocities at a few spot

frequencies and amplitudes. A design for such a box is available on request from Ottawa. The test box is connected directly to the calibration coil of the seismometer by the field technician and is removed on completion of the test sequence.

8.3 Spares

A minimum of one of each of the following items should be stocked ready for deployment:

1. Seismometer
2. Amplifier-VCO-Muliplexer
3. Transmitter
4. Receiver
5. Demodulator
6. Solar charge regulator
7. Discriminator
8. Digital Multiplexer
9. Solar panel
10. Remote station battery

Special care is in planning for spare transmitters and the receivers since it should be possible to change frequency by changing the crystal without returning these units. If widely separated frequencies are in use it may be advantageous to stock two transmitters and two receivers so that each can cover a band of frequencies without returning. Spare crystals (Tx and Rx) should be stocked for all frequencies in use.

The spare assemblies should in turn be backed by spare transistors, IC's, etc.

9. Conclusions

The report outlines some of the considerations in the design of a telemeterd seismograph network which would transmit data from locations in Oaxaca State to Mexico City using analog FM telemetry. The proposed scheme is ambitious since it attempts to push equipment to the limit of its specifications, and as a result I think that it is unlikely that any company would guarantee the operation of the system as a whole. However, I believe that provided sound equipment is purchased the scheme as proposed is an excellent starting point. Equipment would be installed at the planned locations and then performance would be measured and assessed and the suitability of the sites, transmitter power, antenna gains, etc. reevaluated, possibly leading to a relocation of a station and perhaps the addition of another repeater.

At a later date the digitising equipment, initially at Mexico City could be gradually moved towards the remote sites perhaps one repeater at a time. This would ultimately convert the scheme into an all digital system.

Appendix A is the first draft of a set of specifications which could eventually be used as a basis for procurement after requirements have been finalised.

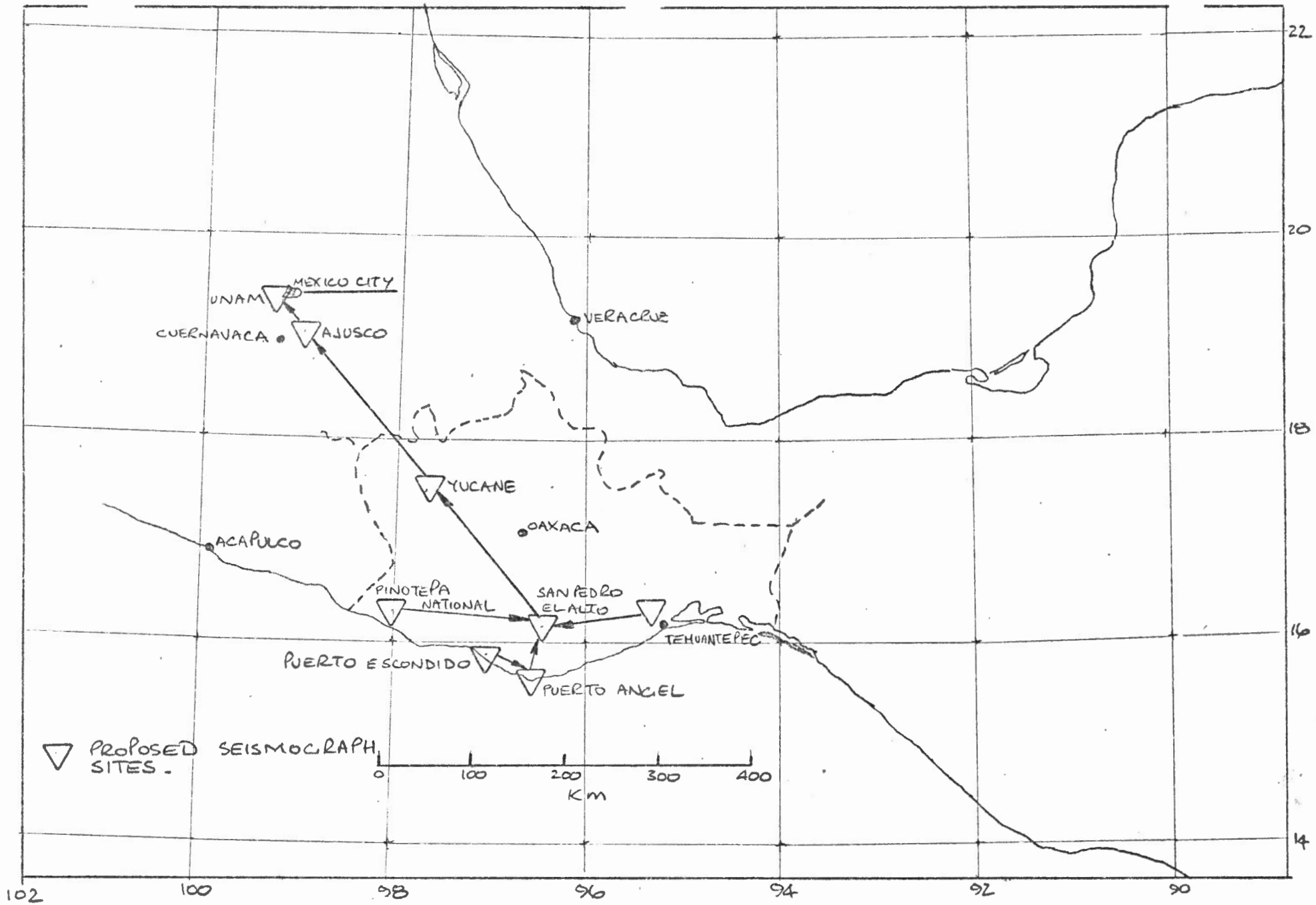

FIG 1 PROPOSED OAXACA SEISMOGRAPH NETWORK

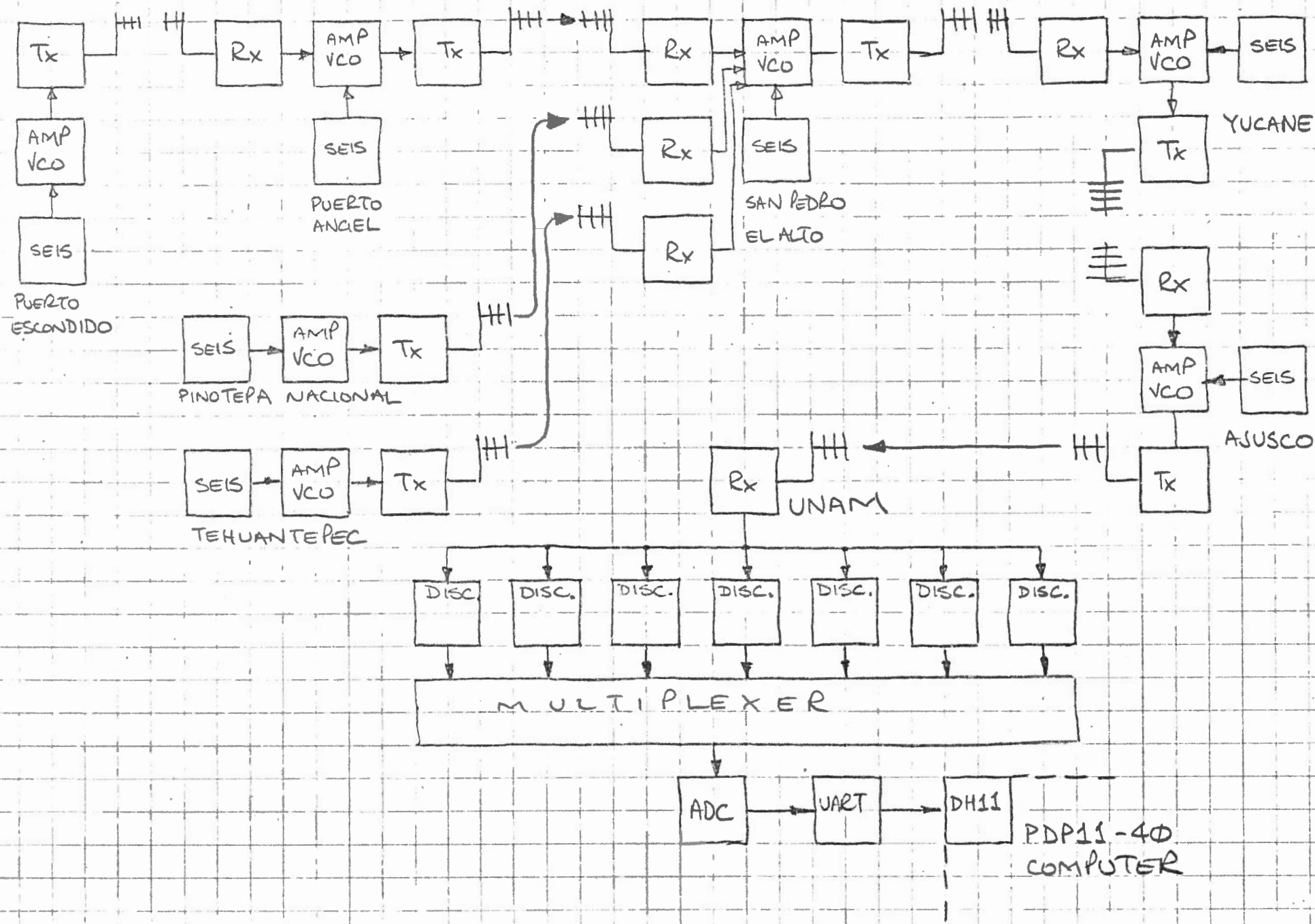

fig. 2. PROPOSED OAXACA SEISMOGRAPH NETWORK: BLOCK DIAGRAM

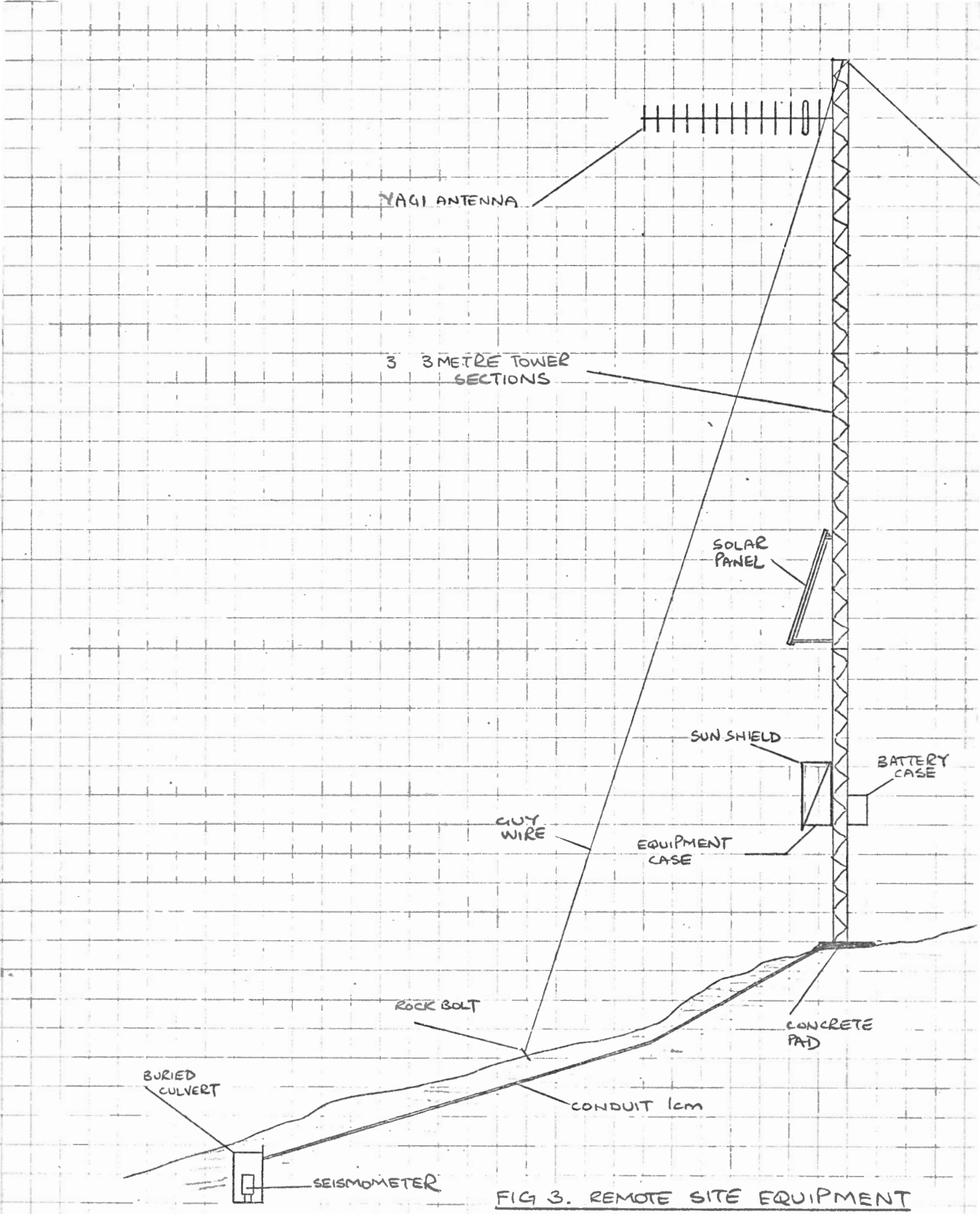

FIG 3. REMOTE SITE EQUIPMENT

APPENDIX A: DRAFT EQUIPMENT SPECIFICATIONS

A.1 Seismometer & Siting

Period	1 second
Calibration coil	to be included
Coil resistance	to be specified
Working damping	.70 critical
Adjustments required	none
Transducer constant	to be specified

The seismometer will be located in a small culvert which will be embedded in concrete and bonded to bedrock. The whole assembly will then be buried. The site should provide good drainage so that the seismometer cannot stand in water for extended periods. An electrical grade steel conduit from the culvert to the mast would permit easy servicing of the cable. The seismometer should be located 10-20m from the mast assembly.

A.2 Enclosure

All equipment, (transmitter, receiver, amplifier regulator and battery) will be placed in a metal enclosures which should be securely attached to the mast. The enclosure should include an access door with a padlock & catch. The enclosure should include provision for cables to exit to (a) seismometer, (b) up to six receiving antennas (c) one solar panel. The enclosure assembly should include a shield to prevent direct solar radiation onto the actual case. The enclosures should include vents and drain holes covered with fine wire mesh.

A.3 Antenna Mast

The enclosure should be of sufficiently heavy construction to prevent rifle

fire damaging the electronic equipment inside. The antenna mast should consist of two or more 3 metre sections of consumer grade steel TV tower (local purchase)

A.4 Antennas

High gain yagi antennas with either six elements or fifteen elements will be required. Antennas should be equipped with clamps for mounting to the steel tower and should use type N connectors.

a. 9.5dB gain 5 element

b. 13.5dB gain 15 element

Polarisation - vertical.

Vertical Separation between transmit & receiver antennas 3 metres minimum.

The long RF links will certainly require the high gain antennas, but some of the shorter links could use low gain antennas.

A.5 Transmitter

It is recommended that the transmitter be enclosed in a shielded metal case in order to minimise RF interference problems.

Frequency range: 450-470 MHZ

Frequency stability: ±.0005% (-10^{o}C to $+50^{o}$C)

RF Power into 50 ohm load: 1W continuous duty

Power supply: 10 - 14 VDC

Power supply current: to be specified; not to exceed .25A

Audio input: 0dBm for ±3.3kHZ deviation

Audio input impedance: 600Ω

Audio response: (with Rx) flat ±3dB, 300 - 3KHZ

Audio distortion: (with Rx) <5% total harmonic distortion

FM Hum & noise: >40dB below 2/3 rated system deviation

Spurious & harmonics: >46dB below carrier

Connector, Power: to be specified

Connector, RF: BNC chassis mount

Case: the transmitter shall be contained in a metal case to prevent spurious radiation and shall include FRI filtering on all power and signal lines

Case size: to be specified

Environmental: -10°C to +50°C, 0 - 95% humidity

Preferred modulation method FM (not Phase Modulation)

A.6 Receiver

Frequency range: 450-470 MHZ

Sensitivity: <.35μV: 12dB SINAD

<.5 μV: 20dB quieting

Spurious Rejection: 60dB

Image Rejection: 40dB

Adj. channel rejection: >70dB (13dB SINAD)

Modulation acceptance ±7.5kHZ (min)

Audio output impedance: 600Ω

Audio output level: 0dBm for ±3.3kHZ deviation

RF input impednace: 50Ω

Supply voltage: 11 - 14 VDC

Supply current drain: to be specified; not to exceed 25 mA

Connector, power: to be specified

Connector, RF: BNC chassis mount

Case: The receiver shall be contained in a metal case to contain or

exclude spurious radiation and should inlcude RFI filtering on all power and signal lines.

Case size: to be specified

Environmental: $-10^{\circ}C$ to $+50^{\circ}C$, 0 - 95% humidity

A.7 Amplifier - VCO - Multiplexer

This assembly shall provide for one seismometer input and a minimum of two received radio tones on appropriate IRIG frequencies. The multiplexer will sum the (up to) three tones and provide for adjustment of each tone so that the summed output will be 0dBm peak when loaded with 600Ω. The composite tone must not drive the transmitter beyond ±3.3KHZ deviation.

A.7.1 Local seismic channel

Sensitivity: 24 μV/Hz nominal, switch adjustable by ±24dB in 6dB steps.

Noise: <.25 μV rms referred to input

Filter: Band pass 0.25Hz to 20Hz (3dB) with 12dB per octave roll-off

Input: differential with transient protection. Common mode rejection: better than 60dB

Input impednace: 20KΩ minimum, with provision for a shunt damping resistor.

A.7.2 VCO

Channels: standard constant bandwidth channels to be chosen from 1020, 1360, 1700, 2040, 2380, 2720, 3060.

Deviation: ±125Hz

Linearity: .1%

Center frequency stability: better than 50ppm/$^{\circ}C$

A.7.3 Multiplexer

Inputs: Local VCO and two external tones

External inputs: 0dB into 600Ω.

Output & controls: three potentiometers to permit amplitude adjustment of all three tones so that composite signal is 0dBm ± 6dB when loaded with 600 Ω.

A.7.4 General

Supply voltage: 11 - 14VDC

Supply current: to be specified; not to exceed 25mA.

Case: the assembly shall be contained in a metal case to exclude spurious RF radiation and should include RFI filtering on all inputs and outputs.

Case size: to be specified.

Environmental: $-10^{o}C$ to $+50^{o}C$, 0 - 95% humidity.

A.8 Solar power system

Specifications for the solar power system can be developed from the request for proposals and pricing which has been extracted from a recent request for quotation and is copied overleaf.

A.9 Discriminator

The discriminators are to be modular plug-in units and should include a chassis and power supplies to accommodate a minimum of eight units. Centre frequencies should match remote site VCO frequencies.

Input sensitivity: 100mV to 3V rms

Channels: to be chosen from 1020, 1360, 1700, 2040, 2380, 2720, 3060HZ .

Bandpass filter: Each unit should include a bandpass filter capable of rejecting signals on an adjacent channel which are 20dB greater than those on the channel under test. Interference shall not be visible when a full deviation 10Hz sine wave test signal is displayed on a chart recorder. The interfering signal should include full deviation 5Hz modulation.

Output level: to be set to ±2 volts pk

Dynamic range: >50dB with 20Hz output filter

Output filter: 10Hz lowpass, third order and .5Hz highpass.

Indicator: low carrier level lamp

Squelch: output clamps to zero when carrier is removed.

Environment: 0 - 60°C, 0 - 95% humidity.

A.10 Multiplexer - ADC - UART

(to be supplied by UNAM)

Input channels: 8

Input level: ±2 volts peak

Input configuration: single ended

ADC sampling rate: 37 s/s or as specified

ADC dynamic range: to be specified

ADC/UART format: to be specified

UART band rate: to be specified

SOLAR POWER SYSTEM

1. APPLICATION

Proposals are invited for solar power systems to provide power for continuous operation of a telemetry transmitter. Up to fifteen systems are planned. Representative coordinates are listed below. Exact power consumption at each site has not yet been determined, but the final value will be chosen from three possible options (according to the required RF power).

Site 1: James Bay - Lat. 52^{o} - Long. 77^{o}
Site 2: Strait of Georgia - Lat. $49\frac{1}{2}^{o}$ - Long. 124^{o}
Site 3: Oaxaca, Mexico - Lat 17^{o} - Long. 97^{o}

2. SYSTEM DESIGN

Proposals should take into account published weather data for the regions specified including ambient temperature and the effects of snowfall and freezing rain. Recommendations should include:

a) total peak power required from the solar panels,
b) panel orientation (elevation & azimuth),
c) battery type and capacity,
d) some indication of the margin of safety built in to the recommendations. (Perhaps a computer printout).

3. DESIGN LOAD

Option 1

Voltage	-	12-14 volts
Duty	-	continuous
Current	-	.3A
Power	-	4 watts
Ampere-hours	-	7.2 ampere-hours/day

Option 2

Voltage	-	12-14 volts
Duty	-	continuous
Current	-	.6A
Power	-	8 watts
Ampere-hours	-	14.4 ampere-hours/day

Option 3

Voltage	-	12-14 voltage
Duty	-	continuous
Current	-	.150A
Power	-	2 watts
Ampere-hours	-	3.6 ampere-hours/day

4. SUB ASSEMBLIES

Proposals should include data as specified for each component of the system as follows.

4.1 Panels

Type number
Operating temperature
Number of cells
Cell diameter
Voltage
Current
Peak power @ 100mW/cm^2, 28^{o}C cell temperature
Is a blocking diode included?
Panel dimensions & outline drawing
Description of panel construction & encapsulation
The effect of .303 rifle fire on the panel

4.2 Battery

Recommendations on the battery should include:

Nominal terminal voltage
Battery type & number
Nominal capacity at 25^{o}C in ampere-hours
Nominal capacity at -30^{o}C in ampere-hours
Battery dimensions, weight

4.3 Regulator

Type number
Operating temperature
Storage temperature
Humidity
Regulation voltage
Maximum current dissipation
Outline drawing

4.4 Panel mounting hardware

Panels will be mounted on triangular steel tower. If hardware exists for mounting panels to steel tower, outline drawings should be included.

5. PRICING

Prices for a system should be broken down by sub assembly (4.1 through 4.4) so variations in system design can be considered without further quotation.

List of Attachments and References

1. Newspaper clipping: Ottawa Citizen April 21, 1978.
2. Ohtake, M., Matumoto, T., Latham, G.V., Seismicity Gap near Oaxaca, Southern Mexico as a probable precursor to a large earthquake, Pageoph, 115, 1977, 375-385.
3. Test instrumentation: partial specifications.
4. Specifications: PDP11 parallel I/O interfaces.
5. Solar arrays: correspondence and proposal from Philps Electronics, Ltd.
6. Solar-cell technology. Electronic Design, Dec. 1977.
7. Bullington, K.,'Radio Propagation Fundamentals', Bell Sys. Tech. J., 1957, 36, 3, 593-626.

Other useful references:

'Transmission systems for communications', Bell Telephone Laboratories. (Textbook).

Scientists plan to be there when quake hits Mexico

By Ann Arnold
CP staff writer

AUSTIN, Texas — University of Texas scientists, using space-shot technology to forecast disasters on earth, predict a massive earthquake will occur soon in the state of Oaxaca in southern Mexico and plan to be there to record it.

UT researchers expect the quake to be stronger than those that shook Managua, Nicaragua, and Guatemala City.

Dr. Creighton A. Burk, director of UT's Marine Science Institute, said the evidence is based on statistics generated by the university's new computerized seismic monitoring system.

"We have discovered a large area in the state of Oaxaca, at the southern tip of Mexico, where no major earthquakes have occurred for more than almost five years," Burk said. "This is extremely unusual."

Burk said the area is part of the very active Central American seismic zone that undergoes continual movement as the result of shifting and crumbling of the Earth's crust.

"Prior to mid-1973 large earthquakes were as characteristic of Oaxaca as anywhere else in this belt," Burk said. "The only reasonable interpretation is that this part of the Earth's crust has become locked in place so that seismic stresses are being released in adjacent areas but continue to build up here.

"It seems inevitable that all of these accumulated stresses will yield a very major and destructive earthquake in Oaxaca."

Burk said he anticipates a quake of magnitude 8 on the Richter scale, or two quakes of magnitude 6 or 7, the size that struck Managua and Guatemala City.

Researchers cannot say how soon the quake will come, but are readying a specially-equipped van and team of investigators to go to Mexico this summer in hopes of studying the quake as it occurs.

"It's still just as quiet as hell," Burk said. "I'm pushing for us to get down there as soon as possible. The worst thing that could happen is for it to happen next week. Chances to capture an earthquake don't occur that frequently."

Scientists say studying an earthquake as it occurs could provide vital information needed to learn how to predict the timing and location of future quakes.

"We've got a chance here to really catch a quake," Burk said. "It's been almost five years that it's been locked which is fantastic. Stress keeps building up and building up and finally it has to fail. The longer it builds up the bigger quake that's going to occur."

Researchers plan to monitor everything from changes in magnetic and gravitational fields to erratic behavior of animals preceeding the quake.

"We're convinced all these reports about unusual animal activity (before a quake) are true. If we could find out what they're sensitive to, there is no doubt we can measure it better than them. We've got to depend on the animals to tell us what it is that's bothering them," said Burk.

Pageoph, Vol. 115 (1977), Birkhäuser Verlag, Basel

Seismicity Gap near Oaxaca, Southern Mexico as a Probable Precursor to a Large Earthquake

By Masakazu Ohtake[1]), Tosimatu Matumoto[2]) and Gary V. Latham[2])

Summary – An area of significant seismic quiescence is found near Oaxaca, southern Mexico. The anomalous area may be the site of a future large earthquake as many cases so far reported were. This conjecture is justified by study of past seismicity changes in the Oaxaca region. An interval of reduced seismicity, followed by a renewal of activity, preceded both the recent large events of 1965 and 1968. Those past earthquakes have ruptured the eastern and western portions of the present seismicity gap, respectively, so that the central part remaining is considered to be of the highest risk of the pending earthquake.

The most probable estimates are: $7\frac{1}{2} \pm \frac{1}{4}$ for the magnitude and $\varphi = 16.5° \pm 0.5°$N, $\lambda = 96.5° \pm 0.5$W for the epicenter location. A firm prediction of the occurrence time is not attempted. However, a resumption of seismic activity in the Oaxaca region may precede a main shock.

Key words: Seismicity; Earthquake prediction.

Introduction

From studies of the seismicity of the northwestern Circum-Pacific seismic belt, Fedotov (1965) and Mogi (1968a) found that 'gaps' in activity have been successively filled within several tens of years by a series of great earthquakes without significant overlap of their rupture zones. More detailed investigations by Utsu (1968), Mogi (1968b, 1969) and Nagumo (1973) revealed that some of the greatest earthquakes ($M \geq 8$) which occurred in and near Japan were preceded by seismically quiescent periods of several to a few tens of years. Similar phenomena have been reported also from other seismic zones including Alaska and the Aleutians (Sykes, 1971), South America (Kelleher, 1972), and major portions of the Circum-Pacific belt (Kelleher *et al.*, 1973; Kelleher, 1972; Kelleher and Savino, 1975). The search for pre-seismic reduction in regional seismicity has been successfully extended to smaller earthquakes of magnitude 6 to 7 (*e.g.*, Borovik *et al.*, 1971; Ohtake, 1976).

As a result of these studies, the recognition of seismicity gaps in active seismic zones is considered to be a promising method for prediction of major earthquakes. This notion was suggested for California earthquakes in an earlier study by Allen

[1]) International Institute of Seismology and Earthquake Engineering, Hyakunin-cho 3-28-8, Shinjuku-ku, Tokyo, Japan. On leave from the Marine Science Institute, University of Texas, USA.

[2]) Marine Science Institute, Geophysics Laboratory, University of Texas, 700 The Strand, Galveston, Texas 77550, USA.

et al. (1965). Some investigators, on the other hand, have emphasized that strong earthquakes are frequently preceded by a marked increase in local seismicity (*e.g.*, FEDOTOV, 1967; SADOVSKY *et al.*, 1972; SUYEHIRO and SEKIYA, 1972; WESSON and ELLSWORTH, 1973). KELLEHER and SAVINO (1975), however, revealed that prior seismic activity, if any, is generally confined to the vicinity of the epicenters of pending large earthquakes, and extensive portions of the future rupture zones commonly remain aseismic until the time of the main shocks.

SCHOLZ *et al.* (1973) ascribed both the quiescence and resumption of seismic activity, together with other premonitory phenomena, to pre-seismic dilatancy of the crust and consequent fluid diffusion. According to this hypothesis, seismic quiescence is attributed to the increased strength of a medium as pore pressure drops in the dilatancy-hardening stage; while the renewal of seismic activity occurs with the recovery of pore pressure and consequent weakening of the medium under shear stress. Further investigations of the nature of seismicity gaps can be expected to break new ground, not only for phenomenological earthquake prediction, but in the physical understanding of earthquake occurrence.

The present paper reports a significant decrease in shallow seismicity near Oaxaca,

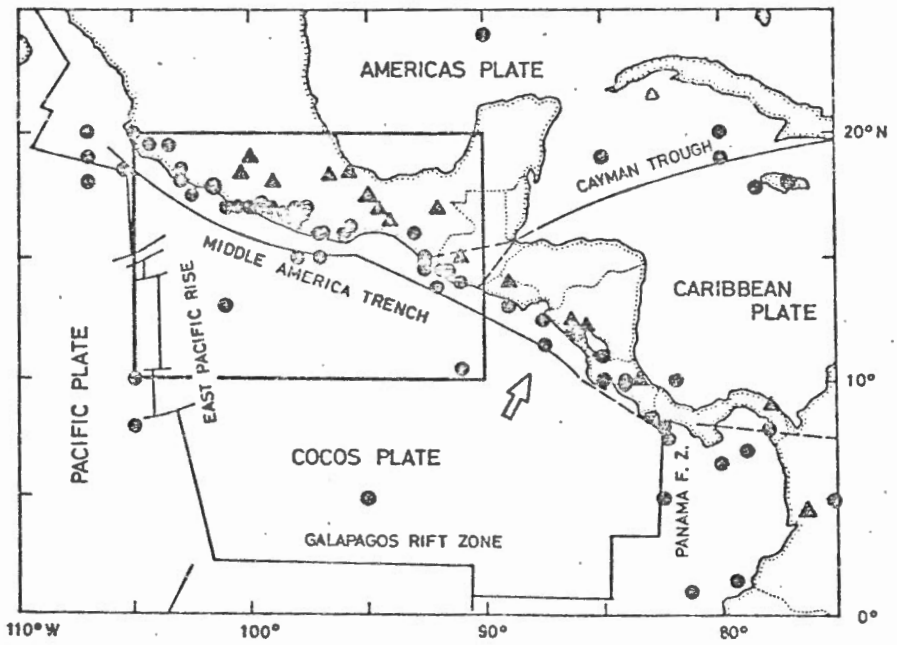

Figure 1

Seismicity and tectonic setting of the Mexico-Middle American region. Small circles and triangles are epicenters of major shallow ($H \leq 65$ km) and deep ($H > 65$ km) focus earthquakes, respectively. The seismic data are taken from the table compiled by DUDA (1965) for the period 1897–1964 ($M_L \geq 7$), and PDE for 1965–1975 ($Ms \geq 7$ or $mb \geq 6.5$). Plate boundaries are delineated after MOLNAR and SYKES (1969). The region of the present study is shown by a rectangle covering southern Mexico and western Guatemala.

southern Mexico, in recent years. Based on this finding, we attempt to predict some of the characteristics of future earthquakes which may take place in this region.

2. Tectonic setting

Figure 1 shows the epicenters of major earthquakes which have occurred in the Mexico-Central America region since 1897. The tectonic elements of MOLNAR and SYKES (1969) are also given in this figure. An active seismic belt follows the Pacific margin of Mexico and Central America, paralleling the Middle America Trench. This activity is associated with the subduction of the Cocos plate under the Americas and the Caribbean plates. The pattern of activity is typical of island arcs, and the deep seismic zone is well delineated down to a depth of 250 km (MOLNAR and SYKES, 1969; STOIBER and CARR, 1973). The greatest earthquakes of this region have occurred along the Pacific coast, and were mostly of the low-angle underthrusting type in accordance with the subduction model (MOLNAR and SYKES, 1969). The region of our present study includes the most active part of the seismic belt as outlined by a rectangle in Fig. 1.

3. Seismicity gap

Figure 2 compares the shallow seismicity ($H < 60$ km) of the southern Mexico-Guatemala region for two successive time intervals: (a) June 1971–May 1973, and (b) June 1973–May 1975. The data are taken from the *Preliminary Determination of Epicenters* (PDE) published by the National Earthquake Information Service (NEIS) of the United States Geological Survey.

For period (b), an area bounded by 95.5°W and 98°W, as outlined by a rectangle, is almost completely free of shallow earthquakes of sufficient magnitude to be reported by PDE ($M \cong 4$ or larger). Assuming that epicenters are distributed randomly throughout the active belt, the probability that this gap could occur by chance in a given 2-year period is about 1 in 36,000 (See Appendix). An additional 40 to 50 earthquakes have been located by the NEIS in the seismic zone of Fig. 2 between 1 June and 31 December, 1975 (latest data available to us). None of these occurred within the quiescent zone, so that the assertion of nonrandomness is further strengthened.

The seismic history of the anomalous area is illustrated in Fig. 3 by a magnitude versus time diagram for shallow earthquakes ($H < 60$ km) which occurred in the present seismicity gap since 1963. This figure demonstrates a clear reduction in earthquake occurrence, starting in mid-1973, followed by complete quiescence for at least 2.5 years. Such a prolonged period of quiescence is clearly unusual for this region.

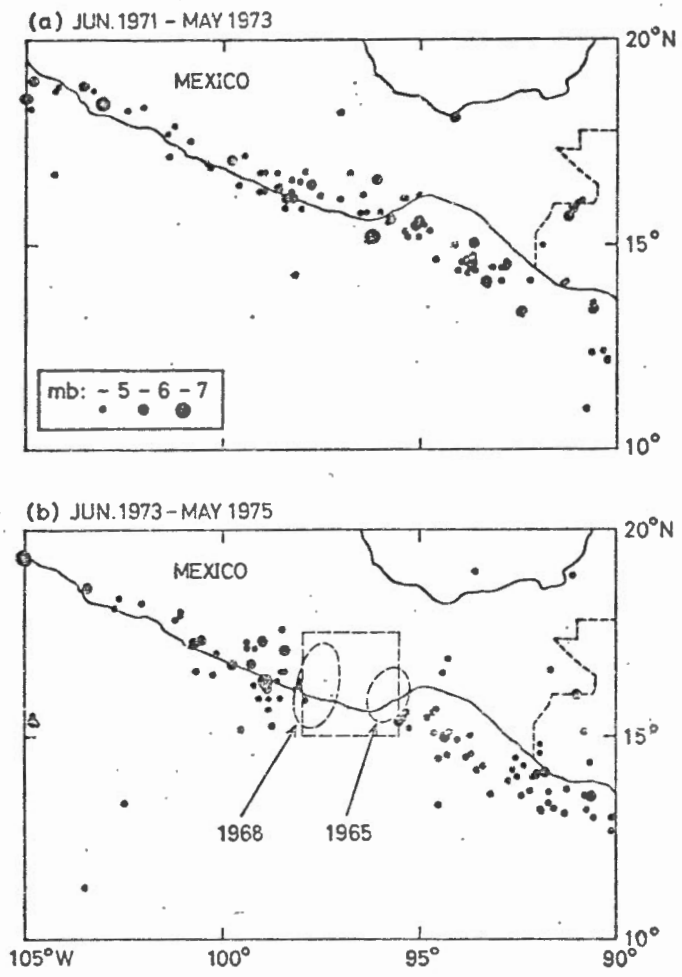

Figure 2
Epicentral distribution of shallow earthquakes ($H < 60$ km) which occurred in the southern Mexico-Guatemala region during the period of (a) June 1971–May 1973, and (b) June 1973–May 1975. The area of seismic quiescence during the latter period is outlined by a square. Two ellipses show aftershock zones of the Oaxaca earthquakes of 1965 and 1968, respectively.

4. Oaxaca earthquakes of 1965 and 1968

Two large earthquakes have occurred in the Oaxaca region during the past decade:

Aug. 23, 1965 $\varphi = 16.33°\text{N}, \lambda = 95.80°\text{W}, H = 29$ km, $Ms = 7\frac{1}{2} - 7\frac{3}{4}$
Aug. 2, 1968 $\varphi = 16.56°\text{N}, \lambda = 97.79°\text{W}, H = 36$ km, $Ms = 7.5$

(after the *Bulletin of the International Seismological Centre*). The approximate

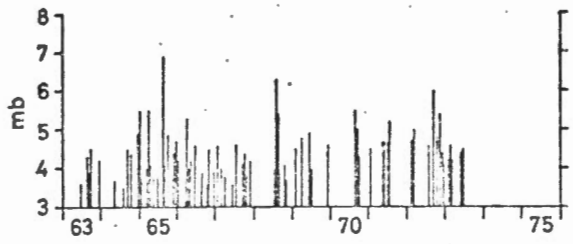

Figure 3
Magnitude versus time diagram of shallow earthquakes ($H < 60$ km) which took place within the square in Fig. 2(b) since 1963. Each event reported by PDE is plotted by a vertical segment of which length corresponds to its body wave magnitude.

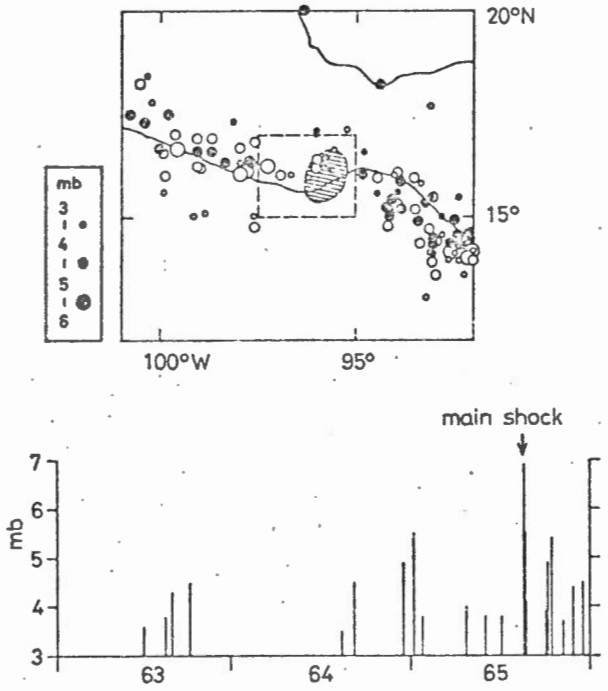

Figure 4
Change in regional seismicity prior to the Oaxaca earthquake of August 23, 1965. Upper: Solid and open circles indicate shallow earthquakes ($H < 60$ km) for the periods of seismic quiescence and resumption preceding the main shock, respectively. The shaded area is the aftershock zone of the main shock (cross mark). Lower: Magnitude versus time diagram for the earthquakes which took place inside of the rectangular area shown in the upper figure.

aftershock zones of these events are plotted in Fig. 2(b) by ellipses. Both of these earthquakes were preceded by anomalous changes in local seismicity. For the former case, local seismicity exhibited a quiescent stage from late 1963 to mid 1964, followed by a renewal of activity prior to the main shock (Fig. 4). For the latter case, preseismic quiescence was more distinct while resumption of activity was weak (Fig. 5).

In this paper, we refer to the period of quiescence as the α stage, and to the period of renewed activity as the β stage. The time interval between the onset of the α stage and occurrence of main shock was 1.5 to 2 years for the Oaxaca earthquakes. It is not clear whether the activities of the β stage were confined in the vicinity of the epicenters of the main shocks or not. Such a detailed analysis seems to require more reliable location of the epicenters, and also more complete coverage of small earthquakes.

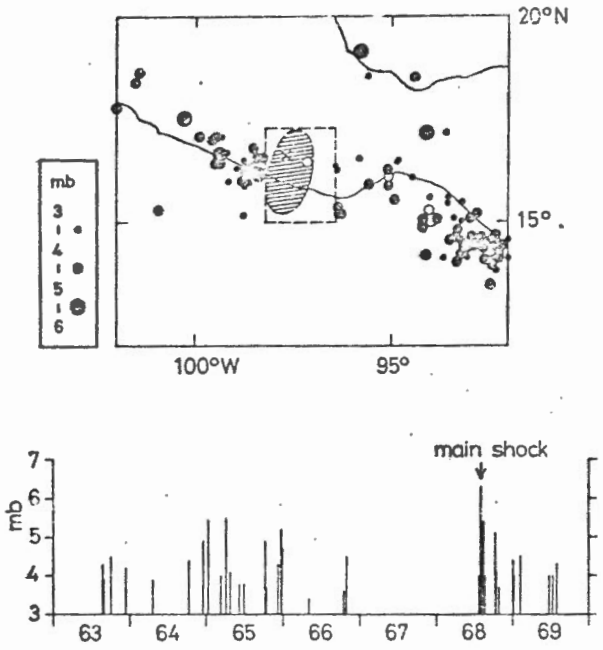

Figure 5
Change in regional seismicity prior to the Oaxaca earthquake of August 2, 1968. See Fig. 4 for explanation.

It is interesting to note that aftershocks did not completely fill the seismicity gap suggesting the smaller dimension of the rupture zone compared with the seismically anomalous area.

The focal mechanisms of the earthquakes were typical underthrust with shallow dip angle. The azimuth and plunge of the slip vector for the 1965 earthquake is reported by MOLNAR and SYKES (1969) as ϕ = N36°E and δ = 14°, respectively. Fig. 6 shows distribution of P initial motions of the 1968 event based on readings from microfilm records of the World-Wide Standard Station Network. The slip corresponds to a low angle thrust with ϕ = N49°E and δ = 6°.

Both of the main shocks were located near the northern extremes of their aftershock zones. This suggests that the rupture started at depth beneath the landward (NE) end of the dislocation, and unilaterally propagated towards shallower depth along the subducted plate interface. This pattern of rupture propagation is frequently found for large, thrust-type earthquakes as discussed by KELLEHER *et al.* (1973).

Summarizing the above discussions, the Oaxaca earthquakes of 1965 and 1968 are characterized by marked similarities in magnitude, space-time patterns of precursory seismicity change, focal mechanisms, and rupture patterns. These systematics may be useful in predicting the characteristics of future earthquakes in this region.

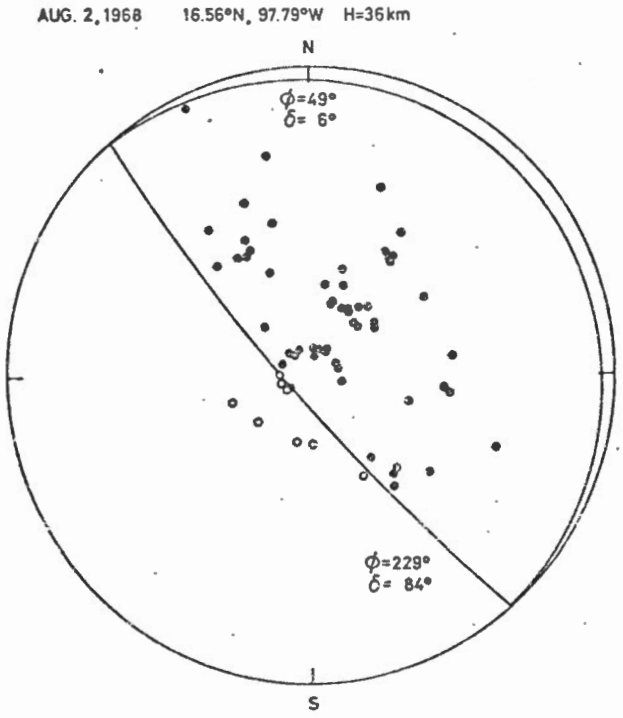

Figure 6
Equal area projection (lower hemisphere) of seismic radiation pattern for the Oaxaca earthquake of August 2, 1968. Solid and open circles indicate compressional and dilatational initial motions of *P* wave, respectively. This radiation pattern can be interpreted as representing underthrusting on a fault plane dipping at a shallow angle to the northeast.

5. *The impending earthquake*

The arguments presented above suggest to us that the relative seismic quiescence near Oaxaca may be signaling the eventual occurrence of a large earthquake in this region. We try to predict the most probable characteristics of the anticipated earthquake in the following.

Magnitude

The size of the present seismicity gap is roughly 7×10^4 km^2 in area, and 300 km in linear dimension, respectively. UTSU and SEKI (1955) and UTSU (1961) found

statistical relations between the magnitude of a main shock M and area A or linear dimension l of its aftershock zone:

$$\log A = 1.02\,M - 4.0 \quad (1)$$

$$\log l = 0.5\,M - 1.8 \quad (2)$$

Direct application of those formulae results in magnitude $8.6 \sim 8.7$ for the future earthquake if we assume that the aftershock zone will completely cover the present zone of quiescence. This seems unlikely, however, based upon the data presented above which suggests that the size of the aftershock zone is normally smaller than the preceding seismicity gap, at least in the Oaxaca region. Moreover, strain energy has been released in the eastern and western parts of the seismicity gap by the recent earthquakes of 1965 and 1968 (see Fig. 2). Thus, we would expect that the central area between those aftershock zones is the most likely site of the next large earthquake in this region. The separation between those two previous aftershock zones is roughly comparable with their dimensions. Therefore, the magnitude of the predicted earthquake may also be comparable to the previous events, that is, $7\frac{1}{2} \sim 7\frac{3}{4}$.

According to ANDERSON and WHITCOMB (1975), the linear dimension, L, of an area showing anomalous behaviour prior to an earthquake is empirically related to l by a simple formula,

$$\log l/L^2 = -3. \quad (3)$$

Combining (3) with (2), magnitude 7.3 is predicted for $L^2 = 7 \times 10^4\ \mathrm{km}^2$. In conclusion, $7\frac{1}{2} \pm 1/4$ is the best estimate we can make for the magnitude.

Location

As stated above, it appears likely that the aftershock zone of a future earthquake will occupy the central part of the present seismicity gap. The earthquake will probably be of the thrust type. The rupture is likely to begin in the northern portion of the zone and propagate southward, judging from the past instances. If this is the case, the epicenter of the main shock should be in the region, $\varphi = 16.5° \pm 0.5°$N and $\lambda = 96.5° \pm 0.5°$W.

Occurrence time

More than three years have passed since the onset of seismic quiescence in the Oaxaca region. This is substantially longer than the precursor times of the previous Oaxaca earthquakes. As yet, we have no reliable basis for predicting the time of occurrence. The precursor times observed for the 1965 and 1968 Oaxaca earthquakes (magnitude $7\frac{1}{2} \sim 7\frac{3}{4}$) were much shorter than the 13 to 31 years expected from the magnitude-precursor time relations by WHITCOMB *et al.* (1973), SCHOLZ *et al.* (1973),

and RIKITAKE (1976). This suggests that precursory time relations may vary greatly between various tectonic provinces. It may also indicate that some completely different phenomenon from the previous studies is being observed. In any case, previous *standard* magnitude-precursor time relations do not seem to be applicable in the present examples. However, a resumption of seismic activity corresponding to the β stage of activity, may be expected prior to the future, large earthquake as in the cases of 1965 and 1968.

6. *Discussions and conclusions*

Since June 1973, the frequency of shallow earthquakes in the area of Oaxaca, southern Mexico, has been unusually low, This area experienced two major earthquakes in the past decade: an event of magnitude 7.5 in 1965, and one of magnitude $7\frac{1}{2}$–$7\frac{3}{4}$ in 1968. These were both preceded by intervals of quiescence (α stage) and following resumption (β stage) of local seismicity in advance of the main shocks.

Previous case studies suggest that the β stage is not a universal phenomenon as is the α stage. Although it may partly be attributed to insufficient detection capability, there are some cases which definitely contradict our finding. KELLEHER and SAVINO (1975), for instance, reported that the prior seismic activity was not detected with reasonable coverage of small earthquakes for the Sitka earthquake of 1972, $Ms = 7.6$ and others. However, the contrast is no wonder because the pattern of earthquake sequences greatly depends on regional characteristics of the lithosphere. Based on laboratory experiments of rock fracture, MOGI (1968) revealed that the main rupture of nonuniform medium tends to accompany distinct activity of foreshocks, which does not appear for a uniform medium. Structural irregularity of the medium and consequent local concentration of stress is considered to be the basic precondition for increase in seismicity prior to the main shocks.

Therefore, the β stage is expected to appear only for regions of nonuniform structure. Really, the region of our present concern exhibits various indications of nonuniform, block-like structure. It is the conclusion of STOIBER and CARR (1973) that the underthrust lithosphere of the Mexico-Central America region is broken along tear faults into 100 to 300 km long segments. In such nonuniform regions, the weakest portions of the lithosphere will sensitively respond to the tectonic force building up so that seismicity change is expected to be a useful measure for predicting large earthquakes.

Based upon the significant scale of the current seismicity gap, both in time and space, together with the previous pattern of earthquake occurrence, the probability of a future, large earthquake in this area is considered to be high. The focal mechanism of the impending earthquake is expected to be a low angle underthrust associated with subduction of the Cocos plate under the Mexico-Middle America arc. The magnitude and epicentral coordinates are estimated to be $Ms = 7\frac{1}{2} \pm \frac{1}{4}$, and $\varphi = 16.5° \pm 0.5°$N, $\lambda = 96{\cdot}5° \pm 0.5°$W. No reliable estimate of occurrence time can be given.

While the evidence presented here is certainly not conclusive, we believe that it is strong enough to justify the initiation of a program of measurements in the Oaxaca region. If possible, the program should include monitoring of microearthquake activity, seismic wave velocity, and crustal deformation. Among these, systematic monitoring of microearthquakes may be the most effective and simplest method since a renewal of activity (β stage) preceding the main event is expected. Detection of a significant increase in seismic activity in the region would not pinpoint the time-of-occurence, but it would serve as a warning that the time remaining before the earthquake might be quite short.

Acknowledgements

We gratefully acknowledge the assistance of Dr. Yoshio Nakamura and Dr. James Dorman for critical review of the manuscript and helpful advice. This work was partially supported by the Harry Oscar Wood Fund, Marine Science Institute, Geophysics Laboratory, Contribution No. 199.

References

ALLEN, C., AMAND, P. ST., RICHTER, C. and NORDQUIST, J. (1965), *Relationship between seismicity and geologic structure in the southern California region*, Bull. Seism. Soc. Amer. *55*, 753–797.

ANDERSON, D. and WHITCOMB, J. (1975), *Time-dependent seismology*, J. Geophys. Res. *80*, 1497–1503.

BOROVIK, N., MISHARINA, L. and TRESKOV, A. (1971), *On the possibility of strong earthquakes in Pribayakalia in the future*, Izv. Acad. Sci. USSR, Phys. Solid Earth, Engl. Transl. 13–16.

DUDA, S. (1965), *Secular seismic energy release in the circum-Pacific belt*, Tectonophys. *2*, 409–452.

FEDOTOV, S. (1965), *Regularities of the distribution of strong earthquakes in Kamchatka, the Kuril Islands, and northeastern Japan*, Trudy Inst. Fiz. Zemli, *36* (203), 66–93 (in Russian).

FEDOTOV, S. (1967), *Long-range seismic forecasting for the Kurile-Kamchatka zone*, Transactions of the Meetings of the Far East Earth Science Division, Akademii Nauk SSSR, Moscow, 1–16 (in Russian).

HOGG, R. and CRAIG, A., *Introduction to Mathematical Statistics*, (MacMillan, New York, 1959), 152–160.

KELLEHER, J. (1972), *Rupture zones of large South American earthquakes and some predictions*, J. Geophys. Res. *77*, 2087–2103.

KELLEHER, J. and SAVINO, J. (1975), *Distribution of seismicity before large strike slip and thrust-type earthquakes*, J. Geophys. Res. *80*, 260–271.

KELLEHER, J., SYKES, L. and OLIVER, J. (1973), *Possible criteria for predicting earthquake locations and their application to major plate boundaries of the Pacific and the Caribbean*, J. Geophys. Res. *78*, 2547–2585.

MOGI, K. (1963), *Some discussions on aftershocks, foreshocks and earthquake swarms —— the fracture of a semi-infinite body caused by an inner stress origin and its relation to the earthquake phenomena*, Bull. Earthq. Res. Inst., Univ. Tokyo, *41*, 615–658.

MOGI, K. (1968a), *Sequential occurrences of recent great earthquakes*, J. Phys. Earth, *16*, 30–36.

MOGI, K. (1968b), *Some features of recent seismic activity in and near Japan (1)*, Bull. Earthq. Res. Inst., Univ. Tokyo, *46*, 1225–1236.

MOGI, K. (1969), *Some features of recent seismic activity in and near Japan (2), Activity before and after great earthquakes*, Bull. Earthq. Res. Inst., Univ. Tokyo, *47*, 395–417.

MOLNAR, P. and SYKES, L. (1969), *Tectonics of the Caribbean and Middle America regions from focal mechanisms and seismicity*, Geol. Soc. Amer. Bull. *80*, 1639–1684.

NAGUMO, S. (1973), *Activation mode of great submarine earthquakes along the Japanese Islands*, Publications for the 50th Anniversary of the Great Kanto Earthquake, 1923, Earthq. Res. Inst., Univ. Tokyo, 273–291.

OHTAKE, M. (1976), *Search for precursors of the 1974 Izu-Hanto-oki earthquake, Japan*, Pure Appl. Geophys. *114* (in press).

RIKITAKE, T., *Earthquake Prediction*, (Elsevier, Amsterdam, 1976), pp. 357.

SADOVSKY, M., NERESOV, I., NIGMATULLAEV, S., LATYNINA, L., LUKK, A., SEMENOV, A., SIMBIREVA, I. and ULOMOV, V. (1972), *The processes preceding strong earthquakes in some regions of middle Asia*, Tectonophys. *14*, 295–307.

SCHOLZ, C., SYKES, L. and AGGARWAL, Y. (1973), *Earthquake prediction: a physical basis*, Science, *181*, 803–810.

STOIBER, R. and CARR, M. (1973), *Quaternary volcanic and tectonic segmentation of Central America*, Bull. Volc. *37*, 304–325.

SUYEHIRO, S. and SEKIYA, H. (1972), *Foreshocks and earthquake prediction*, Tectonophys. *14*, 219–225.

SYKES, L. (1971), *Aftershock zones of great earthquakes, seismicity gaps, and earthquake prediction for Alaska and the Aleutians*, J. Geophys. Res. *76*, 8021–9041.

UTSU, T. (1961), *A statistical study on the occurrence of aftershocks*, Geophys. Mag. *30*, 521–605.

UTSU, T. (1968), *Seismic activity in Hokkaido and its vicinity*, Geophys. Bull. Hokkaido Univ. *20*, 51–75 (in Japanese).

UTSU, T. and SEKI, A. (1955), *A relation between the area of after shock region and the energy of main-shock*, Zisin, J. Seism. Soc. Japan, Ser. 2, *7*, 233–240 (in Japanese).

WESSON, R. and ELLSWORTH, W. (1973), *Seismicity preceding moderate earthquakes in California*, J. Geophys. Res. *78*, 8527–8546.

WHITCOMB, J., GARMANY, J. and ANDERSON, D. (1973), *Earthquake prediction: variation of seismic velocities before the San Fernando earthquake*, Science, *180*, 632–635.

(Received 20th September 1976)

Termaline RF Coaxial Load Resistors

50 ohms nominal

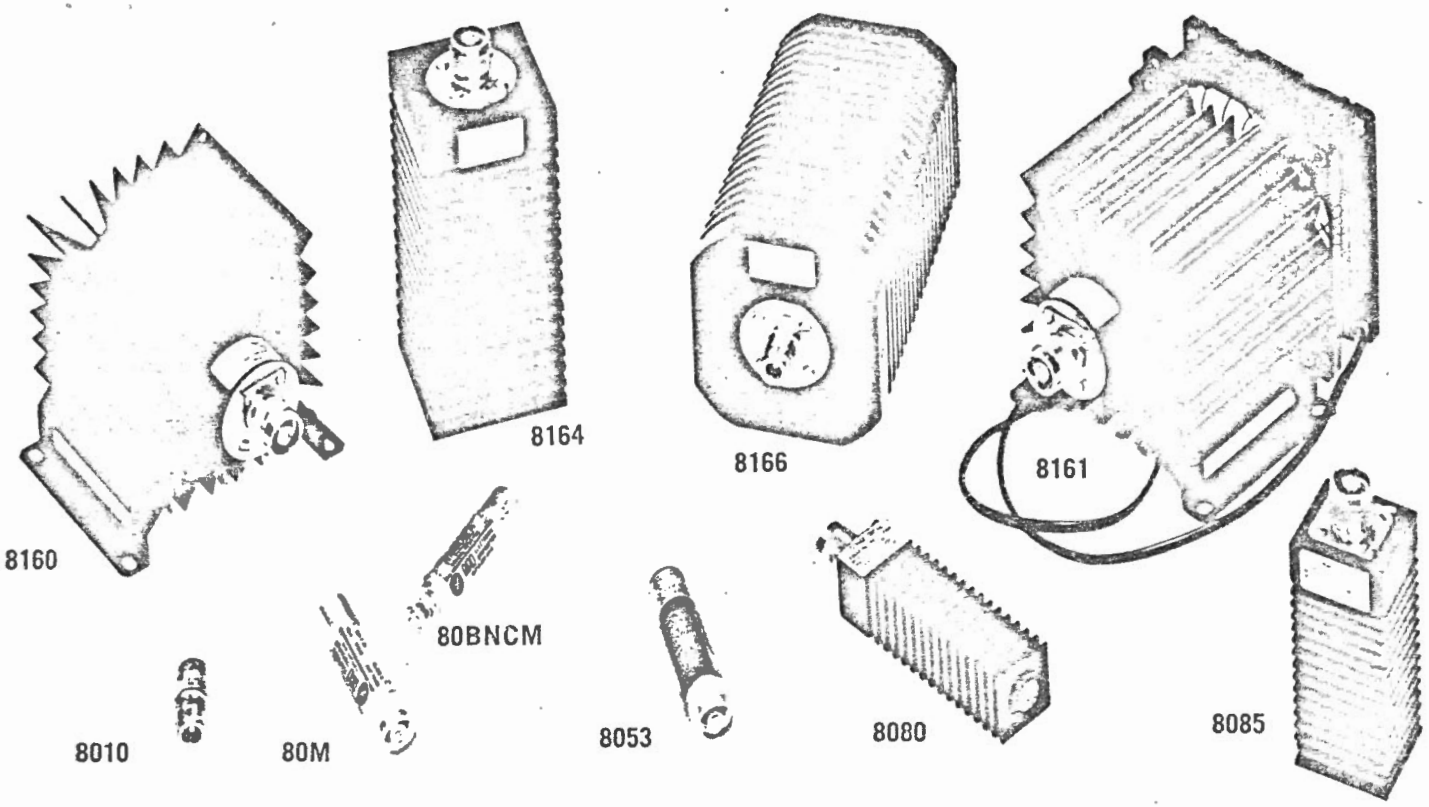

specifications

MODEL	POWER RATING CW	Maximum VSWR Limits and FREQUENCY RANGES DC 1GHz 2 2.5 3.5 4 GHz	INPUT CONN.	NOM. SIZE INCL. CONN.	WEIGHT	FINISH ①
8010	2W	1.04 1.06 1.1	N (F)	11/16 Dia x 1½ L	1¾ oz	BNP
8011	2W	1.04 1.06 1.1	N (M)	11/16 Dia x 1⅝ L	1¾ oz	BNP
80 F	5W	1.1 1.2	N (F)	11/16 Hex x 3¼ L	4 oz	SP
80 M	5W	1.1 1.2	N (M)	11/16 Hex x 3⅜ L	4 oz	SP
80 CF	5W	1.1 1.2	C (F)	11/16 Hex x 3⅜ L	4 oz	SP
80 CM	5W	1.1 1.2	C (M)	11/16 Hex x 3⅜ L	4 oz	SP
80 BNCF	5W	1.1 1.2	BNC (F)	11/16 Hex x 3⅛ L	4 oz	SP
80 BNCM	5W	1.1 1.2	BNC (M)	11/16 Hex x 3⅜ L	4 oz	SP
80 TNCF	5W	1.1 1.2	TNC (F)	11/16 Hex x 3⅛ L	4 oz	SP
80 TNCM	5W	1.1 1.2	TNC (M)	11/16 Hex x 3⅜ L	4 oz	SP
80 SCF	5W	1.1 1.2	SC (F)	11/16 Hex x 3⅜ L	4 oz	SP
80 SCM	5W	1.1 1.2	SC (M)	11/16 Hex x 3⅝ L	4 oz	SP
8052	10W	1.1 1.2	N (F)	11/16 Hex x 3⅜ L	4 oz	LBE
8053	10W	1.1 1.2	N (M)	11/16 Hex x 3½ L	4 oz	LBE
8080	25W	1.1 1.25	QC-N (M)	1¼x1¼x5⅛ L	9 oz	LBE
8085	50W	1.1 1.25	QC-N (M)	1¾x1¾x5⅛ L	15 oz	LBE
8160	100W	1.1 1.2	QC-N (M)	4⅞ x 5 11/16 x 6 L	36 oz	LBE
8164	100W	1.1 1.2	QC-N (F)	2¾ x 2¾ x 7 L	48 oz	LBE
8166	150W	1.1 1.2	QC-N (F)	4 x 4 x 7½ L	96 oz	LBE
8161 ②	225W	1.1 1.2	QC-N (M)	5¼x5 11/16x7 13/16 L	52 oz	LBE

① FINISH: BNP—Bright Nickel Plated; SP—Silver Plated; LBE—Lusterless Black Enamel (Fed. Spec. TT-E-527)

② Model 8161 Fan is 115 Vac 50/60 Hz. Other supply voltages and frequencies on request.

NOTES:

These dry (air) dielectric TERMALINE Load Resistors can be operated in ANY position.

Ambient Air Temperature Range for listed continuous power rating is -40° to +45°C. For higher ambient temperatures, see Power Derating Curves on p. 39.

QC-connector equipped Loads are shown with the QC type normally supplied. For other available types, see p. 36.

the indispensable model 43

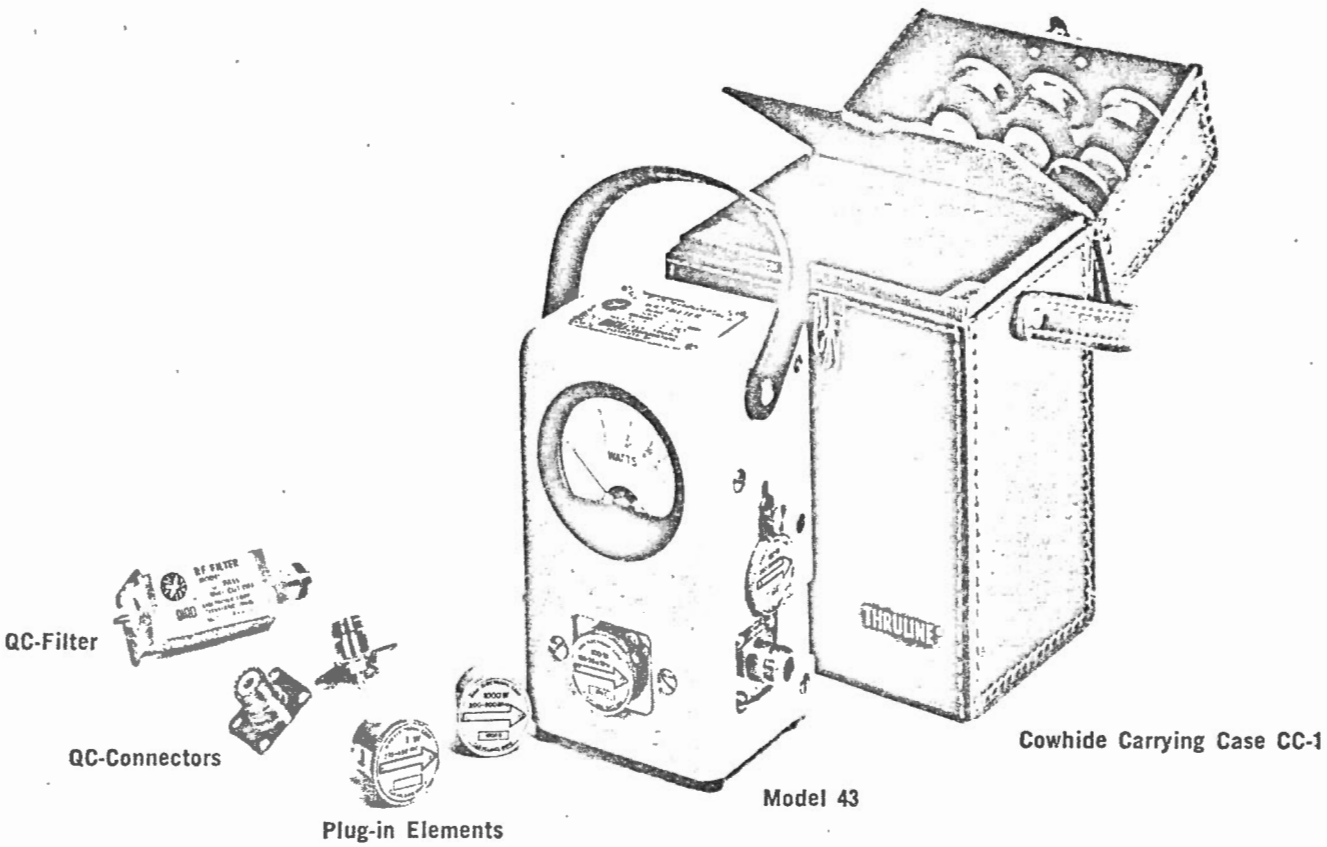

PLUG-IN ELEMENTS for use with Model 43 THRULINE Wattmeter. Select one or more elements to suit your frequency and power ranges. When ordering, specify catalog number and THRULINE model number.

Also for use with Models 4311, 4311-200, 4313, 4501, 4521, 4522, and 4526 THRULINE Wattmeters, 50Ω Line Sections equipped with QC-Connectors or 7/8" EIA Flanges, and TERMALINE Wattmeter Model 6151.

Table I

STANDARD ELEMENTS (CATALOG NUMBERS)

Power Range	Frequency Bands (MHz) 2-30	25-60	50-125	100-250	200-500	400-1000
5 watts	—	5A	5B	5C	5D	5E
10 watts	—	10A	10B	10C	10D	10E
25 watts	—	25A	25B	25C	25D	25E
50 watts	50H	50A	50B	50C	50D	50E
100 watts	100H	100A	100B	100C	100D	100E
250 watts	250H	250A	250B	250C	250D	250E
500 watts	500H	500A	500B	500C	500D	500E
1000 watts	1000H	1000A	1000B	1000C	1000D	1000E
2500 watts	2500H					
5000 watts	5000H					

Table II

LOW-POWER ELEMENTS

1 watt	Cat. No.	2.5 watts	Cat. No.
60-80 MHz	060-1	60-80 MHz	060-2
80-95 MHz	080-1	80-95 MHz	080-2
95-125 MHz	095-1	95-150 MHz	095-2
110-160 MHz	110-1	150-250 MHz	150-2
150-250 MHz	150-1	200-300 MHz	200-2
200-300 MHz	200-1	250-450 MHz	250-2
275-450 MHz	275-1	400-850 MHz	400-2
425-850 MHz	425-1	800-950 MHz	800-2
800-950 MHz	800-1		

Table III

HIGH-FREQUENCY ELEMENTS (CATALOG NUMBERS)

Power Range	Frequency Bands (MHz) 950-1260	1100-1800	1700-2200	2200-2300
1 w	1J	1K	1L	1M
2.5 w	2.5J	2.5K	2.5L	2.5M
5 watts	5J	5K	5L	5M
10 watts	10J	10K	10L	10M
25 watts	25J	25K	25L	25M
50 watts	50J			
100 watts	100J			
250 watts	250J			

Table IV

LOW-FREQUENCY ELEMENTS (CATALOG NUMBERS)

Power Range	Frequency Band .45 to 2.5 MHz
1000 watts	1000P
2500 watts	2500P
5000 watts	5000P
10000 watts	10000P

RF DIRECTIONAL COUPLER PLUG-IN ELEMENTS for sampling of the main line signal at a fixed attenuation level are listed on page 37

Model EC-1 Carrying Case for Plug-in Elements

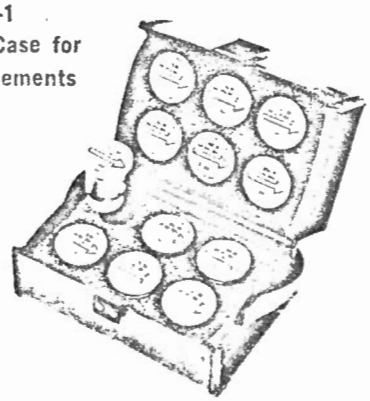

SIGNAL GENERATORS

Precision, high stability, AM-FM, 0.5 to 1024 MHz

Models 8640A, 8640B

- Wide frequency and power range
- Lo[w] broadband and close-in noise
- Ca[li]brated, metered AM and FM
- The 8640B also features:
  internal phase lock synchronizer
  external counter to 550 MHz

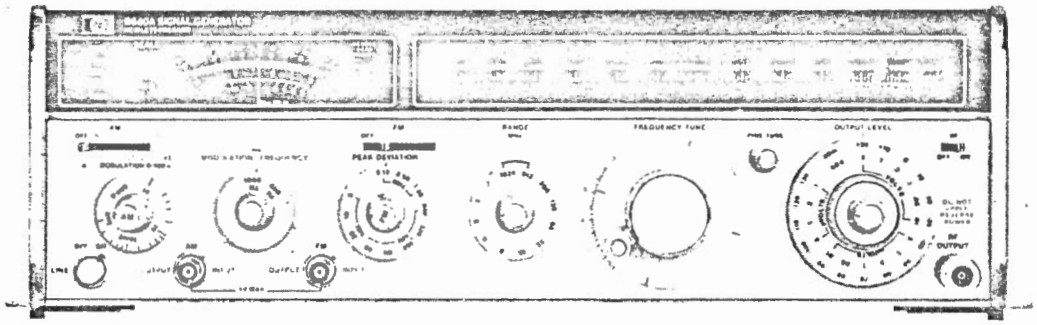

8640A

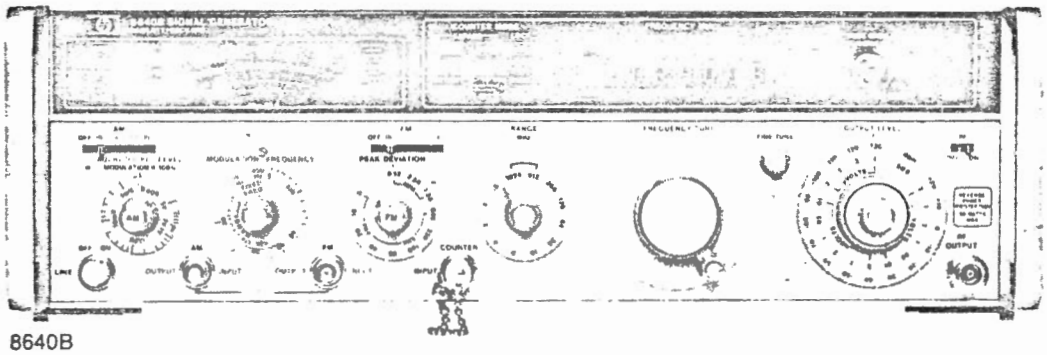

8640B

Description

The 8640 Signal Generator covers the frequency range 500 kHz to 512 MHz (450 kHz to 550 MHz with band overrange) and can be extended to 1100 MHz with an internal doubler (Opt 002). Using the 11710B Down Converter, the 8640 frequency range can be extended down to 10 kHz. An optional audio oscillator is also available with a frequency range of 20 Hz to 600 kHz. This broad coverage, together with calibrated output and modulation, provides for complete RF and IF performance tests on virtually any type of HF, VHF, and UHF receivers.

Both solid state generators 8640A and B have an output level range of +19 to −145 dBm (2 V to 0.013 μV) which is calibrated, metered, and leveled to within ±0.5 dB across the full frequency range of the instrument.

The 8640A/B generators provide AM, FM, and pulse modulation for a wide range of receiver test applications. This modulation is calibrated and metered for direct readout under all operating conditions.

A reverse power protection option (Opt 003) is available to eliminate instrument damage due to accidental transmitter keying. This module protects against up to 50 watts of applied power and automatically resets upon removal of the excessive signal.

Spectrally pure output signals

Noise performance of the 8640 is state-of-the-art for a solid-state generator. The high-Q cavity oscillator has been optimized with use of a low-noise microwave transistor for spectally pure output signals.

At 20 kHz offsets from 230 to 450 MHz, SSB phase noise is >130 dB/P[ ]low the carrier level and rises to 122 dB/Hz at 550 MHz. This [ ]l-to-noise ratio increases by approximately 6 dB for each divi[ ]of the output frequency down to the broadband noise floor of better than 140 dB/Hz. This exceptional noise performance is also preserved during FM modulation and in the phase-locked mode of the 8640B.

Mechanical dial or built-in counter

There are two versions of the 8640 Signal Generators. One, the 8640A, has an easy-to-read slide rule dial with scales for each of the 10 output frequency ranges. There is an additional scale to provide direct readout of the output frequency even in the INTERNAL DOUBLER band, 512-1024 MHz.

The 8640B has the same performance features as the 8640A, but incorporates a built-in 550 MHz frequency counter and phase lock synchronizer.

The built-in 6 digit counter displays the output frequency and can also be used to count external input signals from 20 Hz to 550 MHz. This eliminates the need for a separate frequency counter in many measurement systems.

Internal pushbutton synchronizer

At the push of a button, the 8640B built-in phase lock synchronizer locks the RF output frequency to the crystal time base used in the counter. In this locked mode, the output stability is better than 5×10^{-8}/h and the spectral purity and FM capability of the unlocked mode are preserved. For higher stability, it is possible to lock to an externally applied 5 MHz standard. Two 8640B's can also be locked together for various 2-tone measurements.

In the phase locked mode, increased resolution is available by using the ½ digit increment button. For example, 500 Hz resolution is possible for frequencies between 100 and 1000 MHz.

FM while phase locked

When phase locked, full FM capability is preserved down to modulation rates of 50 Hz. The narrow bandwidth of the phase lock loop (<5 Hz) provides for FM modulation up to 250 kHz rates and assures no degradation in noise from the unlocked mode. This crystal stability, coupled with the precision modulation and low noise, makes the 8640B ideal for testing narrowband FM or crystal-controlled receivers.

M/AM Modulation Meter

MAY MAI 1 0 1978

TF 2304

$1215

- Automatic operation – no tuning or signal levelling required
- Carrier frequency range: 9 to 12·5 MHz and 18 to 1000 MHz
- FM deviation in eight ranges: 1·5 to 150 kHz f.s.d.
- AM depth in three ranges: 10, 30 and 100%
- Two sensitivity versions available
- High and low level indication
- Light and compact; a.c. supply or rechargeable battery operation
- High accuracy, low price
- Optional accessories for mobile radio testing

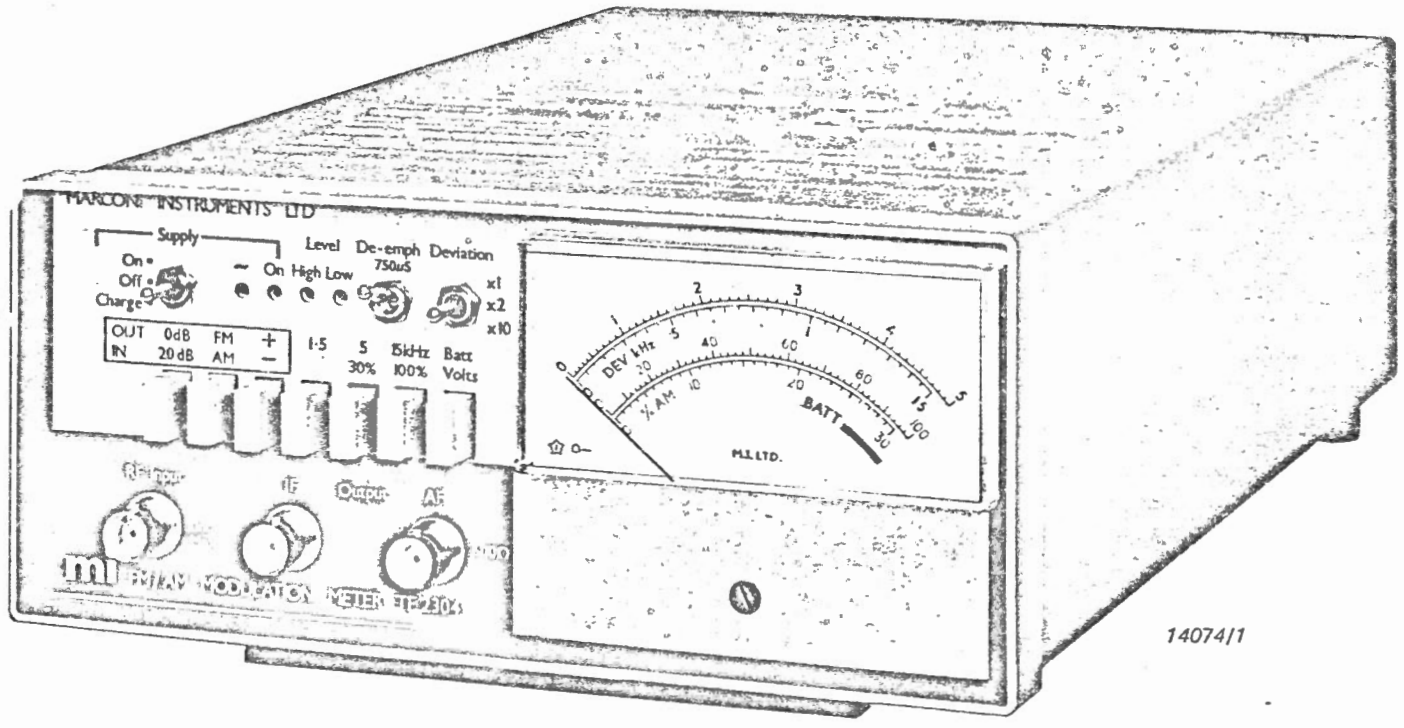

14074/1

FM/AM Modulation Meter TF 2304 combines high accuracy with automatic tuning and automatic level setting. It has been designed primarily for the servicing and production testing of radio communications systems, particularly mobile radio transmitters, and it covers carrier frequencies from 9 to 12·5 MHz and from 18 to 1000 MHz. FM deviation is measured in eight ranges from 1·5 kHz to 150 kHz full scale, and a.m. depth is measured in two ranges of 30% and 100% full scale, with a further uncalibrated range of 10%. Accuracy for both f.m. and a.m. measurements is ±3% of full scale.

An outstanding feature of this instrument is its ease and speed of use – leading to considerable time savings in production testing. To make a measurement it is only necessary to couple the r.f. signal to the input and select the measurement required, the meter will then tune automatically to the carrier frequency, set the signal level and display the f.m. deviation or a.m. depth on the panel meter. The whole measurement process takes only a few seconds.

Applications

This new modulation meter has been designed with

1.3 FEATURES.

1.4 Fully Portable. Operates up to one full year on a single 9-volt (transistor radio type) dry battery. A switch position is provided to measure the battery voltage. The instrument is extremely light, weighing only 1 pound and operates at full accuracy at any angle. A handy carrying case is available.

1.5 Easy to Operate. One switch selects off/on, battery test, and all functions and ranges. Input leads are never required to be moved for a special range, function, or polarity.

1.6 Digital Display. Liquid crystal readout provides large easy to read numbers and decimal placement as well as automatic polarity indication on DC volts and current measurements.

1.7 High Input Resistance. Ten megohms on all d.c.v. ranges and two megohms on all a.c.v. ranges insures higher measurement accuracy in high impedance circuits and minimizes affecting circuit

Table 1.1 - Danameter Specifications (continued)

DC	
Ranges:	2, 20, 200, 1000V
Resolution:	1 mV
Polarity:	Automatic
Accuracy:	2V ±(.25% Rdg + 1 Digit) for 1 year, ±5°C 20, 200, 1 KV ±(.35% Rdg + 1 Digit) for 1 year, ±5°C
Temperature Coefficient:	+0°C to +20°C and 30°C to 50°C ±(.025% Rdg + .05 Digit)/°C
Input Resistance:	10 Megohms, all ranges
NMR:	50 dB Min., at or near 60 Hz
Response Time:	1 second
Maximum Input:	1000 VDC or peak A.C., any range

AC	
Ranges:	2, 20, 200, 1000V
Resolution:	1 mV
Accuracy:	±(.5% Rdg + 2 Digits) for 1 year, ±5°C(f = 60 Hz to 400 Hz)
Bandwidth:	50 Hz to 2 kHz ±(1% Rdg + 2 Digits) for 1 year, ±5°C 45 Hz to 4 kHz ±(1.5% Rdg + 2 Digits) for 1 year, ±5°C (20, 200, 1 KV ranges)
Input Impedance:	2 Megohms in parallel with 50 pF
Response Time:	3 secs, Max.
Maximum Input:	250 VDC + 1 KV peak AC (700 VRMS), any range

OHMS	
Ranges:	2 KΩ, 20 KΩ, 200 KΩ, 20 MΩ
Resolution	1Ω
Accuracy:	20 KΩ, 200 KΩ ±(.5% Rdg + 1 Digit) for 1 year, ±5°C 2 KΩ ±(.5% Rdg + 2 Digits) for 1 year, ±5°C 20 MΩ ±(.75% Rdg + 1 Digit) for 1 year, ±5°C
Response Time	2 seconds
Current Through Unknown:	2 KΩ 100 μA 3.5 V Max. 20 KΩ 100 μA Open cir- 200 KΩ 10 μ cuit 20 MΩ 100 ηA Voltage
Maximum Input Voltage:	250 VDC or RMS AC, any range

CURRENT (DC)	
Ranges:	20 μA, 2 mA, 200 mA, 2A
Resolution:	10 nA
Accuracy:	±(.5% + 2 Digits) for 1 year, ±5°C
Voltage Burden:	.25V Maximum to 1/2 Amp
Response Time:	1 second
Maximum Input Current Voltage	 2 Amps RMS (fuse protected) 250 VDC or RMS AC (5 sec. Max. 20 μA range)

ELECTRONIC COUNTERS

Low cost counters for frequency measurements

Models 5381A, 5382A & 5383A

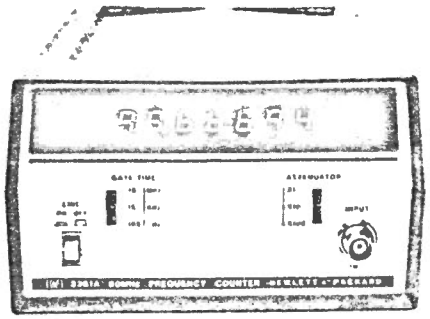

5381A

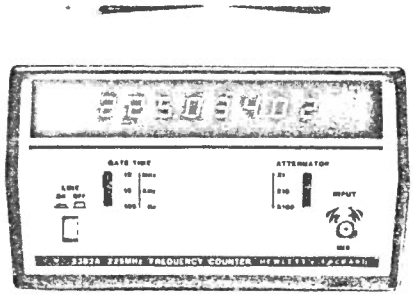

5382A

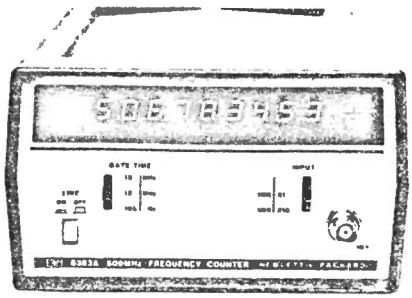

5383A

Description

General

The 5381A, 5382A and 5383A are a logical result of H-P's long standing leadership in frequency counter development. Leadership in quality, technology and efficient production procedures allows H-P to offer a price/performance combination in these three precision instrument unequalled in their product category. These counters are designed to deliver reliable, high quality operation in such diverse areas as: Production Line Testing, Service and Calibration (2-Way Radio and test equipment), Frequency Monitoring, Education and Training.

Resolution

The 5318A, 5382A and 5383A employ the direct counting technique and with 7, 8 and 9 digits respectively offer resolution of 10 Hz in 0.1 sec, 1 Hz in 1 sec and 0.1 Hz in 10 seconds.

Specifications

5381A

Frequency range: 10 Hz to 80 MHz.
Sensitivity: 25 mV rms—30 Hz to 20 MHz, 50 mV rms—10 Hz to 80 MHz.
Input impedance: 1 MΩ, <50 pF.
Input attenuation: X1, X10, X100.
Accuracy: ±1 count ± timebase error.
Resolution: direct count; 1 Hz in 1 second.
Gate times: 0.1 second, 1 second, 10 seconds.
Display: 7 LED Digits.
Rear panel input: sensitivity: TTL levels or 2.5 V rms.
Ratio: Rear Panel Input, 10 kHz to 2 MHz.
External frequency standard: Rear Panel Input, 1 MHz.
Timebase
Frequency: 1 MHz.
Aging: <0.3 ppm/month.
Temperature: ±10 ppm 0°C to 40°C.
Line voltage: ±1 ppm for 10% line change.

5382A

Frequency range: 10 Hz to 225 MHz.
Sensitivity: 25 mV rms–30 Hz to 10 MHz, 50 mV rms–10 Hz to 225 MHz.
Input impedance: 1 MΩ, <40 pF.
Input attenuation: X1, X10, X100.
Accuracy: ±1 count ± timebase error.
Resolution: direct count: 1 Hz in 1 second.
Gate time: 0.1 second, 1 second, 10 seconds.
Display: 8 LED Digits, nonsignificant zero blanking.
Rear panel input: sensitivity: 250 mV rms.
Ratio: Rear Panel Input, 100 kHz to 10 MHz.
External frequency standard: Rear Panel Input, 10 MHz.
Timebase
Frequency: 10 MHz.
Aging: <0.3 ppm/month.
Temperature: ±2.5 ppm 0°C to 40°C.
Line voltage: ±0.5 ppm for 10% line change.

5383A

Frequency range: 10 Hz to 520 MHz.
Sensitivity
1 MΩ: 25 mV rms—20 Hz to 10 MHz.
50 mV rms—10 Hz to 50 MHz.
50Ω: 25 mV rms—20 Hz to 520 MHz.
Input impedance: selectable: 1 MΩ, <40 pF or 50Ω.
Input attenuation: 1 MΩ × 1, × 10; 50Ω × 1—fuse protected.
Accuracy: ±1 count ± timebase error.
Resolution: direct count: 1 Hz in 1 second.
Gate time: 0.1 second, 1 second, 10 seconds.
Display: 9 LED Digits, nonsignificant zero blanking.
Display test: RESET function (activated with GATE TIME switch) illuminates all segments of all digits.
Rear panel input: sensitivity: 250 mV rms.
Ratio: Rear Panel Input, 100 kHz to 10 MHz.
External frequency standard: Rear Panel Input, 10 MHz.
Timebase output
Frequency: 10 MHz timebase.
Voltage: 200 mV p-p into 50Ω load.
Control: active with Rear Panel Internal/External switch in internal position.
Timebase
Frequency: 10 MHz.
Aging: <0.3 ppm/month.
Temperature: ±2.5 ppm 0°C to 40°C.
Line voltage: ±0.5 ppm for ±10% line change.

TCXO Option

Opt 001: (available for all models) Temperature Compensated Crystal Oscillator Timebase
Frequency: 10 MHz.
Aging: <0.1 ppm month.
Temperature: <1 ppm 0°C to 40°C.
Line voltage: ±0.1 ppm for ±10% line change.
Note: Timebase output available for both 5382A and 5383A with Option 001. Rear Panel Input not available.

5380 Family general data

Overflow: LED lamp indicator when most significant digit overflows.
Reset: manual selection of reset occurs when GATE TIME switch is between three normal positions.
Package: rugged, high strength metal case.
Operating temperature: 0°C to 40°C.
Power requirements: 100, 120, 220, 240, V rms (+5%, −10%) 48–440 Hz; 20 VA maximum.
Weight: net, 2.2 kg (4¾ lb). Shipping. 2.8 kg (6 lb).
Dimensions: 98 H × 160 W × 248 mm D (3½" × 6¼" × 9¾").

Ordering information

5381A Frequency Counter
5382A Frequency Counter
5383A Frequency Counter
Opt 001: TCXO (all models)

MARCONI INSTRUMENTS LIMITED

Automatic Distortion Meter TF 2337A

MAY MAI 10 1978

- Indicates distortion factor and signal level simultaneously
- Measures distortion down to 0·01% at signal level down to 100 mV
- Rapid measurement of SINAD ratios
- All push-button controls
- No level-calibration or filter-tuning adjustments
- Unaffected by signal frequency variation up to ± 5%

$1155

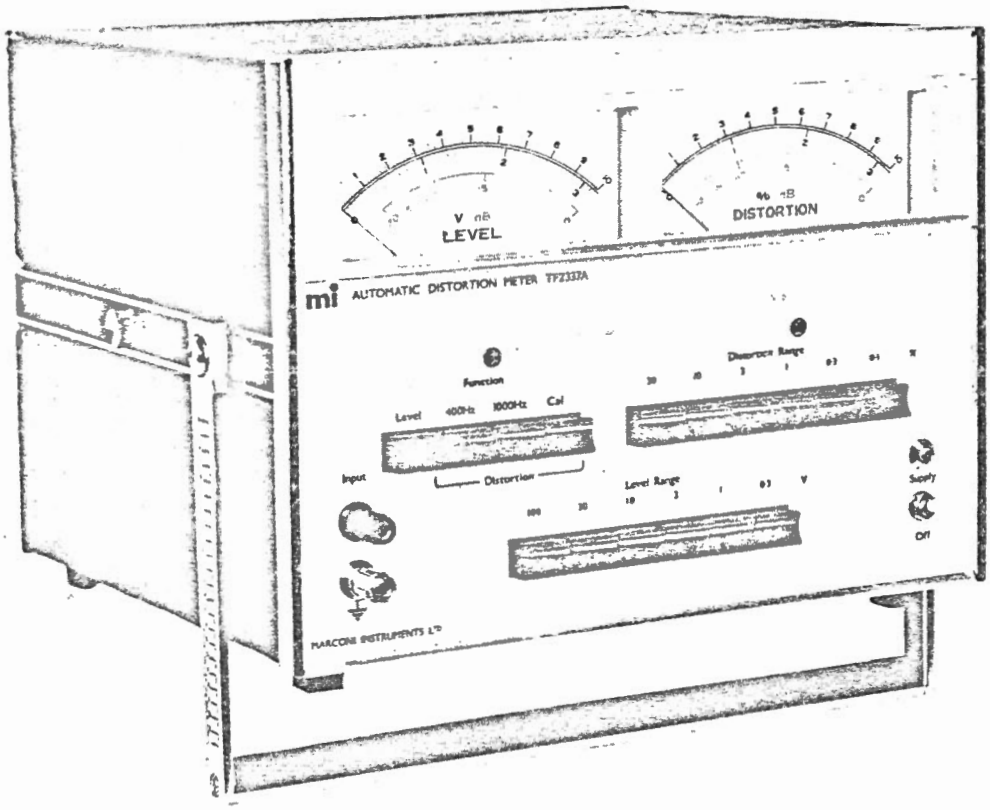

Automatic Distortion Meter TF 2337A enables extremely rapid measurements to be made of both level and distortion factor of audio frequency test signals. Its novel design eliminates the need for setting a reference level and for the usual precise tuning of a fundamental rejection filter. The only controls are push-button switches for selection of input voltage range, distortion range and fundamental frequency.

Once the appropriate ranges have been selected any number of similar distortion and level measurements can be made without further adjustment to the instrument. TF 2337A is thus highly suitable for repetitive measurements, as may occur in factory testing of a.f. amplifiers, oscillators, tape recorders etc.

Internal noise is very low owing to the use of field-effect transistors in the input stages, so that distortion down to 0.01% can be measured with an input signal of 100 mV.

The Measuring System

The instrument measures distortion factor in the conventional way; i.e. by filtering out the fundamental component and comparing the amplitude of the residue with that of the total signal.

A novel ratio circuit is used for making the measurement. The input signal, after impedance conversion and amplification, is split into two parallel paths. One path includes a fundamental rejection filter consisting of an active twin-T four stage element. After rejection of the fundamental, the harmonic and noise content are amplified and fed to an a.c. to d.c. converter. In the parallel path the complete signal, fundamental plus harmonic, is passed through an a.c. to d.c. converter and is then recombined with the filtered signal in a ratio circuit. The output of this circuit is related to the value of the harmonic content of the total signal and is displayed on the front-panel DISTORTION meter.

SIGNAL ANALYZERS

Distortion analyzers

Models 331A, 332A, 333A, 334A

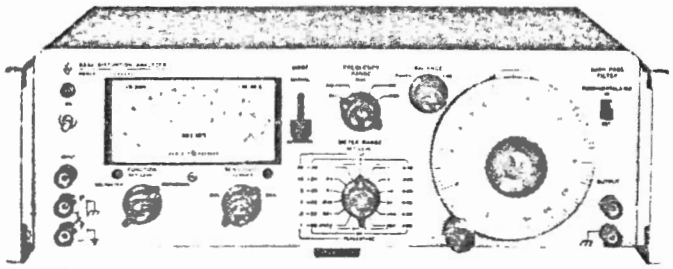

333A

Description

Hewlett-Packard's models 331A, 332A, 333A and 334A Distortion Analyzers measure total distortion down to 0.1% full scale at any frequency between 5 Hz to 600 kHz; harmonics are indicated up to 3 MHz. These instruments measure noise as low as 50 microvolts and measure voltages over a wide range of level and frequency. Refer to table below for available models and features.

Model No.	Auto Nulling	Hi-Pass Filter	Lo-Pass Filter	AM Detector
331A				
332A				X
332A Opt. H05			X	X
333A	X	X		
334A	X	X		X
334A Opt. H05	X		X	X

Option 001, for each model, features VU meter characteristics conforming to FCC requirements.

331A Specifications

Distortion measurement range: any fundamental frequency, 5 Hz to 600 kHz. Distortion levels of 0.1%–100% are measured full scale in 7 ranges.

Distortion measurement accuracy

Harmonic measurement accuracy (full scale)

Fundamental Input Less Than 30 V

Range	±3%	±6%	±12%
100%–0.3%	10 Hz–1 MHz	10 Hz–3 MHz	
0.1%	30 Hz–300 kHz	20 Hz–500 kHz	10 Hz–1.2 MHz

Fundamental Input Greater Than 30 V

Range	±3%	±6%	±12%
100%–0.3%	10 Hz–300 kHz	10 Hz–500 kHz	10 Hz–3 MHz
0.1%	30 Hz–300 kHz	20 Hz–500 kHz	10 Hz–1.2 MHz

Elimination characteristics: fundamental rejection >80 dB. Second harmonic accuracy for a fundamental of 5 to 20 Hz; better than +1 dB; 20 Hz to 20 kHz: better than ±0.6 dB; 20 kHz to 100 kHz: better than −1 dB; 100 kHz to 300 kHz: better than −2 dB; 300 kHz to 600 kHz: better than −3 dB.

Distortion introduced by instrument: >−70 dB (0.03%) from 5 Hz to 200 kHz. >−64 dB (0.06%) from 200 kHz to 600 kHz. Meter indication is proportional to average value of a sine wave.

Frequency calibration accuracy: better than ±5% from 5 Hz to 300 kHz. Better than ±10% from 300 to 600 kHz.

Input impedance: distortion mode; 1 MΩ ±5% shunted by <70 pF (10 MΩ shunted by <10 pF with HP 10001A 10:1 divider probe).

Voltmeter mode: 1MΩ ±5% shunted by <35 pF 1 to 300 V rms; 1 MΩ ±5% shunted by <70 pF, 300 μV to 0.3 V rms.

Input level for distortion measurements: 0.3 V rms for 100% set level or 0.245 V for 0 dB set level (up to 300 V may be attenuated to set level reference).

DC isolation: signal ground may be ±400 V dc from external chassis.

Voltmeter range: 300 μV to 300 V rms full scale (13 ranges) 10 dB per range.

Voltmeter accuracy: (using front panel input terminals)

Range	±2%	±5%
300 μV	30 Hz–300 kHz	20 Hz–500 kHz
1 mV–30 V	10 Hz–1 MHz	5 Hz–3 MHz
100 V–300 V	10 Hz–300 kHz	5 Hz–500 kHz

Noise measurements: voltmeter residual noise on the 300 μV range: <25 μV rms, when terminated in 600 (shielded) ohms, <30 μV rms terminated with a shielded 100 kΩ resistor.

Output: 0.1 ±0.01 V rms open circuit and 0.05 ±0.005 V rms into 2 kΩ for full scale meter deflection.

Output impedance: 2 kΩ.

Power supply: 115 or 230 V ±10%, 50 to 66 Hz, approximately 4 VA.

332A Specifications

Same as Model 331A except as indicated below:

AM detector: high impedance DC restoring peak detector with semi-conductor diode operates from 550 kHz to greater than 65 MHz. Broadband input, no tuning is required.

Maximum input: 40 V p-p AC or 40 V peak transient.

Distortion introduced by detector: carrier frequency: 550 kHz–1.6 MHz: <50 dB (0.3%) for 3–8 V rms carriers modulated 30%. 1.6 MHz–65 MHz: <40 dB (1%) for 3–8 V rms carriers modulated 30%. Note: Distortion introduced at carrier levels as low as 1 Volt is normally <40 dB (1%) 550 kHz to 65 MHz for carriers modulated 30%.

333A Specifications

Same as Model 331A except as indicated below:

Automatic nulling mode: set level: at least 0.2 V rms

Frequency ranges: X1, manual null tuned to less than 3% of set level; total frequency hold-in ±0.5% about true manual null. X10 through X10 k, manual null tuned to less than 10% of set level; total frequency hold-in ±1% about true manual null.

Automatic null accuracy: 5 Hz to 100 Hz: meter reading within 0 to +3 dB of manual null. 100 Hz to 600 kHz: meter reading within 0 to +1.5 dB of manual null.

High-pass filter: 3 dB point at 400 Hz with 18 dB per octave roll off. 60 Hz rejection 40 dB. Normally used with fundamental frequencies greater than 1 kHz.

Power supply: same as Model 331A.

334A Specifications

Same as Model 333A except includes AM Detector described under Model 332A:

General

Dimensions: 426 mm W × 126 mm H × 337 mm D (16.75" × 5" × 13.25").

Weight: net, 7.98 kg (17.75 lb). Shipping, 10.35 kg (23 lb).

Ordering instructions

Option 001, indicating meter has VU characteristics conforming to FCC requirements for AM/FM and TV broadcasting

H05-332A (meets FCC requirements)

H05-334A (meets FCC requirements)

331A Distortion Analyzer

332A Distortion Analyzer

333A Distortion Analyzer

334A Distortion Analyzer

OSCILLATORS & FUNCTION GENERATORS

0.0005 Hz to 5 MHz function generators

Model 3310A/B

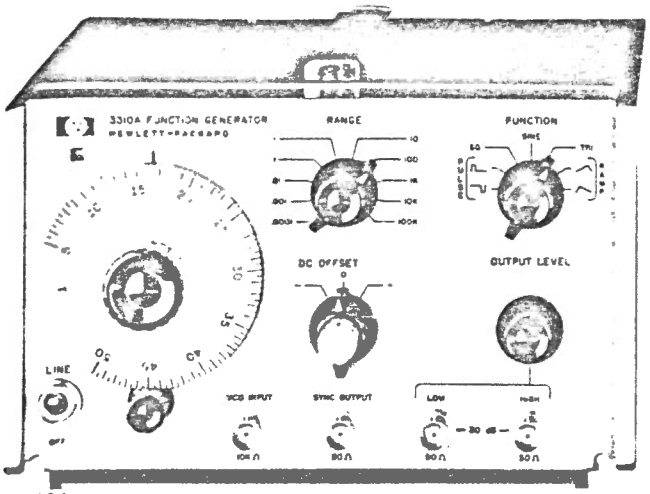

3310A

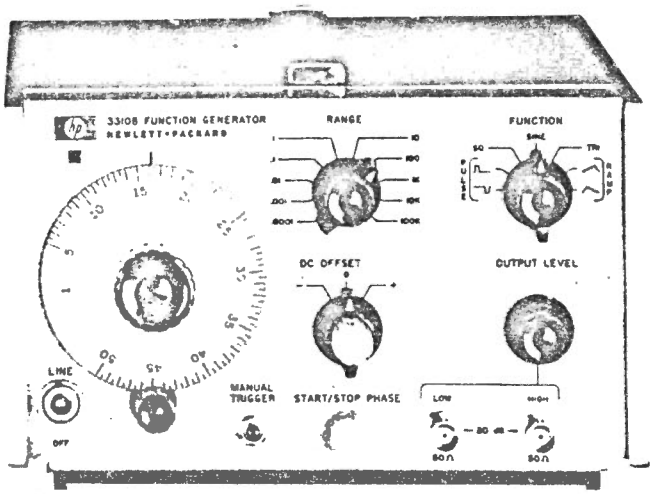

3310B

Description

The 3310A Function Generator is a compact voltage-controlled generator with 10 decades of range. Ramp and pulse functions are available in addition to sine, square and triangle. DC offset and external voltage control provide wide versatility. A fast rise time sync output is provided. Aspect ratio of nonsymmetrical function is 15%/85%.

The 3310B has all the features of the standard 3310A plus single and multiple cycle output capability.

3310A Specifications

Output waveforms: sinusoidal, square, triangle, positive pulse, negative pulse, positive ramp and negative ramp. Pulses and ramps have a fixed 15% or 85% duty cycle.

Frequency range: 0.0005 Hz to 5 MHz in 10 decade ranges.

Sine wave frequency response

0.0005 Hz to 50 kHz: ±1%; 50 kHz to 5 MHz: ±4%. Reference, 1 kHz at full amplitude into 50Ω.

Dial accuracy

0.0005 Hz to 500 kHz all functions: ±(1% of setting + 1% of full scale).

500 kHz to 5 MHz sine, square and triangle: ±(3% of setting + 3% of full scale).

500 kHz to 5 MHz pulse and ramps: ±(10% of setting + 1% of full scale).

Maximum output on high: >30 V p-p open circuit: >15 V p-p into 50Ω (except for pulses at frequency >2 MHz).

Pulse (frequency >2 MHz): >24 V p-p open circuit: >12 V p-p into 50Ω.

Minimum output on low: <30 mV p-p open circuit: <15 mV p-p into 50Ω.

Output level control: range >30 dB. High and low outputs overlap for a total range of >60 dB; low output is 30 dB down from high output.

Sine wave distortion

0.0005 Hz to 10 Hz; >40 dB (1%).

10 Hz to 50 kHz (on 1 k range): >46 dB (0.5%).

50 kHz to 500 kHz: >40 dB (1%).

500 kHz to 5 MHz: >30 dB (3%).

Square wave and pulse response: <30 ns rise and fall times at l output.

Iangle and ramp linearity: 0.0005 Hz to 50 kHz, <1%.

-mpedance: 50Ω.

Sync

Amplitude: >4 V p-p open circuit, >2 V p-p into 50Ω.

DC offset

Amplitude: ±10 V open circuit, ±5 V into 50Ω (adjustable).

Note: max V ac p + V dc offset is ±15 V open circuit, ±7.5 V into 50Ω.

External frequency control: 50:1 on any range.

Input requirement: with dial set to low end mark, a positive ramp of 0 to +10 V ±1 V will linearly increase frequency 50:1. With dial set at 50, a linear negative ramp of 0 to −10 V ±1 V will linearly decrease frequency 50:1. An ac voltage will FM the frequency about a dial setting within the limits ($1 < f < 50$) × range setting.

Linearity: ratio of output frequency to input voltage ($\Delta F/\Delta V$) will be linear within 0.5%.

Sensitivity: approximately 100 mV/minor division.

Input impedance: 10 kΩ.

General

Power: 115 V or 230 V ±10%, 48 Hz to 440 Hz, <20 VA max.

Dimensions: 114 mm H (without removable feet), 197 mm W, 203 mm D (4½" × 7¾" × 8").

Weight: net, 2.7 kg (6 lb); shipping, 4.5 kg (10 lb).

Accessories available

HP Part No. 5060-8540 filler strip for use with HP 1051A Combining Case or HP 5060-8762 Rack Adapter Frame.

3310B Specifications

Same as 3310A with the following additions:

Modes of operation: free run, single cycle, multiple cycle.

Frequency range: 0.0005 Hz to 50 kHz (usable to 5 MHz).

Single cycle:** ext trigger (ac coupled) requires a positive-going square wave or pulse from 1 V p-p to 10 V p-p. The triggering signal can be dc offset, but (V ac peak + V dc) ≤±10 V ext gate (dc coupled) will trigger a single cycle on any positive waveform ≥1 V but ≤10 V which has a period greater than the period of the 3310B output, and a duty cycle less than the period of the 3310B output. The gate signal cannot exceed 10 V.

Multiple cycle:** manual trigger will cause the 3310B to free run when depressed. When the trigger button is released, the waveform will stop on the same phase as it started. Ext gate will cause the 3310B to free run when the gate is held at between +1 and +10 V. When the gate signal goes to zero, the 3310B will stop on the same phase as it started.

Start-stop phase: the start-stop phase can be adjusted over a range of approximately ±90°.

Ordering information

3310A Function Generator

3310B Function Generator

**This specification applies on the X.0001 to X1 k range only.

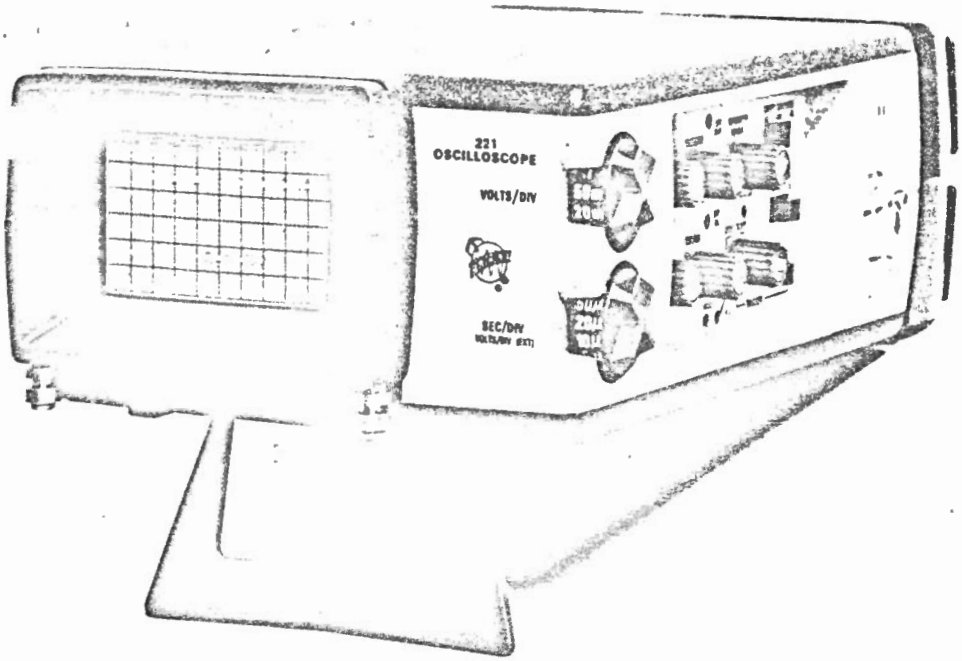

5-MHz, 5 mV/div to 100 V/div

Internal Battery Pack

Integral 1 MΩ probe

The 221 miniscope weighs just 3.5 pounds and easily fits into a tool box or brief case; it measures only 3 x 5¼ x 9½ inches. Yet it ... the capability needed for on-site service ... much of today's complex equipment. This versatile miniscope has a 5-MHz bandwidth, 5 mV/div sensitivity, and 0.1 μs/div sweep speed (using X10 magnifier) packaged in an impact-resistant case.

Internal rechargeable batteries allow at least three hours' operation away from external power sources. And the 221 will operate and charge from practically all the world's principal line voltages: 90 to 250 V, 48 to 62 Hz ac, or 80 to 250 V dc (all without making any change to the instrument).

The 1 MΩ low-capacitance probe minimizes circuit loading. And because it's attached, it's always there when you need it. Vertical deflection factors extend from 5 mV/div, allowing on-screen measurement of signals up to 600 V dc + peak ac. The 1 μs/div to 200 ms/div time base is enhanced by a X10 magnifier that extends the fastest range to 0.1 μs/div. A variable control will slow the sweep to about 0.5 s/div.

A single rotary control on the 221 is used for all trigger level and slope functions. Controls are side mounted and recessed for protection, yet are highly accessible.

In applications where it is necessary to "float" the oscilloscope to make your measurements, these can be elevated to 700 V + peak ac) above ground when operated from batteries. Although insulated, caution should be observed when connecting the probe to test points.

The 221 is used in a wide assortment of service applications. For example, in data transmission systems, the 221 is preferred for maintenance and testing of modems, because of its ability to see higher frequency noise. It can even help in building roads... by spot checking motors in a road grader's closed loop servo system that controls blade angle, depth of cut, and machine direction.

VERTICAL DEFLECTION

Bandwidth — Dc to 5 MHz (−3 dB point) at all calibrated deflection factors. Lower −3 dB point ac coupled is approx 2 Hz.

Deflection Factor — 5 mV/div to 100 V/div, accurate 3% from 0°C to +40°C and ±5% from −15°C to 0°C and +40°C to 55°C. Uncalibrated, continuously variable between steps to at least 300 V/div.

Input R and C — Approx 1 MΩ paralleled by approx 29 pF via attached signal acquisition probe.

Max Input Voltage — 600 V (dc + peak ac), 600 V p-p ac, 5 MHz or less.

HORIZONTAL DEFLECTION

Time Base — 1 μs/div to 200 ms/div, accurate ±3%.

Magnifier — Increases all sweep speeds X10 with a max sweep speed of 0.1 μs/div.

Variable Time Control — Extends minimum sweep rate to approx 0.5 s/div. Continuously variable between calibrated settings.

TRIGGER

Modes — Automatic or manual. Level and slope selected with a single control. Automatic operation minimizes trigger adjustment and provides a bright baseline with no input.

Trigger Sensitivity

Mode	To 1 MHz	At 5 MHz
Internal	0.5 div	1 div
External	0.5 V	1 V

X-Y OPERATION

Input — X-axis input is via the external trigger or the external horizontal input.

X-axis Deflection Factor — 1 V/div ±10%, dc to 500 kHz. Sensitivity is increased by a factor of 10 (0.1 V/div) using horizontal magnifier.

Max External Horizontal Input Voltage — 200 (dc + peak ac), 200 V (p-p ac) to 500 kHz, decreasing to 20 V p-p ac at 5 MHz.

Input Impedance — Approx 0.5 MΩ paralleled by approx 30 pF.

DISPLAY

Crt — 6 x 10 div (0.5 cm/div) display. P31 phosphor normally supplied; P7 optional without extra charge. 1 kV accelerating potential.

Graticule — Internal, black line, non-illuminated.

ENVIRONMENTAL CAPABILITIES

Ambient Temperature — Operating: (battery only), −15°C to +55°C. Charging or operating from ac line: 0°C to +40°C. Nonoperating: −40°C to +60°C.

Altitude — Operating: 25,000 ft, decrease max temperature by 1°C/1000 ft above 15,000 ft. Nonoperating: 50,000 ft.

Vibration — Operating and nonoperating: 15 minutes along each of the 3 major axes, .06 cm (0.025 in) p-p displacement (4 g's at 55 Hz) 10 to 55 to 10 Hz in one minute cycles. Held for 3 min at 55 Hz.

Humidity — 5 days at +50°C, 95% humidity.

Shock — Operating and nonoperating: 100 g's, ½ sine, 2 ms duration each direction along each major axis. Total of 12 shocks.

OTHER CHARACTERISTICS

Power Sources — Internal NiCd batteries provide at least 3 hours operation at max trace intensity for a charging and operating temperature between +20°C and +30°C. Internal charger charges the batteries when connected to an ac line with instrument turned on or off. Dc operation is automatically interrupted when battery voltage drops to approx 10 V to protect batteries against deep discharge. Full recharge requires approx 16 hours. Extended time charges will not damage the batteries. An expanded scale battery meter indicates full, low, and recharge. External power source, 90 to 250 V ac (48 to 62 Hz) or 80 to 250 V dc, 5 W or less.

Insulation Voltage — 500 V rms or 700 V (dc + peak ac) when operated from internal batteries, with the line cord stored and the plug protected. When operated from an external line, line voltage plus floating voltage not to exceed 250 V rms; or 1.4 x line + (dc + peak ac) not to exceed 350 V.

Dimensions	In	cm
Height	3.0	7.6
Width	5.2	13.3
Depth	9.0	22.8
Weights (approx)	**lb**	**kg**
Net (without accessories)	3.5	1.6
Shipping	≈8.0	≈3.6

INCLUDED ACCESSORIES

Viewing hood (016-0199-01), carrying case (016-0512-00), neck strap (346-0104-00), Two spare fuses (159-0080-00).

ORDERING INFORMATION

221 Oscilloscope, including batteries and probe

INSTRUMENT OPTION

Option 76, P7 Phosphor

OPTIONAL ACCESSORIES

Alligator Clip Kit — A pair of alligator clips that allow connecting the probe and ground lead to large (up to ⅜ in) conductors. Includes: red clip (015-0229-00); yellow clip (015-0230-00); 6-32 to probe adapter (103-0051-01).
Order 015-0231-00

Probe-tip to BNC Panel Connector Adapter
Order 013-0084-01

Probe-tip to BNC Cable Adapter
Order 103-0096-00

Power Cable Adapter Assembly — A short length of two-wire power cord. One end has a female NEC socket fitting the 200-Series power cords; the other end is left open so that the wires can be attached to a non-NEC male power plug. Plugs not supplied.
Order 161-0077-01

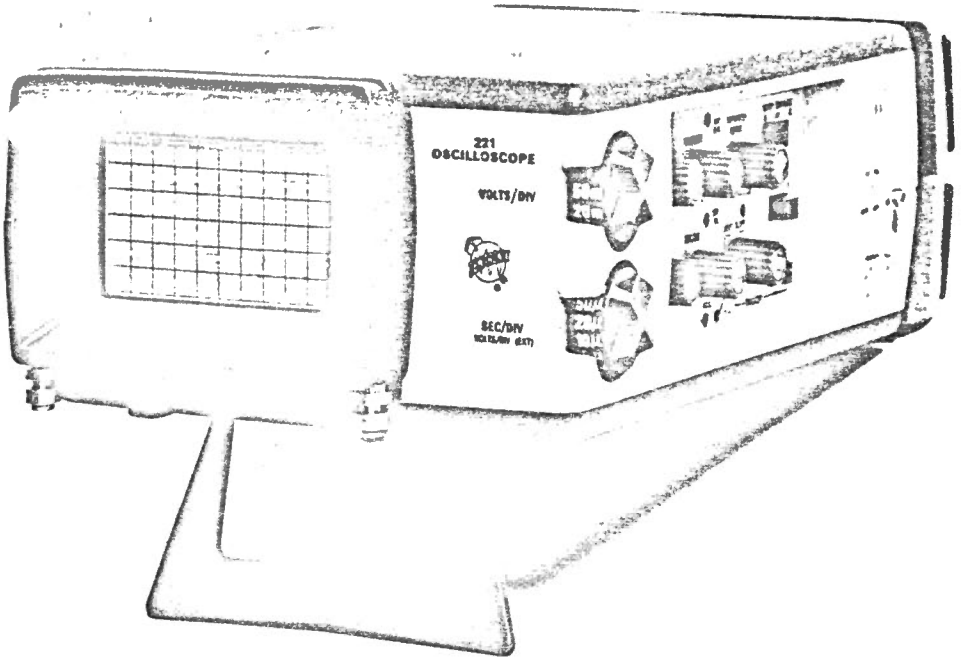

5-MHz, 5 mV/div to 100 V/div

Internal Battery Pack

Integral 1 MΩ probe

The 221 miniscope weighs just 3.5 pounds and easily fits into a tool box or brief case; it measures only 3 x 5¼ x 9½ inches. Yet it has the capability needed for on-site service of much of today's complex equipment. This versatile miniscope has a 5-MHz bandwidth, 5 mV/div sensitivity, and 0.1 μs/div sweep speed (using X10 magnifier) packaged in an impact-resistant case.

Internal rechargeable batteries allow at least three hours' operation away from external power sources. And the 221 will operate and charge from practically all the world's principal line voltages: 90 to 250 V, 48 to 62 Hz ac, or 80 to 250 V dc (all without making any change to the instrument).

The 1 MΩ low-capacitance probe minimizes circuit loading. And because it's attached, it's always there when you need it. Vertical deflection factors extend from 5 mV/div, allowing on-screen measurement of signals up to 600 V dc + peak ac. The 1 μs/div to 200 ms/div time base is enhanced by a X10 magnifier that extends the fastest range to 0.1 μs/div. A variable control will slow the sweep to about 0.5 s/div.

A single rotary control on the 221 is used for all trigger level and slope functions. Controls are side mounted and recessed for protection, yet are highly accessible.

In applications where it is necessary to "float" the oscilloscope to make your measurements, these can be elevated to 700 V + peak ac) above ground when operated from batteries. Although insulated, caution should be observed when connecting the probe to test points.

The 221 is used in a wide assortment of service applications. For example, in data transmission systems, the 221 is preferred for maintenance and testing of modems, because of its ability to see higher frequency noise. It can even help in building roads... by spot checking motors in a road grader's closed loop servo system that controls blade angle, depth of cut, and machine direction.

VERTICAL DEFLECTION

Bandwidth — Dc to 5 MHz (−3 dB point) at all calibrated deflection factors. Lower −3 dB point ac coupled is approx 2 Hz.

Deflection Factor — 5 mV/div to 100 V/div, accurate 3% from 0°C to +40°C and ±5% from −15°C to 0°C and +40°C to 55°C. Uncalibrated, continuously variable between steps to at least 300 V/div.

Input R and C — Approx 1 MΩ paralleled by approx 29 pF via attached signal acquisition probe.

Max Input Voltage — 600 V (dc + peak ac), 600 V p-p ac, 5 MHz or less.

HORIZONTAL DEFLECTION

Time Base — 1 μs/div to 200 ms/div, accurate ±3%.

Magnifier — Increases all sweep speeds X10 with a max sweep speed of 0.1 μs/div.

Variable Time Control — Extends minimum sweep rate to approx 0.5 s/div. Continuously variable between calibrated settings.

TRIGGER

Modes — Automatic or manual. Level and slope selected with a single control. Automatic operation minimizes trigger adjustment and provides a bright baseline with no input.

Trigger Sensitivity

Mode	To 1 MHz	At 5 MHz
Internal	0.5 div	1 div
External	0.5 V	1 V

X-Y OPERATION

Input — X-axis input is via the external trigger or the external horizontal input.

X-axis Deflection Factor — 1 V/div ±10%, dc to 500 kHz. Sensitivity is increased by a factor of 10 (0.1 V/div) using horizontal magnifier.

Max External Horizontal Input Voltage — 200 (dc + peak ac), 200 V (p-p ac) to 500 kHz, decreasing to 20 V p-p ac at 5 MHz.

Input Impedance — Approx 0.5 MΩ paralleled by approx 30 pF.

DISPLAY

Crt — 6 x 10 div (0.5 cm/div) display. P31 phosphor normally supplied; P7 optional without extra charge. 1 kV accelerating potential.

Graticule — Internal, black line, non-illuminated.

ENVIRONMENTAL CAPABILITIES

Ambient Temperature — Operating: (battery only), −15°C to +55°C. Charging or operating from ac line: 0°C to +40°C. Nonoperating: −40°C to +60°C.

Altitude — Operating: 25,000 ft, decrease max temperature by 1°C/1000 ft above 15,000 ft. Nonoperating: 50,000 ft.

Vibration — Operating and nonoperating: 15 minutes along each of the 3 major axes, .06 cm (0.025 in) p-p displacement (4 g's at 55 Hz) 10 to 55 to 10 Hz in one minute cycles. Held for 3 min at 55 Hz.

Humidity — 5 days at +50°C, 95% humidity.

Shock — Operating and nonoperating: 100 g's, ½ sine, 2 ms duration each direction along each major axis. Total of 12 shocks.

OTHER CHARACTERISTICS

Power Sources — Internal NiCd batteries provide at least 3 hours operation at max trace intensity for a charging and operating temperature between +20°C and +30°C. Internal charger charges the batteries when connected to an ac line with instrument turned on or off. Dc operation is automatically interrupted when battery voltage drops to approx 10 V to protect batteries against deep discharge. Full recharge requires approx 16 hours. Extended time charges will not damage the batteries. An expanded scale battery meter indicates full, low, and recharge. External power source, 90 to 250 V ac (48 to 62 Hz) or 80 to 250 V dc, 5 W or less.

Insulation Voltage — 500 V rms or 700 V (dc + peak ac) when operated from internal batteries, with the line cord stored and the plug protected. When operated from an external line, line voltage plus floating voltage not to exceed 250 V rms; or 1.4 x line + (dc + peak ac) not to exceed 350 V.

Dimensions	in	cm
Height	3.0	7.6
Width	5.2	13.3
Depth	9.0	22.8
Weights (approx)	**lb**	**kg**
Net (without accessories)	3.5	1.6
Shipping	≃8.0	≃3.6

INCLUDED ACCESSORIES

Viewing hood (016-0199-01), carrying case (016-0512-00), neck strap (346-0104-00), Two spare fuses (159-0080-00).

ORDERING INFORMATION

221 Oscilloscope, including batteries and probe

INSTRUMENT OPTION

Option 76, P7 Phosphor

OPTIONAL ACCESSORIES

Alligator Clip Kit — A pair of alligator clips that allow connecting the probe and ground lead to large (up to ⅜ in) conductors. Includes: red clip (015-0229-00); yellow clip (015-0230-00); 6-32 to probe adapter (103-0051-01).
Order 015-0231-00

Probe-tip to BNC Panel Connector Adapter
Order 013-0084-01

Probe-tip to BNC Cable Adapter
Order 103-0096-00

Power Cable Adapter Assembly — A short length of two-wire power cord. One end has a female NEC socket fitting the 200-Series power cords; the other end is left open so that the wires can be attached to a non-NEC male power plug. Plugs not supplied.
Order 161-0077-01

DIGITAL EQUIPMENT CORPORATION

OPTION BULLETIN

LOGIC PRODUCTS

APRIL 1975

DR11-M Two-word Output UNIBUS Interface

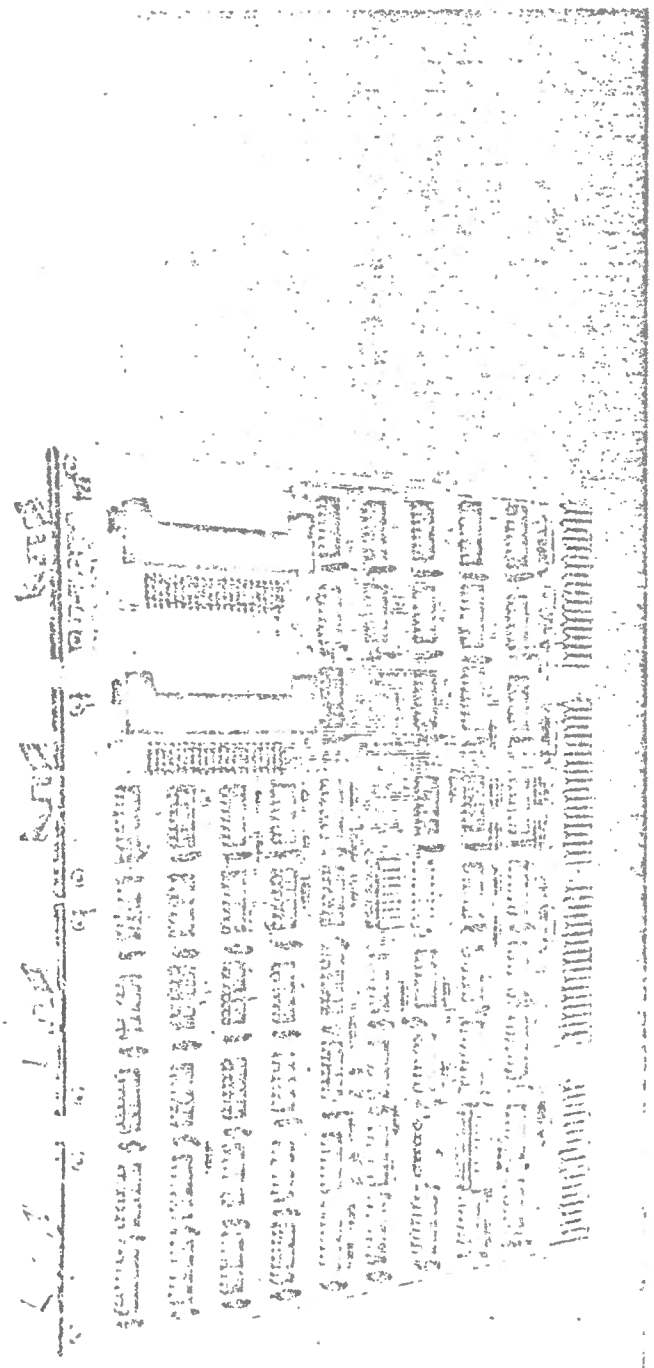

DESCRIPTION

The DR11-M is a complete, self-contained output interface used to transfer two independent 16-bit, parallel data words from the PDP-11 computer system to a user's peripheral device. It is directly compatible with the PDP-11 UNIBUS and is designed for installation into one of the available Small Peripheral Controller slots (SPCs) of a BB11-M, DD11-A, DD11-B System Interfacing Unit or into the PDP-11 processor unit.

The DR11-M consists of address selection logic, interrupt control and priority level select logic, two Data Buffer Registers (DBRs), one for each word, and two independent Control/Status Registers (CSRs).

Each register is word or byte addressable, and the register contents can be read back into the processor under program control, allowing the full range of PDP-11 instructions to be used. Two control and two status lines between the user's device and the interface permit the establishment of a handshake routine to efficiently control the transfer of data.

Data, status, and control signals from the interface to the user's device are supplied from open collector output drivers capable of sinking 32 mA of load current. Each output is connected to +5 V through a pull-up resistor. This feature allows a variety of user devices to be directly connected to the interface without the need of external line drivers and discrete components.

All address selection, interrupt priority selection, and vector address selection is performed using Dual In-line Package (DIP) switches mounted on the module. These switches facilitate the installation of the module by eliminating the need for priority plugs and soldering or removing jumper leads for address and priority selection.

The DR11-M is designed for user applications and requires a minimum of external hardware to implement into the PDP-11 system. Two 40-pin connectors are conveniently mounted near the edge of the board. These connectors permit either one or two external devices to be easily connected using BC08R or BC04Z flat cables available from DIGITAL. These cables have the mating connectors premounted and are supplied in any specified length.

The interface module occupies one SPC slot and is a quad-height, extended-length, single-width module.

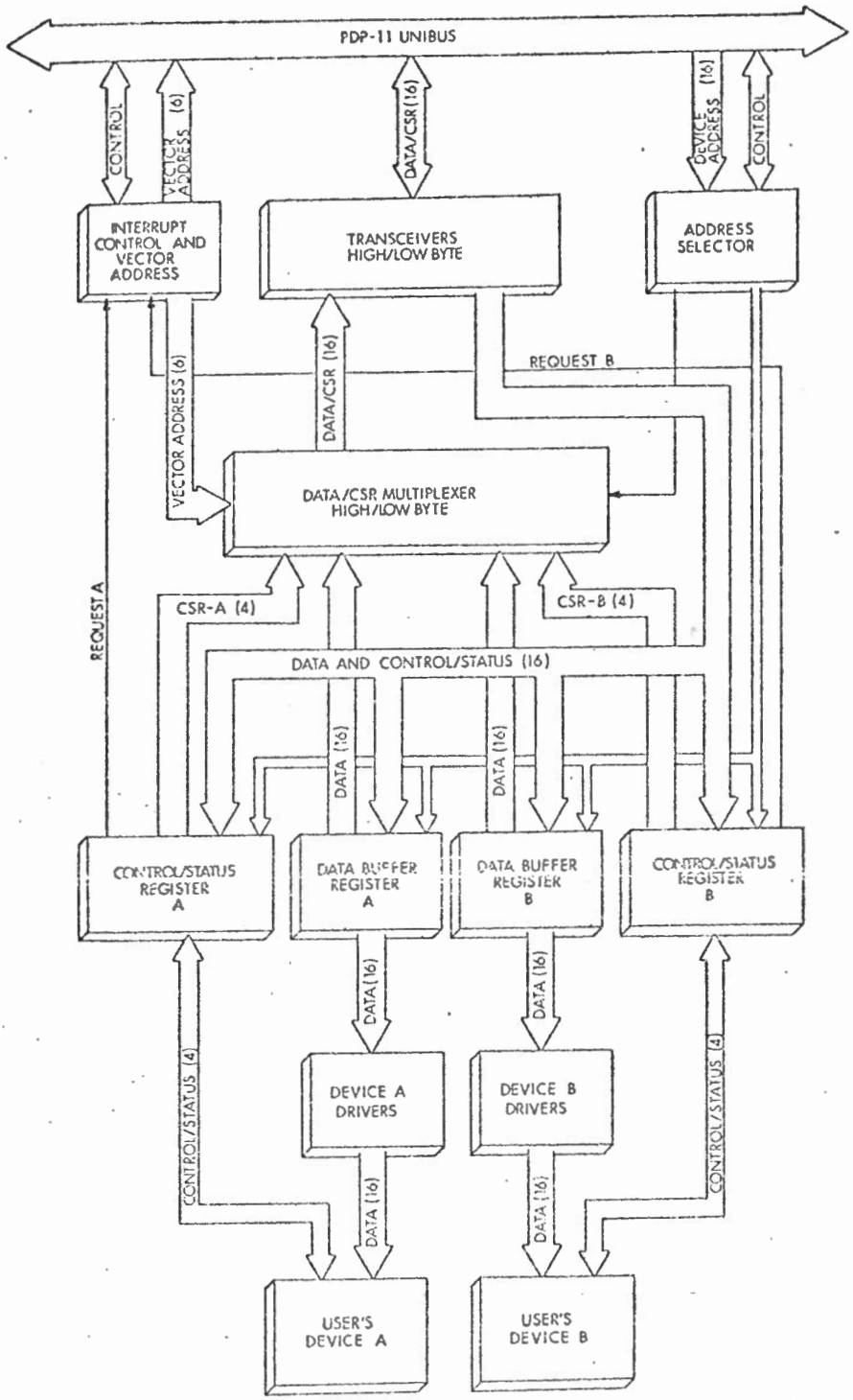

DR11-M Two-word Output UNIBUS Interface Module

FEATURES

- Self-contained interface for mounting in SPC slot of PDP-11 System Interfacing Unit.
- Dual 16-bit data word outputs.
- Dual interrupt logic contained on module.
- Output word or byte addressable storage register for each word.
- Switch-programmable device and vector address and priority level assignments.
- Two independent CSR registers with identical bit assignments.
- CSR contains vector address and interrupt priority in addition to normal status and control bits.
- Additional one-bit input and buffered one-bit output in each CSR that can be defined by user.
- Signal outputs to devices supplied from open collector line drivers.
- Handshake signals controlled by interrupts or under program control.
- Program-controlled Data Ready handshake signal.
- Presents only one unit load on UNIBUS.

SWITCH PROGRAMMABLE FUNCTIONS

The DR11-M module contains two DIP switch banks used to conveniently select the device address, the vector address, and the priority level of the interrupt requests.

Vector Address Switches—	The vector address of the interrupt routine pointer located in memory is selected by six of the DIP switches, allowing vectors of up to 774_8 to be specified.
Priority Level Switches—	Two switches are provided to select one of the four Bus Request priority levels (BR4 through BR7) of the UNIBUS.
Device Address Switches—	The address of the device is assigned with ten switches, allowing the module address to be located within the upper 4K address block dedicated to peripherals and user's devices.

DR11-M ELEMENTS AND SIGNAL FLOW

The main elements of the DR11-M interface module and the data, control, and status signal flow are shown on the diagram. The module provides the complete interface logic necessary to allow the efficient transfer of data from the UNIBUS to a user's device.

CONTROL/STATUS REGISTERS

Each CSR is a 16-bit register used to supply control and status information to the user's device and to provide control and status indicators of the user's device and interface to the processor. Each CSR is byte- or word- addressable.

DATA BUFFER REGISTERS

Each DBR is used to store 16 bits of data for transfer to the device. The DBR is a read/write register allowing the full range of PDP-11 instructions to be used.

DATA/CSR MULTIPLEXER

The multiplexer is controlled by the decoded device address and selects either 16 bits of data from a DBR or 16 bits of status and control information from a CSR for transfer to the UNIBUS. The selected output of the multiplexer is transferred to the processor under program control through the UNIBUS transceivers.

ADDRESS SELECTION LOGIC

The address selection logic decodes the addresses associated with each CSR and DBR and specifies the direction of data transfer.

INTERRUPT CONTROL LOGIC

The interrupt control logic requests bus mastership on one of the four bus request lines of the UNIBUS, produces the interrupt request, and specifies the vector addresses of the interrupt routine pointers located in memory.

INTERFACE SIGNALS

UNIBUS Signals-The input and output data, control, and status signals conform to the UNIBUS signal specifications outlined in the *PDP-11 Peripherals Handbook* published by Digital Equipment Corporation. The DR11-M module presents no more than one unit load on any UNIBUS signal line.

Device Signals-Four lines provide TTL-compatible signals between each CSR and the external device and can be used to establish a handshake routine for positive-control data transfers. Two lines can be used for status information to and from the processor, and two lines provide controlling information for data transfers. The 8-bit byte or 16-bit data word from the interface to the device is supplied by the 16 Data Out lines. The general function of the device interface signals is described as follows; however, the actual function can be determined by the user.

DATA ACCEPTED IN Signals	Input from the user's device indicating that data has been accepted. One line for each word.
DATA READY OUT Signals	Input to the user's device to specify that data is ready for transfer. One line for each word.
STATUS IN Signals	Additional input from the user's device to the CSR. One line for each word. Function can be defined by the user.
STATUS OUT Signals	Additional input to the user's device from the CSR. One line for each word. Function can be defined by the user.
DATA OUT Signals	Sixteen parallel lines to a user's device providing up to 30 V open collector breakdown and capable of sinking up to 32 mA of current from the load. Each output has a 750 ohm resistor to +5 V. Resistors can be removed to drive a higher current up to 40 mA.

GENERAL SPECIFICATIONS

Output Data Configuration	Two parallel 16-bit data lines to a device providing TTL-compatible levels.
UNIBUS Signals	Presents a maximum of one unit load on a UNIBUS line.
Operating Temperature	5°C (41°F) to 50°C (122°F)
Relative Humidity	10% to 90%, without condensation
Size	Quad height—10.5 in. (26.67 cm); single width—0.5 in. (1.27 cm); extended length—8.5 in. (21.59 cm)
Power	+5 V ±5% at 1.5 A nominal

DIGITAL EQUIPMENT CORPORATION

OPTION BULLETIN

LOGIC PRODUCTS

APRIL 1975

DR11-L Two-word Input UNIBUS Interface

1172

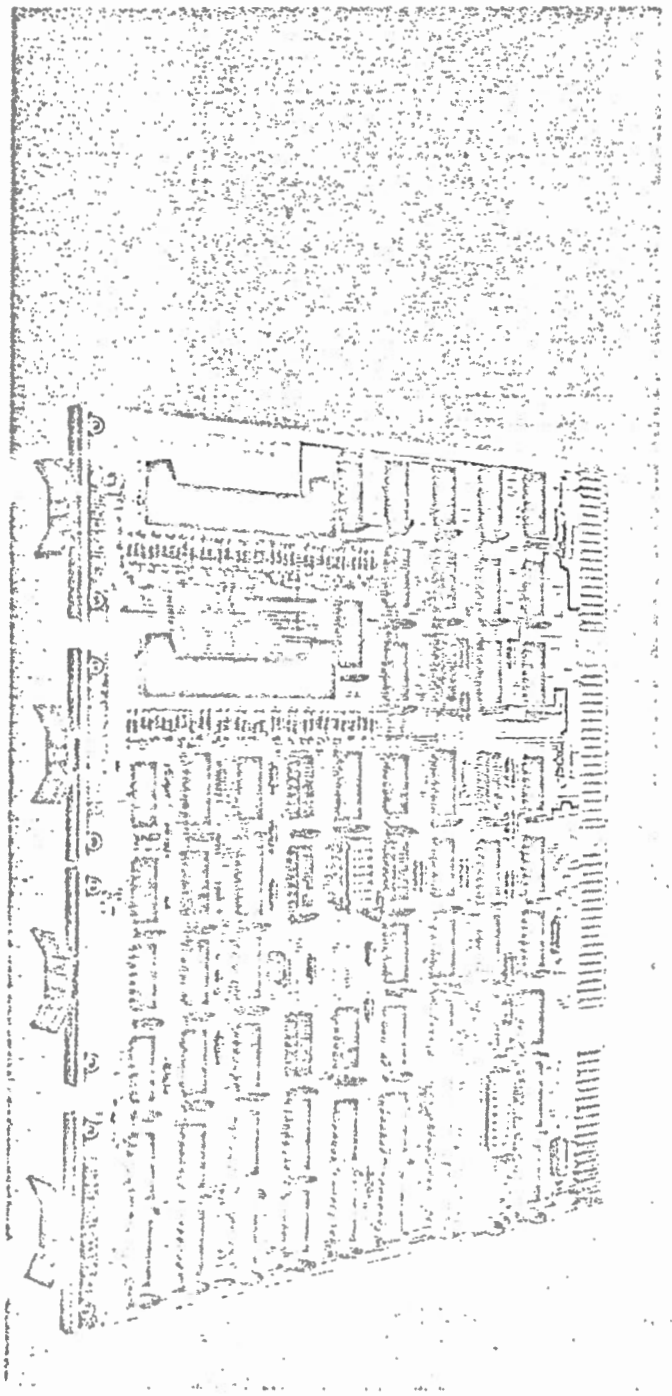

DESCRIPTION

The DR11-L is a complete, self-contained input interface used to transfer two independent 16-bit, parallel data words from a user's peripheral device to the PDP-11 computer system. It is directly compatible with the PDP-11 UNIBUS and is designed for installation into any one of the available Small Peripheral Controller slots (SPC) of a BB11-M, DD11-A, or DD11-B System Interfacing Unit and the PDP-11 processor unit.

The DR11-L consists of address selection logic, interrupt control and priority level select logic, two Data Buffer Registers (DBRs), one for each word, and two independent Control/Status Registers (CSRs). One CSR is assigned to each input data word and provides status and control information during a word transfer.

Two control and two status lines between the user's device and the interface module permit the establishment of a handshake routine to efficiently control the data transfers.

The input signal lines are TTL-compatible with high threshold receiver inputs and built-in hysteresis for both high and low threshold, providing substantial noise immunity. Input data lines are diode-clamped to +5 V and ground. Control lines from the user's device are diode-clamped to ground and pulled up to +5 V by a resistor.

All address selection, interrupt priority selection, and vector address selection is performed using Dual In-line Package (DIP) switches mounted on the module. These switches facilitate the installation of the module by eliminating the need for soldering or removing jumper leads for address and priority selection.

The DR11-L is designed for user applications and requires a minimum of external hardware to implement into the PDP-11 system. Two 40-pin connectors are conveniently mounted near the edge of the board. These connectors permit either one or two external devices to be easily connected using BC08R or BC04Z flat cables available from DIGITAL. These cables have the mating connectors premounted and are supplied in any specified length.

The interface module occupies one SPC slot and is a quad-height, extended-length, single-width module.

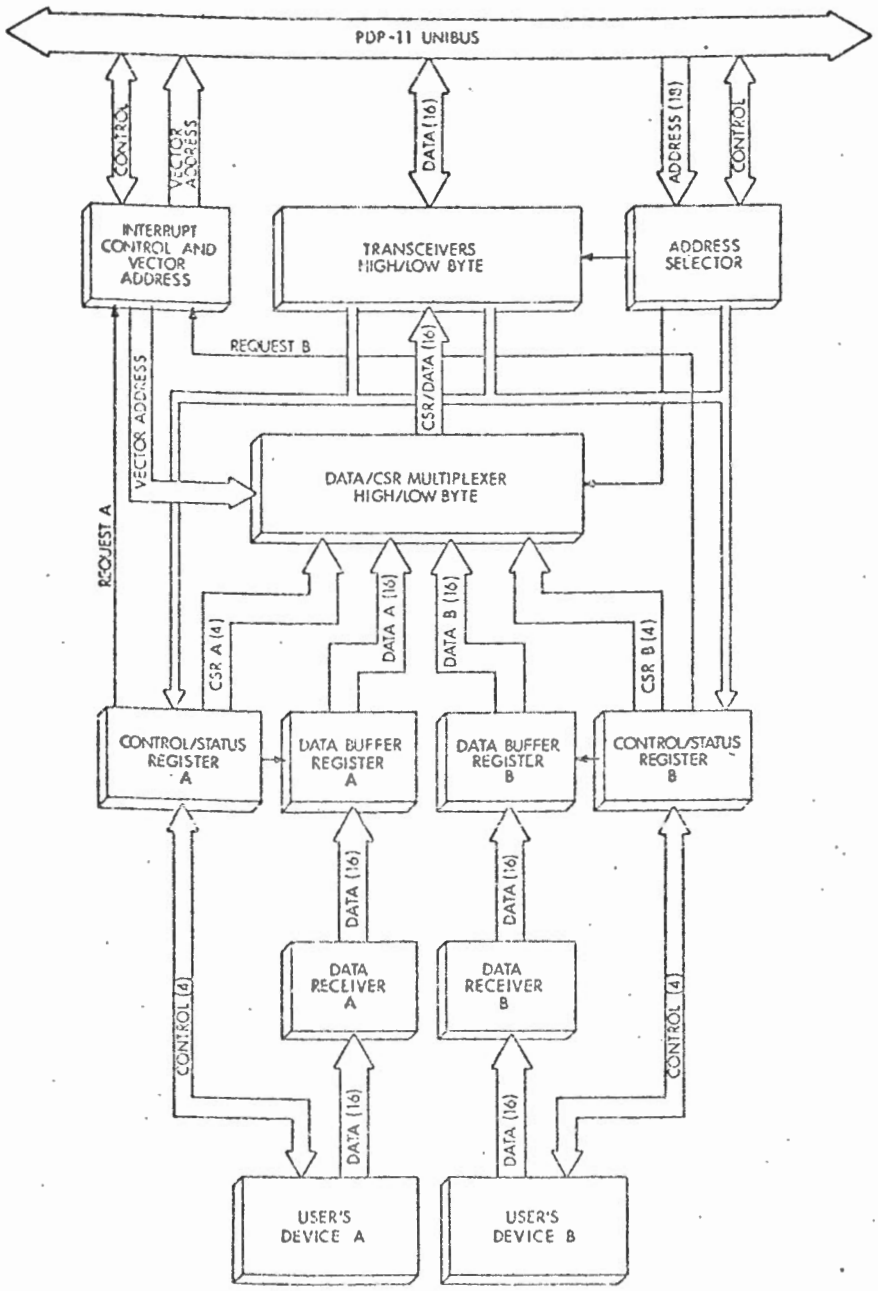

DR11-L Two-word Input UNIBUS Interface Module

FEATURES

- Self-contained interface for mounting in SPC slot of PDP-11 System Interfacing Unit.
- Dual 16-bit data word inputs.
- Dual interrupt logic contained on module. User-defined functions, such as module address, vector address, and interrupt priority, are configured by switches to eliminate soldered jumpers and priority plugs.
- Input data buffer for each word.
- Two independent CSR registers with identical bit assignments.
- CSR contains vector address and interrupt priority in addition to normal status and control bits.
- Additional one-bit input and buffered one-bit output in each CSR that can be defined by user.
- Handshake signals controlled by interrupts or under program control.
- Program-controlled Data Ready handshake signal.
- Presents only one unit load on UNIBUS.

SWITCH PROGRAMMABLE FUNCTIONS

The DR11-L module contains two DIP switch banks used to conveniently select the device address, the vector address, and the priority level of the interrupt requests.

ector Address—Switches	The vector address of the interrupt routine pointer located in memory is selected by six of the switches, allowing vectors up to 774_8 to be specified.
Priority Level—Switches	Two switches are provided to select one of the four Bus Request priority levels (BR4 through BR7) of the UNIBUS.
Device Address—Switches	The address of the device is assigned with ten switches, allowing the module address to be located within the upper 4K address block dedicated to peripherals and user's devices.

DR11-L ELEMENTS AND SIGNAL FLOW

The main elements of the DR11-L interface module and the data, control, and status signal flow are shown on the diagram. The module provides the complete interface logic necessary to allow the efficient transfer of data from the UNIBUS to a user's device.

CONTROL/STATUS REGISTERS

Each CSR is a 16-bit register used to supply control and status information to the user's device and to provide control and status indicators of the user's device and interface to the processor. Each CSR is byte- or word-addressable.

DATA BUFFER REGISTER

Each DBR is used to store 16 bits of data from a device. The contents of the DBR are transferred to the processor under program control as a 16-bit data word or 8-bit byte. When addressed by the processor or when an interrupt request is asserted, the device data is latched into the DBR. Input data is not required to be held by the device for the entire transfer operation, thereby permitting faster data transfers.

DATA/CSR MULTIPLEXER

The multiplexer is controlled by the decoded device address and selects either 16 bits of data from a DBR or 16 bits of status and control information from a CSR for transfer to the UNIBUS. The selected output of the multiplexer is transferred to the processor under program control through the UNIBUS transceivers.

ADDRESS SELECTION LOGIC

The address selection logic decodes the addresses associated with each CSR and DBR and specifies the direction of data transfer.

INTERRUPT CONTROL LOGIC

The interrupt control logic requests bus mastership on one of the four bus request lines of the UNIBUS, produces the interrupt request, and specifies the vector addresses of the interrupt routine pointers located in memory.

INTERFACE SIGNALS

UNIBUS Signals-The input and output data, control, and status signals conform to the UNIBUS signal specifications outlined in the *PDP-11 Peripherals Handbook* published by Digital Equipment Corporation. The DR11-L module presents no more than one unit load on any UNIBUS signal line.

Device Signals-Four lines provide TTL-compatible signals between each CSR and the external device and can be used to establish a handshake routine for positive-control data transfers. Two lines can be used for status information to and from the processor, and two lines provide controlling information for data transfers. The 8-bit byte or 16-bit data word from the device to the interface is supplied by the 16 Data In lines. The general function of the device interface signals is described as follows:

DATA READY IN Signals	From each user's device indicating that a data word or byte is ready for transfer. One line for each input word. Causes a computer interrupt if interrupt-enable CSR bit is set.
DATA ACCEPTED OUT Signals	From each CSR indicating that a data byte or word has been received by the DR11-L. One line for each input word.
STATUS IN Signals	Additional input from user's device to CSR. One line for each input word. Function can be defined by user.
STATUS OUT Signals	Additional output from the CSR. One line for each input word. Function can be defined by user.
DATA IN Signals	Sixteen data input lines from each user's device or 32 data lines from one device. Each line is diode-clamped to +5 V and ground at the DR11-L.

GENERAL SPECIFICATIONS

Input Data Configuration	Two parallel 16-bit data lines from a device.
UNIBUS Signals	Presents a maximum of one unit load on a UNIBUS line.
Operating Temperature	5°C (41°F) to 50°C (122°F)
Relative Humidity	10% to 90%, without condensation
Size	Quad height—10.5 in. (26.67 cm); single width—0.5 in. (1.27 cm); extended length—8.5 in. (21.59 cm)
Power	+5 V ±5% at 1.5 A nominal

DRS11 AND DSS11
AVAILABLE NOW!!

DRS11

- 48 DIGITAL OUTPUT POINTS
- PLUS 1 INTERRUPT INPUT POINT
- SIGNAL CONDITIONING OPTIONAL
- DSP11 SCREW TERMINAL PANEL OPTIONAL
- RSX-11M, RSX-11S, RT11 SOFTWARE SUPPORT
- PRICE $ 830
- FS BMC $ 20

DSS11

- 48 DIGITAL INPUT POINTS
- PLUS 1 INTERRUPT INPUT POINT
- SIGNAL CONDITIONING OPTIONAL
- DSP11 SCREW TERMINAL PANEL OPTIONAL
- RSX-11M, RSX-11S, RT11 SOFTWARE SUPPORT
- PRICE $ 990
- FS BMC $ 15

OFF THE SHELF DELIVERY

- RIGHT NOW -

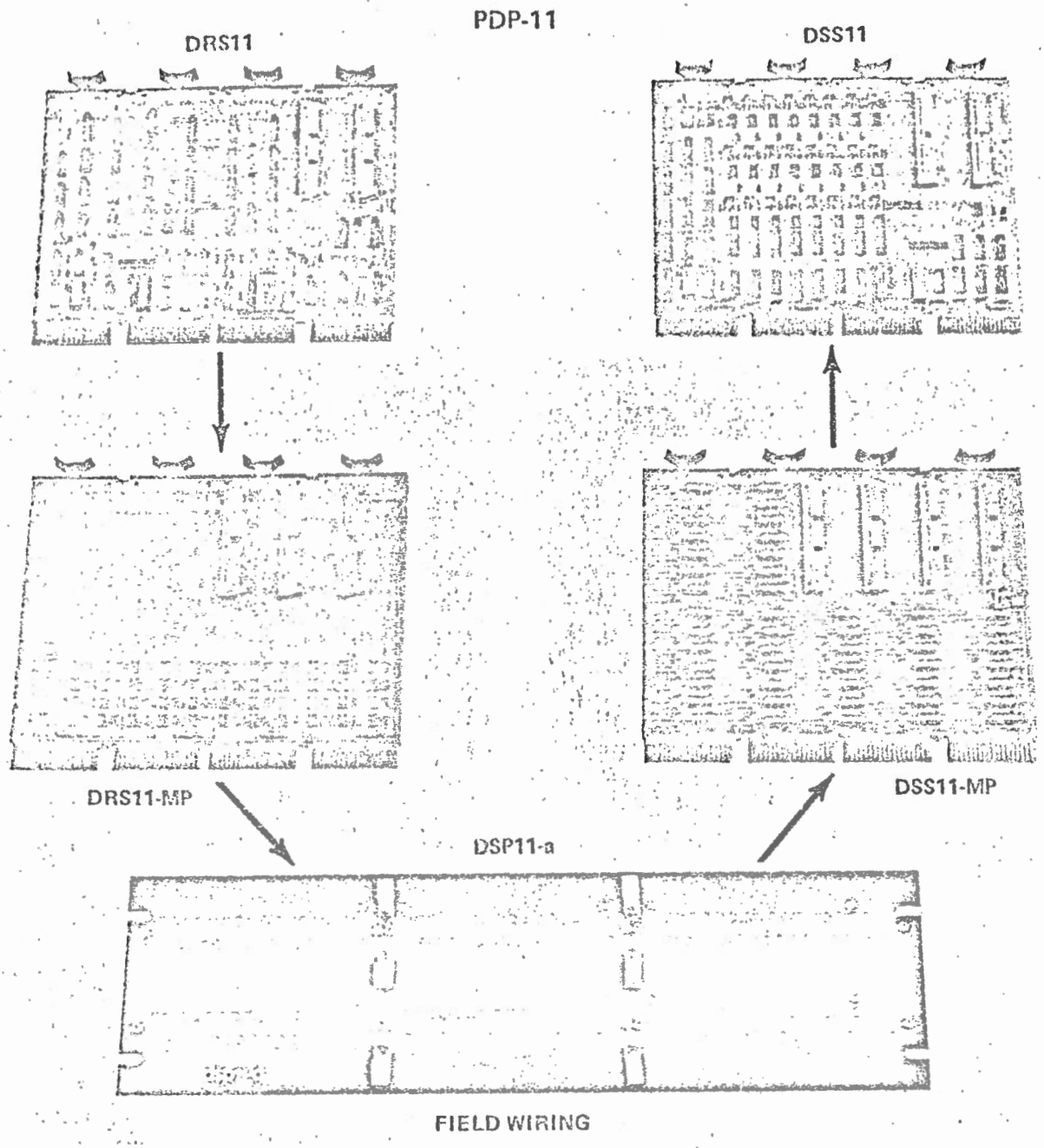

CE, MA, NE REGION

APPLICATION ENGINEER CONTACT LIST

CSS MAIN NUMBER (603) 889-8900

IPG/LDP/EPG	COMMERCIAL PL'S	OEM/COMP
Dan Bowser (X355)	Ram Chandran (X337)	Bob Brown (X244)
Frank Elia (X359)	Chuck Cobb (X456)	Brint Ferguson (X243)
Doug Forsberg (X354)	John Defilippo (X336)	Steve Laden (X245)
Louise Potter (X358)	Roy Hugenberger (X344)	
John Sutherland (X353)	Herb Mark (X345)	
	Joe Smyjunar (X343)	

DIGITAL EQUIPMENT CORPORATION

Computer Special Systems

OPTION BULLETIN
Section 4.3-15

JULY, 1977

DRS11 and DSS11 Digital Input and Output Options

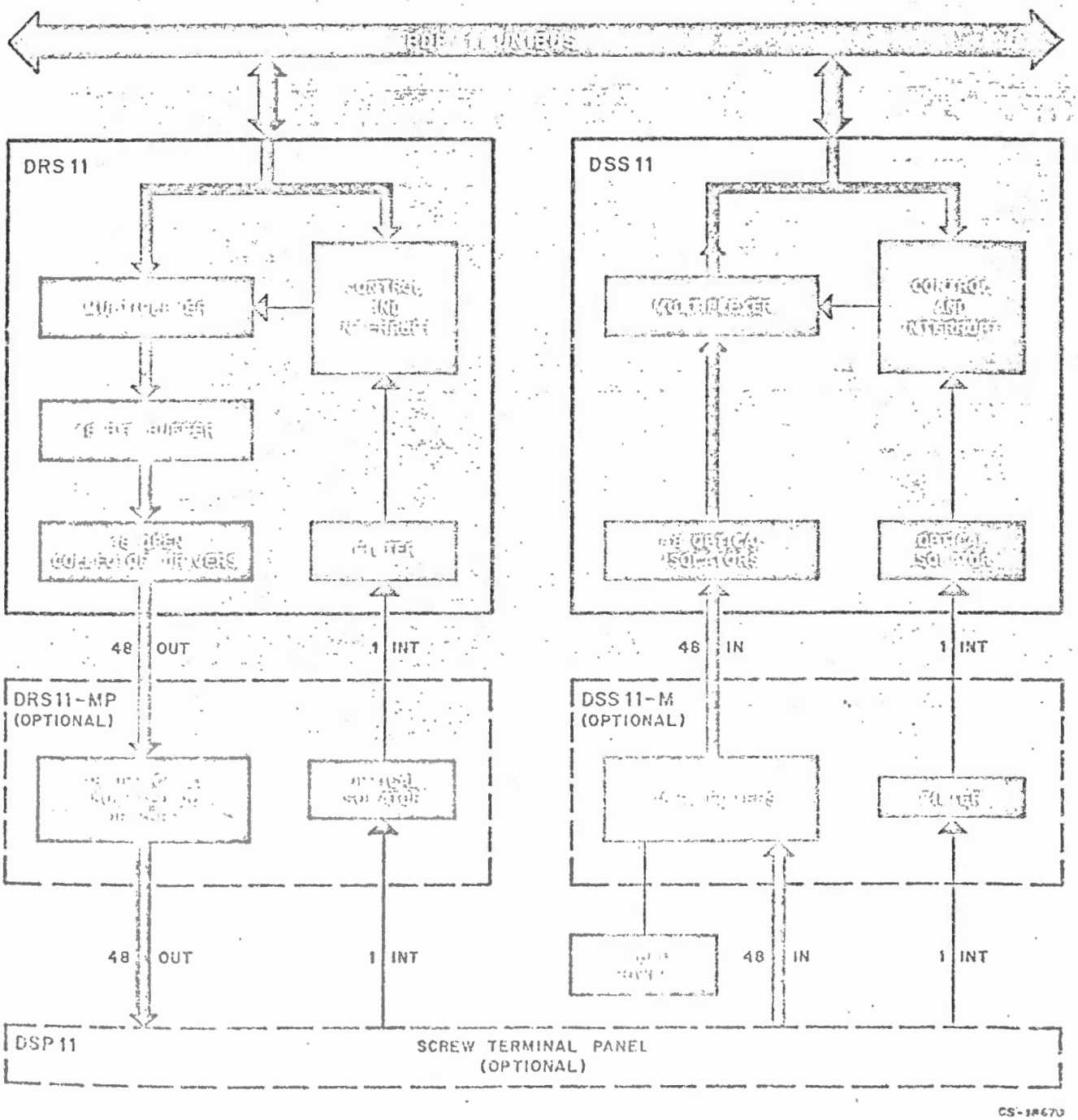

FEATURES

- 48 optically isolated inputs plus one interrupt (DSS11)
- 48 buffered outputs, TTL or open collector, plus one interrupt (DRS11)
- RC input filters (optional)
- Optically isolated output drivers (optional)
- Screw terminal panel (optional)

THE DRS11 AND DSS11

The DRS11 and DSS11 provide 48 digital inputs and outputs for the PDP-11 computer systems. The DRS11 and DSS11 options consist of two basic modules which are Small Peripheral Slot (SPC)-compatible. The output module (DRS11) provides the user with 48 buffered outputs plus one RC filtered interrupt input. The input module (DSS11) provides the user with 48 optically isolated inputs plus one optically isolated interrupt input.

In addition to the basic modules, optional signal conditioning I/O modules and screw terminal panels can be added to the basic modules to meet the requirements of small industrial data acquisition and control systems.

DRS11 DIGITAL OUTPUT MODULE

The DRS11 is an SPC-compatible module which provides 48 buffered outputs. The two basic module types include the DRS11-A with TTL-compatible outputs, and the DRS11-B with open collector drivers. Both the DRS11-A and DRS11-B include one RC filtered interrupt input. The outputs are organized in three 16-bit words, loaded by the computer system under control of the program. The DRS11 includes two 10-foot flat ribbon cables (50 conductors) terminated into 50 pin Berg connctors for connection to field output signals.

DSS11 DIGITAL INPUT MODULE

The DSS11 is an SPC-compatible module which provides 49 optically isolated inputs consisting of 48 non-buffered sense data inputs plus one interrupt input. The sense inputs are organized in three 16-bit words, and are read by the computer system under control of the program. The DSS11 includes two 10-foot flat ribbon cables (50 conductors) terminated into 50 pin Berg connectors for connection to field input signals.

SIGNAL CONDITIONING

When specific input filtering or output drivers are required, signal conditioning modules may be optionally added to the basic DRS11 and DSS11 modules. The standard options which are available are described below.

DRS11-MP OPTICALLY ISOLATED DC DRIVER

The DRS11-MP is an SPC-compatible module which mounts next to the DRS11-B basic module. It provides 48 optically isolated DC drivers and one optically isolated interrupt input.

DSS11-MP CONTACT SENSE INPUTS

The DSS11-MP is an SPC-compatible module which mounts next to the associated DSS11 basic module. The DSS11-MP provides RC-filtered 24 volt (user supplied) contact sense inputs for the basic DSS11. It provides over-voltage protection, and is prewired for use with externally supplied DC power.

DSS11-MR AND DSS11-MS VOLTAGE SENSE INPUTS

The DSS11-MR and DSS11-MS are SPC-compatible modules which mount next to the associated DSS11 basic module. The DSS11-MR provides 49 RC-filtered 24 volt inputs for voltage sensing applications. The DSS11-MS provides 49 RC-filtered 48 volt inputs for voltage sensing applications.

DSP11 SCREW TERMINAL PANEL

The DSP11 is an optional terminal panel providing 100 pair of screw connections for the DRS11 and DSS11 or the associated signal conditioning module. It provides for connection of 96 input or output signals plus two interrupt inputs and two field power inputs. DSP11 is a standard 5-1/4-inch by 19-inch rackmounted assembly.

CONFIGURATION GUIDELINES

Any mixture of DRS11 and/or DSS11 modules may be mounted in a PDP-11 system provided that the total does not exceed 16, and subject to the normal constraints of mounting space, bus loads, and 5-volt power.

SOFTWARE SUPPORT

The DRS11 and DSS11 are fully supported by Digital's Real-Time Operating Systems, RSX-11M, RSX-11S, and RT11. The support includes conventional Instrument Society of America (ISA) FORTRAN and calls for digital input and output operations. Also included is the capability to schedule Tasks (programs) for execution upon the occurrence of an interrupt from the DRS11 and/or the DSS11. This software support is compatible with the RSX11-M and RSX11-S support of the Industrial Control Subsystems (ICS and ICR), allowing the user to transport programs between systems with a minimal conversion effort.

DIGITAL INPUTS – DSS11

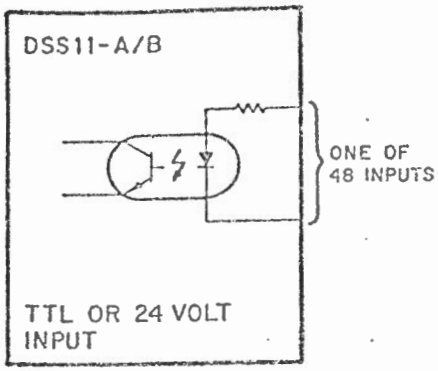

CS-18671

DIGITAL OUTPUTS – DRS11

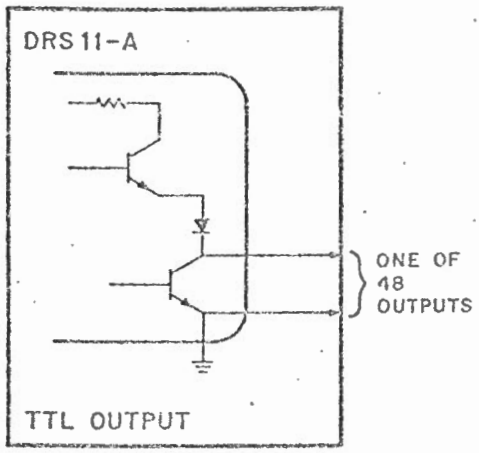

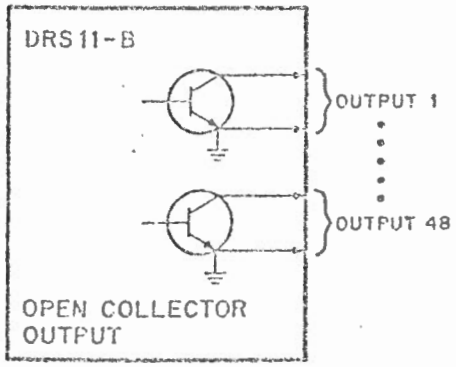

CS-18671

INPUT SIGNAL CONDITIONING – DSS11-M

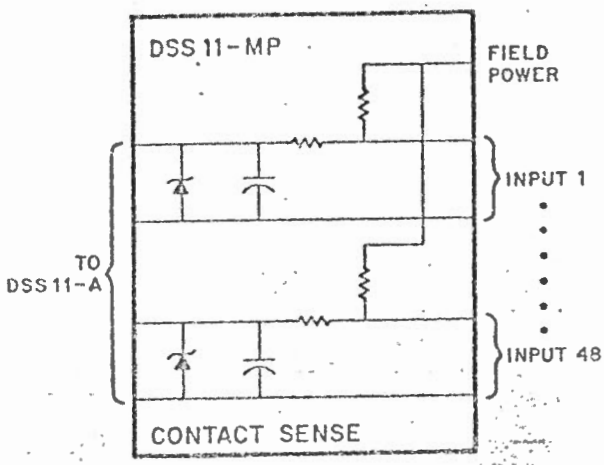

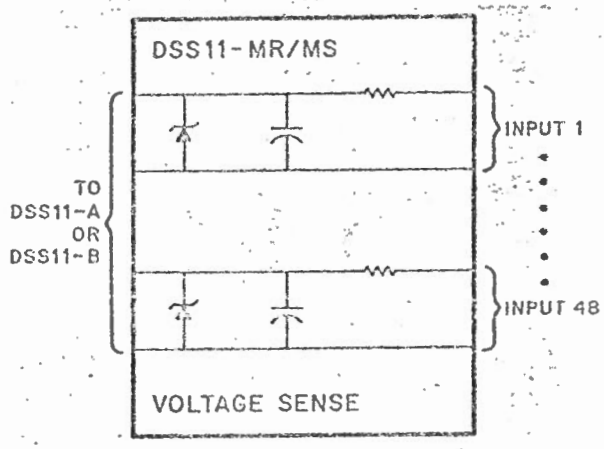

CS-18671

OUTPUT SIGNAL CONDITIONING – DRS11-MP

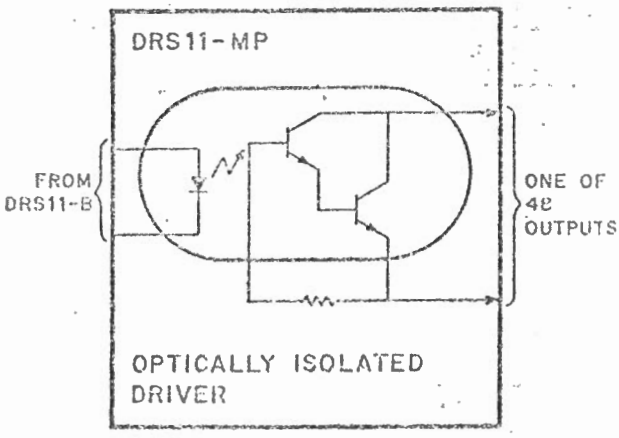

CS-18671

DIGITAL INPUTS – DSS11

DESCRIPTION	DSS11-A 48 Inputs (TTL) Plus One Interrupt	DSS11-B 48 Inputs (24 V) Plus One Interrupt
Input Voltage Range (on state)	4–7 Volts	24 Volts ±15%
Input Current	7–21 mA	16 mA Nominal
Isolation Voltage	500 Volts	500 Volts
Prerequisite	PDP-11	PDP-11
Mounting	1 SPC	1 SPC
Unibus Loads UNIBUS	1 LOAD	1 Load
Amps at +5	1.6 Amps	1.6 Amps

INPUT SIGNAL CONDITIONING – DSS11-M

DESCRIPTION	DSS11-MP RC-Filtered Contact Sense	DSS11-MR RC-Filtered Voltage Sense	DSS11-MS RC-Filtered Voltage Sense
Input Voltage Range (on state)	24 Volts ±15%	24 Volts ±15%	48 Volts ±10%
Input Current	User supplied	13 mA @ 24 V	13 mA @ 48 V
Contact Current	15 mA nominal	–	–
Prerequisite	DSS11-A	DSS11-A Plus Power Supply	DSS11-B
Mounting	1 SPC Next to DSS11-A	1 SPC Next to DSS11-A	1 SPC Next to DSS11-B
Unibus Loads UNIBUS	–	–	–
Amps at +5	–	–	–

DIGITAL OUTPUTS – DRS11

DESCRIPTION	DRS11-A 48 Outputs Plus One Interrupt	DRS11-B 48 Outputs Plus One Interrupt
Type Output	TTL Driver	Open Collector
Output Voltage		
Off State	TTL	30 Volts Maximum
On State	Compatible	.7 Volts @ 40 mA
Output Current	16 mA @ 0.4 Volts	40 mA @ 0.7 Volts
Prerequisite	PDP-11	PDP-11
Mounting	1 SPC	1 SPC
Unibus Loads UNIBUS	1 Load	1 Load
Amps at +5	2.5 Amps	2.5 Amps

OUTPUT SIGNAL CONDITIONING – DRS11-MP

DESCRIPTION	48 Optically Isolated DC Drivers Interrupt Input RC Filter
Type Output	Open Collector
Output Voltage	
Off State	50 Volts Maximum
On State	1 Volt Maximum at 75 mA
Output Current	75 mA at 1 Volt
Isolation Voltage	500 Volts Maximum
Prerequisite	DRS11-B
Mounting	1 SPC Next to DRS11
Unibus Loads UNIBUS	–
Amps at +5	1.5 Amps

PRINTED IN U.S.A.

DRS11-C

DIRECT MEMORY ACCESS INTERFACE

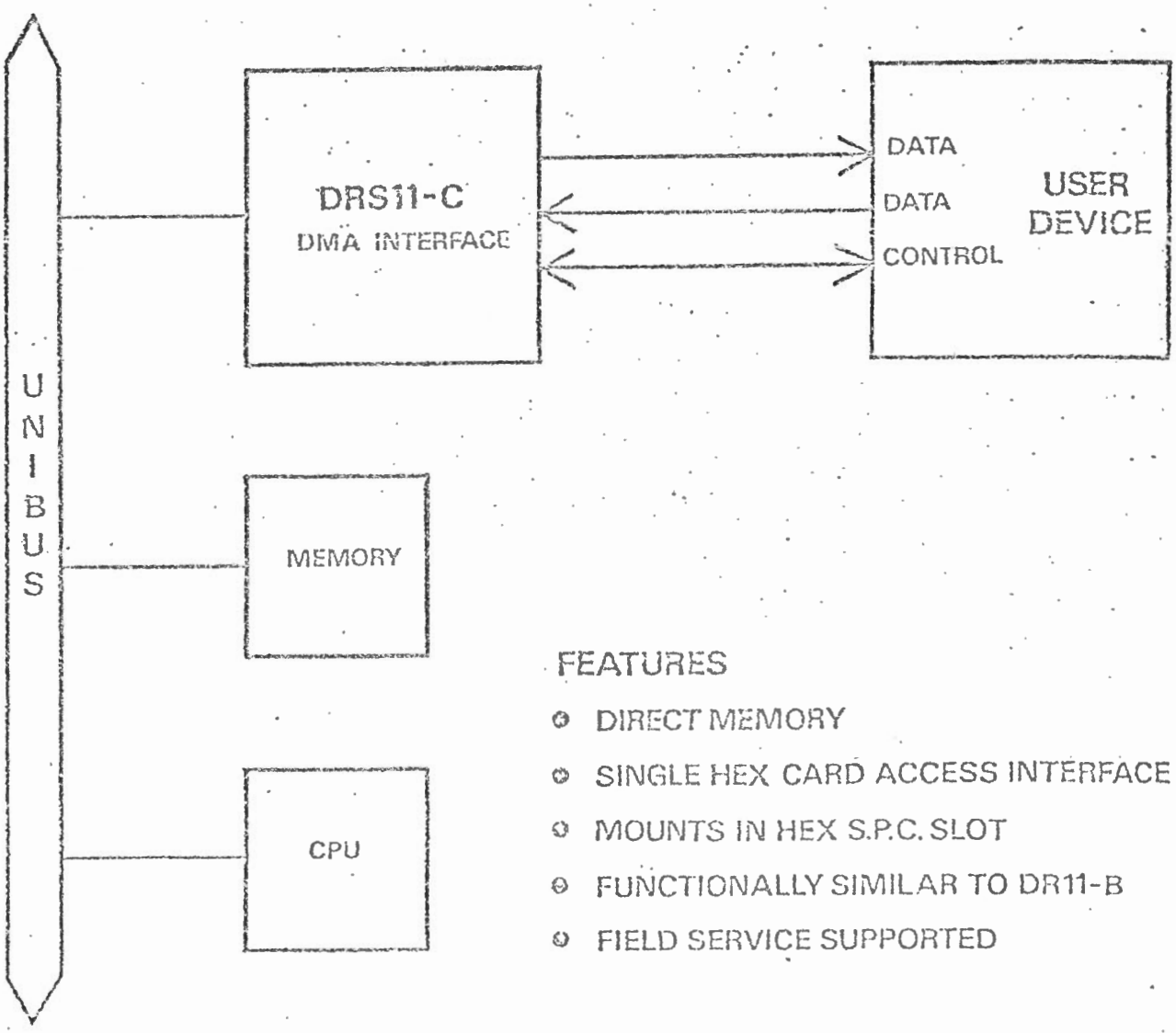

FEATURES

- DIRECT MEMORY
- SINGLE HEX CARD ACCESS INTERFACE
- MOUNTS IN HEX S.P.C. SLOT
- FUNCTIONALLY SIMILAR TO DR11-B
- FIELD SERVICE SUPPORTED

GENERAL DESCRIPTION

Operation

The DRS11-C is a general purpose, direct memory access interface to the PDP-11 Unibus. The DRS11-C operates directly to or from memory, moving data between the Unibus and the user device, rather than using program controlled data transfers.

The interface consists of four registers: command and status, word count, bus address and data. Operation is initialised under program control by:

(a) Loading word count with the 2's compliment of the number of transfers.

(b) Specifying the initial memory or bus address where the block transfer is to begin.

(c) Loading the command/status register with the appropriate function bits.

The user device recognises these function bits and responds by setting up the control inputs. If the user device requests data from memory or a UNIBUS device, the DRS11-C performs a UNIBUS data transfer (DATI) and loads its data register with the information held in the referenced bus address. The outputs of this register are available to the user device. This output data is buffered in a 16 bit flip flop register.

If the user device requests data to be written into memory, the DRS11-C interface performs a UNIBUS Data Transfer (DATO), moving data from the user device to the referenced bus address. This input data from the user is not register buffered and must be held as levels for the duration of the UNIBUS transfer. Transfers normally continue at a user defined rate until the specified number of words is transferred.

The user is given a number of control lines which provide flexible operation. Read-modify-restore in addition to normal word operations are possible.

SPECIFICATION

Mechanical

The DRS11-C is configured on one HEX Printed Circuit Board designed to fit in a Unibus S.P.C. slot.

User input/output signals are connected via two 40 way Berg sockets mounted on the top edge of the board.

Cable length is constrained by standard T.T.L. input/outputs, and the cable attenuation must be sufficiently low to enable transmission of a 100nSec positive pulse. A cable length of 3 feet and within the same box is recommended.

Electrical

Power Consumption	2·5 Amps at +5V from backplane supply.
Logic Voltage Levels	T.T.L. L,+0V; H, +3V.
Unibus Loading	1 unit load.
Priority Interrupt Levels	Selectable by priority plug.
User Input/ Output Signals	T.T.L. levels.

AVAILABILITY

The DRS11-C is a product of Digital's Computer Special Systems Group.

For further information please contact your local Digital Representative.

'All specifications are subject to change without notice.

OPERATIONAL DIFFERENCES BETWEEN DRS11-C AND DR11-B

DRS11-C	DR11-B
1. The interface is configured on one HEX board with edge connectors for a HEX S.P.C. slot. (Edge connector signals are all in columns C, D, E and F).	1. The interface is configured on a 4 slot wide systems Unit.
2. Interface priority is set by a priority plug which inserts into a I.C. type socket.	2. The priority is back-plane wired to level 5. Changing priority levels involves rewiring the back-plane.
3. User cables are fitted with 40 way Berg type plugs for connection to the interface.	3. User cables are connected (solder connection) to M957 cable connections.
4. Outputs from the interface to user are T.T.L. totem pole with a maximum fan out of 10 (ten) units (=10mA). Some signal fanouts are less than 10.	4. Outputs from the interface to user are 30mA open collector drivers.
5. The interface has one CYCLE REQUEST input from the user.	5. The interface has two CYCLE REQUEST inputs, which are logic ORed on the interface.
6. DMA transfers are initiated by the user signal CYCLE REQUEST after the program has set up the interface registers. There is no CYCLE bit as in the DR11-B for program initiation of DMA transfers.	6. In addition to normal initiation of DMA transfers by CYCLE REQUEST, the DR11-B has the extra facility to initiate transfers using the CYCLE bit in DRST.
7. The DRS11-C can perform DMA transfers across 32K core boundaries because extended bus address bits XBA17 and XBA16 increment as a modulo four counter when DRBA overflows as a 16 bit register. As a consequence, there is no error condition when DRBA overflows.	7. The DR11-B cannot perform transfers across 32K core boundaries. When DRBA overflows, an error interrupt occurs and further DMA transfers are inhibited.
8. The DRS11-C cannot perform a DATOB (user to Unibus device byte) transfer. However, C0 is still under user control to enable read-modify-restore transfers. DRS11-C is intended for DMA word transfer operations.	8. The DR11-B can be used for DATOB byte transfers.
9. When the DRS11-C becomes Unibus Master, the assertion and dissertion times are precisely controlled by a delay line. This allows an accurate definition of speed.	9. The DR11-B bus master logic has logic times determined by R, C networks allowing for a 25 per cent error margin. No speed specifications are quoted.
10. In the DRST, when maintenance bit is set, FNCT 1 toggles as a modulo 2 counter on alternate NPR cycles.	10. When maintenance is set, Function bits 1, 2 and 3 act as a modulo 8 counter, clocking after each NPR cycle.
11. After the last NPR cycle and subsequent interrupt, DRBA shows the address of the last DMA transfer plus four.	11. After the last NPR cycle and subsequent interrupt, DRBA shows the address of the last DMA transfer plus two.

PROGRAMMING THE DRS11-C

Register Addresses and Interrupt Vector

The DRS11-C interface consists of four registers: ommand and status word, bus address, word count and data.

These registers are assigned the following bus addresses.

WORD COUNT REGISTER (DRWC)	77XXX0
BUS ADDRESS REGISTER (DRBA)	77XXX2
STATUS REGISTER (DRST)	77XXX4
DATA BUFFER REGISTER (DRDB)	77XXX6

Note address bits 12 to 3 are selectable by wire links on the DRS11-C module allowing the device addresses to be selected within the normal peripheral address space.

The status register has an interrupt vector address YYY also selected by wire links on the module for bits 8 to 2.

Word Count Register (DRWC)

DRWC is a 16 bit read/write register. It is initially loaded with the 2's complement of the number of transfers to be made and increments up towards all 1's after each bus cycle. Incrementation can be inhibited by the user device; (refer to WC INC ENB user signal). When overflow occurs (all 1's to all 0's), the READY bit of DRST is set and the bus cycle stops. DRWC is cleared by the initialise pulse INIT.

Note:
DRWC is a word register; do not use byte instructions when loading; if this is done, the byte not referenced is loaded with the same data pattern as the referenced byte.

Data Buffer Register (DRDB)

The DRDB serves two distinct functions:

(a) A 16 bit write only register. The outputs of this register are available to the user device. The register, which can be loaded under program control, is also used to buffer information when data is being transferred from the UNIBUS to the user device (when the DRS11-C Interface does a DATI cycle).

(b) A 16 bit read only register. Information to be read is provided by the user device on the DATA IN signal lines. These lines are not buffered and must be held until either read under program or transferred directly to memory (DATO Bus Cycle).

DRDB output buffer is cleared by the initialise pulse.

Bus Address Register (DRBA)

The DRBA is a 16 bit read/write register. However, bit zero is permanently held to a zero, thus restricting the operation of the DRS11-C interface into word operation only. Along with XBA 16 and 17 in DRST, DRBA is used to specify BUS A 17; 01. The register is normally incremented (+2) after each bus cycle, advancing the address to the next sequential word location on the bus. If DRBA (corresponding to A 15; 01) overflows, XBA 16 and 17, acting as a modulo four counter will be incremented. This allows DMA transfers across 32K boundaries.
Incrementation of DRBA can be inhibited by the user device; refer to BA INC ENB user signal. DRBA is cleared by INIT.

Status Register (DRST)

DRST is used to give commands to the user device and to provide status indicators of the DMA Interface Control and the user device (refer to Table 1).

BIT	NAME	FUNCTION
15	Error	Set to indicate an error condition: either NEX (BIT 14), ATTN (BIT 13). Sets READY (BIT 7) and causes interrupt if IE (BIT 6) is set. ERROR is cleared by removing all possible error conditions: NEX is cleared by loading bit 14 with a zero; ATTN is cleared by user device. Read only.
14	Non-existent Memory (NEX)	Set to indicate that as Unibus master, the DRS 11-C did not receive a SSYN response 20 usec after asserting MSYN. Cleared by INIT or loading with a 0; cannot be loaded with a 1. Sets ERROR. Read Only.
13	Attention (ATTN)	Attention bit that reads the state of the ATTN user signal. Sets ERROR. (Used for device initiated interrupt). Set and cleared by user control only. Read Only.
12	Maintenance	Set for maintenance programs only when the interface is disconnected from the user device. When set, FNCT1 is forced to toggle on alternate bus cycles. Set and cleared by program. Read/Write.
11-9	Device Status (DSTST A. B. C)	Device Status bits that read the state of the DSTST A, B and C user signals. (Not tied to interrupt). Set and cleared by user control only. Read only.
8	NOT USED	
7	Ready	Set on word count overflow to indicate that the DRS11-C is able to accept a new command. Causes interrupt if bit 6 is set. Forces the device to release control of the Unibus and prevents further DMA cycles. Read Only.
6	Interrupt Enable (IE)	Set to allow ERROR or READY=1 to cause an interrupt. Cleared by INIT. Read/Write.
5-4	Extended Bus Address	Extended bus address bits 17 and 16 that in conjunction with DRBA specify A (17:00) in direct memory transfers. Cleared by INIT. XBA17 and 16 are incremented when DRBA overflows.
3-1	Function 3, 2, 1	Three bits made available to the user device. User defined. Cleared by INIT. Read/Write.
0	Go	Set to cause a pulse to be sent to the user device indicating a command has been issued. Clears READY. Always reads as a zero. Write only.

INPUT/OUTPUT SIGNALS

Tables 1a and 1b list signals available to the user device. For input signals loading refers to the number of T.T.L. unit loads the input signal must drive; for output signals loading refers to number of T.T.L. loads in the user device that the signal can drive.

User input and output signals are connected to p.c. board via two BERG sockets designated J1 and J2. Table 2 shows signals and associated pin connections.

NOTE: Unassigned connections must be left open circuit. Some signals have more than one pin connection for either test purposes or paralleling of signals to both sockets.

TABLE 1a
USER OUTPUT SIGNALS

Name	No. of Signals	Loading	Description
DATOUT 15 - 0	16	10	Data output to user device. These signals represent the contents of the DRDB register, which is loaded either under program control (e.g. MOV RO, DRDB) or when the DR11-B performs a DATI cycle. Levels are: +3V = logical 1; ground = logical 0. All lines cleared to 0 by INIT.
INITIALISE	1	10	This line is true (+3V) whenever the Unibus is initialised, which occurs on power up, power down, console start, or RESET instruction.
FNCT 3, 2, 1	3	9	These 3 lines are derived from the function bits in DRST (bits 3, 2, 1) and are used to specify device operation. Levels are: +3V = logical 1; ground = logical 0. Clear by INIT.
READY	1	8	This signal is derived from the READY bit in DRST (bit 7). This signal is true (+3V) after INIT; it becomes false (ground) when the GO bit is loaded, indicating that a command has been given; and it becomes true again when word count overflows or an error condition developes.
BUSY	1	9	BUSY indicates that a bus sequence is in progress. It becomes true (+3V) on the trailing edge of CYCLE REQUEST and becomes false (ground) when the bus cycle is complete.
END CYCLE	1	5	This pulse is a 100-ns positive pulse that indicates that the bus cycle is complete.
GO	1	10	This pulse is a 200-ns positive pulse that results from the setting of the GO bit in DRST. Indicates that a new operation is to be performed.

TABLE 1b
USER INPUT SIGNALS

Name	No. of Signals	TTL Loads	Description
DATIN 15 - 0	16	1 each	Data input from user device. The levels presented on these lines can be examined by reading the DRDB register (e.g. MOV DRDB, RO) and are transferred directly to memory when the DRS11-C performs a DATO bus cycle. Levels are +3V = Logical 1; Ground = Logical 0.
C1 CONTROL C0 CONTROL	1 1	3 1	These two control signals specify the type of Unibus cycle the DRS11-C is to perform. They correspond logically with the Unibus signals C1 and C0. Levels are +3V = logical 1; Ground = logical 0. Note: polarities on Unibus are inverted. DATIP is used for read-modify-restore operation. C1 Control / C0 Control / Cycle Performed 0 / 0 / DATI — To transfer data 0 / 1 / DATIP — from Unibus to the user device 1 / 0 / DATO — To transfer data from user device to Unibus.
CYCLE REQUEST	1	1	CYCLE initiates the sequence of requesting bus use and triggering the Unibus Cycle after the DRS11-C device obtains control of the bus. This input should be pulsed positive for 100ns minimum duration to initiate a bus transfer sequence. CYCLE REQUEST sets BUSY on the +3V-to-ground transition of the input.
DSTAT A, B, C	3	1 each	Device Status Bits A, B, C. The signal levels applied to these lines appear as bits 11, 10 and 09 of DRST. Levels are: +3V = logical 1; ground = logical 0.
ATTN	1	2	Attention. The signal level applied to this line appears as bit 13 of DRST. A logical 1(+3V) forces an error condition in the option and stops further bus cycles. An interrupt occurs if IE is set. Must be grounded if not used.
WC INC ENB	1	1	Word Count Increment Enable. In most operations this signal is wired to a logical 1(+3V) source, allowing the DRWC register to count each bus cycle performed by the DRS11-C. However, in read-modify-write sequences, for example, incrementation would be disabled for the DATIP cycle and enabled for the subsequent DATO.
BA INC ENB	1	2	Bus Address Increment Enable. In most operations, this signal is tied to a logical 1 (+3V) source, allowing the DRBA register to step after each bus cycle. However, in read-modify-restore operations, for example, incrementation must be inhibited for the DATIP cycle and enabled for the subsequent DATO.

INPUT/OUTPUT CONNECTIONS

Signal List. Table 2

Signal Name	Pin	Signal Name	Pin	Signal Name	Pin
DATOUT 00	J1-A	DATIN 00	J2-UU	FNCT 1	J1-U, J1-V, J2-L
DATOUT 01	J1-B	DATIN 01	J2-VV	FNCT 2	J1-W, J2-H
DATOUT 02	J1-C	DATIN 02	J2-SS	FNCT 3	J1-X, J2-J
DATOUT 03	J1-D	DATIN 03	J2-TT	END CYCLE	J1-Y, J2-E
DATOUT 04	J1-E	DATIN 04	J2-PP	GO	J1-Z, J2-F
DATOUT 05	J1-F	DATIN 05	J2-RR	READY	J1-BB, J2-V
DATOUT 06	J1-H	DATIN 06	J2-MM	BUSY	J1-CC, J2-S
DATOUT 07	J1-J	DATIN 07	J2-NN	INITIALISE	J1-DD, J2-T
DATOUT 08	J1-K	DATIN 08	J2-KK	GROUND	J1-AA, J2-C
DATOUT 09	J1-L	DATIN 09	J2-LL	+3V	J1-EE, J1-FF
DATOUT 10	J1-M	DATIN 10	J2-HH	C0 CONTROL	J1-SS, J2-K
DATOUT 11	J1-N	DATIN 11	J2-JJ	C1 CONTROL	J1-HH, J2-AA
DATOUT 12	J1-P	DATIN 12	J2-EE	REQUEST	J1-JJ, J2-X
DATOUT 13	J1-R	DATIN 13	J2-FF	ATTN	J1-KK, J2-U
DATOUT 14	J1-S	DATIN 14	J2-CC	DSTATA	J1-UU, J2-A, J1-NN
DATOUT 15	J1-T	DATIN 15	J2-DD	DSTATB	J1-TT, J2-Y
				DSTATC	J1-VV, J2-BB
				WC INC ENB	J2-P
				BA INC ENB	J2-R

Timing Considerations

The negation of READY, as well as the GO signal, indicates to the user device that GO bit has been set and the FNCT bits now indicate a valid command. The user device responds by providing the following set of signals: DATA 15: 00 IN, C1 CONTROL, C0 CONTROL, WC INC ENB, BA INC ENB. This set of signals must be established 100ns prior to the negative transition of REQUEST and held for the duration of the bus cycle. The trailing edge of REQUEST causes BUSY to become true, indicating that DRS11-C is requesting bus use or in the process of executing a bus cycle. At the completion of the bus cycle, the END CYCLE pulse is generated, and BUSY goes false. For the duration of BUSY (from REQUEST to END CYCLE), the above set of signals must be held with the exception of BA INC ENB which must be held until the end of the END CYCLE pulse. No new request should be made while BUSY is set.

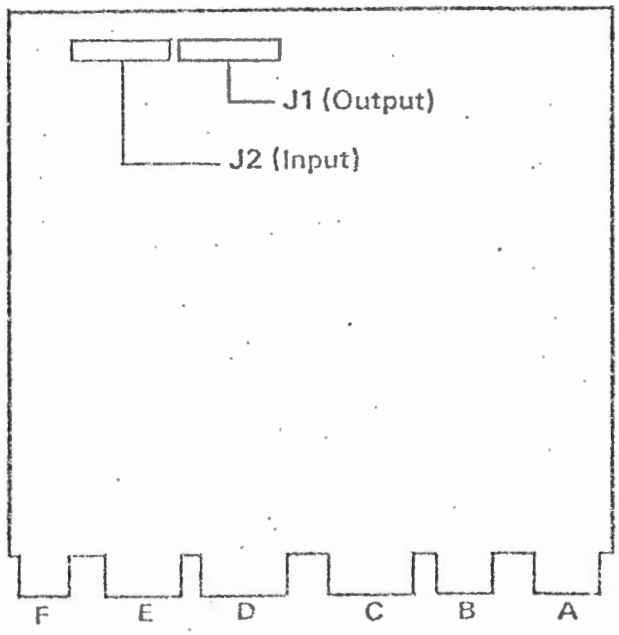

DRS11-C USER CONNECTORS

Philips Electronics Ltd
Energy Systems

PHILIPS

601 Milner Avenue
Scarborough, Ontario
M1B 1M8

April 4, 1978.

Mr. R. Hayman,
Seismological Instrumentation
Laboratory,
Earth Physics Branch,
Energy, Mines and Resources,
1 Observatory Crescent,
Ottawa, Ontario.

Dear Mr. Hayman:

Further to our telephone conversation of today, please find enclosed the literature I promised to send you on the Philips solar cells.

I have worked out your requirements for a 12 volt 4 watt continuous system for the three areas you mentioned (53°N, 49°N and 17°N) and find that 3 modules tilted at 60° with two 6 volt DD-3-5 ESB 200 Ahr batteries will be necessary for the northern locations. To prevent snow build up you might wish to have the panels vertical (90°) and in this case you will require 4 panels. For the Mexican location the DD-3-3 batteries can be used with 2 panels at 45° tilt. These are estimates. I shall run our computer programme and give you the exact figures in a few weeks (as I am in Europe on business for the coming three weeks).

$275 / 10.7 watts = $25/W

The solar cell array BXP47A is priced at $275 each excluding duty and taxes and the charge regulator is $100. The prices of the batteries are indicated in the enclosed sheet. (Please add approximately 25% for 1978 prices and the exchange rate.) Framing for the arrays can be custom made. I enclosed a copy of frame we have supplied to MOT.

I shall write to you when I have the detailed computer calculations.

Yours truly,

Frank Snapp, Ph.D.,
Manager.

telephone: (416) 292-5161
telex: 065-25100
065-25103
065-25104

PHILIPS

TECHNICAL
INFORMATION
ENERGY SYSTEMS

PHOTOVOLTAIC SOLAR GENERATORS

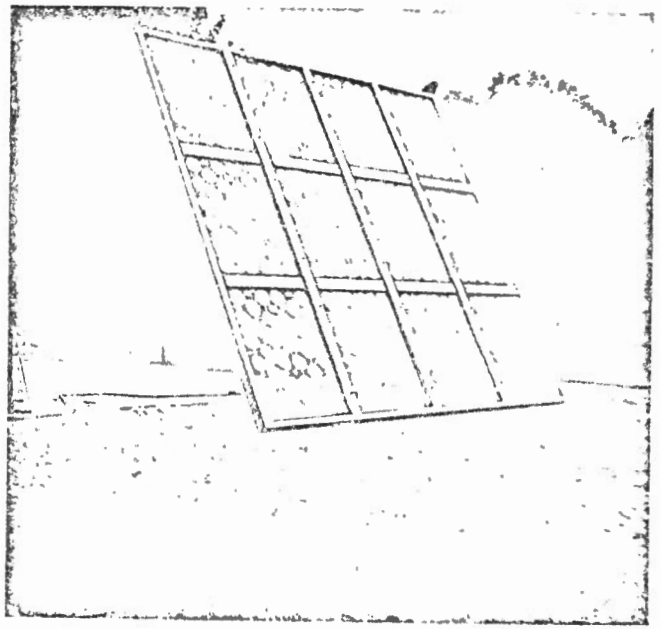

SERIES SG

A range of Photovoltaic Solar Generators for controlled energy supply by direct conversion of solar radiation. Each generator contains a specific number of solar cell modules (BPX 47A) mounted in an aluminium frame and is designed to charge lead acid batteries. The generators are provided with charge regulators for battery protection. End of discharge situation is indicated by a signalling voltage at the output terminals.
The SG Series is a family of three solar generators: the SG 447, SG 847 and SG 1247 providing respectively 40, 80 and 120 watts at 1 kW/m² radiation. Where higher power is required additional solar generators can be connected in parallel.
In addition to the standard range, engineered "tailor-made" systems can be produced when required.

DESCRIPTION

Each solar generator consists of three parts:

- A set of solar cell modules (BPX 47A) to convert solar energy into electrical energy.
- Supporting frame of four major parts for easy assembly in remote and difficult to get to sites: these are a flat carrier frame for the solar modules and cables which includes a bird screen for the top of the generator; a two-part mast which also carries the output cable; a knee to provide optimum inclination for site. The frame is constructed of anodized aluminium, painted to prevent corrosion.
- One/two (depending on requirements) charge regulators to protect the battery from overcharge and excessive gassing.

FEATURES

- Outstanding reliability by use of highly reliable solar modules
- Solar modules designed to withstand severe climatic conditions
- "Worst case" circuit design based on "end of life" data on components
- Sturdy mechanical construction to withstand strong winds

APPLICATIONS

For use in locations where utility-grid electricity is not available for:
Communications systems
Railway signalling systems
Forestry equipment
Weather monitors
Cathodic protection
Navigational aids
Remote datametric equipment
Water supply systems

PHILIPS

PHOTOVOLTAIC SOLAR GENERATORS

PROVISIONAL
P10
PE

CHARACTERISTICS

TEMPERATURE RANGE
Operating temperature range —40°C to 45°C (in the shadow)
Storage temperature —40°C to 85°C
Temperature rise by 1 kW/m² solar radiation typical 15°C

OUTPUT CURRENT
At E_e = 1 kW/m² (irradiance from the sun at sea level) and T_e 25°C the output current in Amps can be read from the table

Nominal Voltage	12	24	36	48
SG 447	2,75	1,35	n.a.	0,65
SG 847	5,6	2,75	n.a.	1,35
SG 1247	8,4	4,2	2,75	2,05

CHARGE REGULATOR
The charge regulator switches off the photovoltaic current if the output voltage exceeds V_{max}. The current is switched on as soon as the output voltage is lower than $V_{max} - V_{hys}$. The voltages can be read from the table:

Nominal Voltage		12	24	36	48
Hysteresis	V_{max}	13,6	27,2	40,8	54,4
	V_{hys}	0,8	1,6	2,4	5,2

SIGNALLING CIRCUIT
The signalling circuit switches a voltage at the output terminals from high to low as soon as the output voltage is lower than V_{min} which can be read from the table:

Nominal Voltage	12	24	36	48
V_{min}	11,4	22,8	34,2	45,6

Signal voltage (low battery voltage) $V_{snl} = R_{ex} \cdot I_{snl}$ (is max. 5 V)
Signal current (low battery voltage) I_{snl} between 10 and 15 mA
Signal voltage (high battery voltage) $V_{snl} = R_{ex} \cdot I_{snl}$
Signal current (high battery voltage) I_{snl} max. 0.1 mA
Signal output will withstand a short circuit.
(R_{ex} = terminating resistance)

STANDARD SERIES AVAILABLE

Type	No of panels	Weight kg ±	Nominal voltage
SG 447	4	35	12 24 48
SG 847	8	50	12 24 48
SG 1247	12	65	12 24 36 48

Each type and nominal voltage is available with knee for one of the four recommended angles of inclination.

RECOMMENDED INCLINATION ANGLES

Climate	Inclination degrees
Wet tropical	30
Arid tropical	45
Moderate	60
Expectation of snow	90

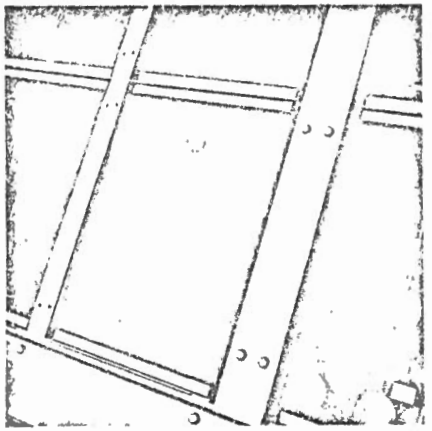

Solar cell module BPX 47A

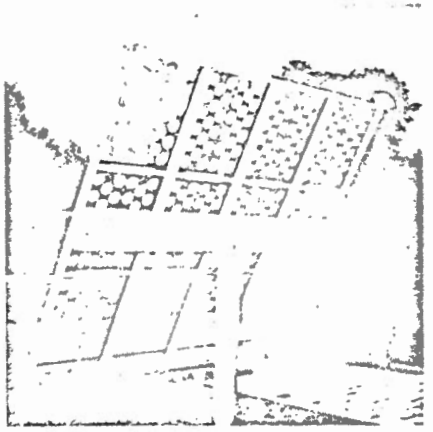

Rear view of Solar Generator

DIMENSIONS OF SOLAR GENERATOR

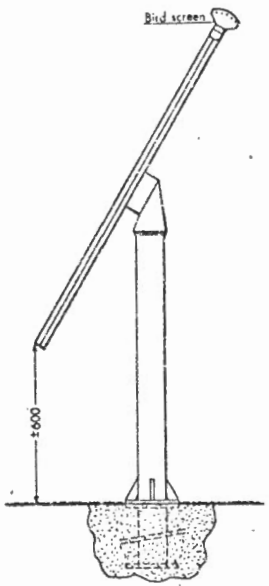

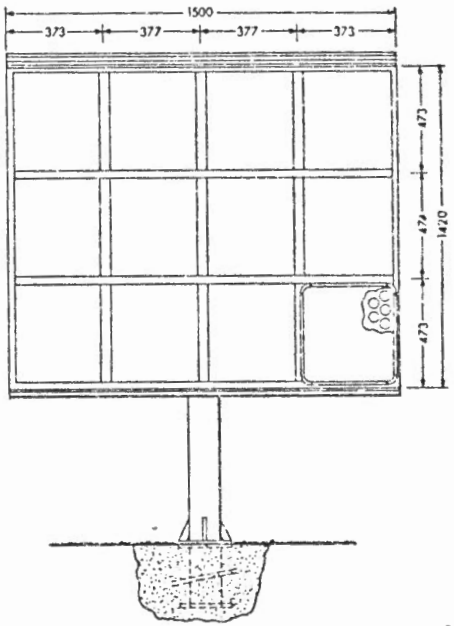

PRINCIPLE OF OPERATION
(Example SG 1247)

12 Volt system

24 Volt system

48 Volt system

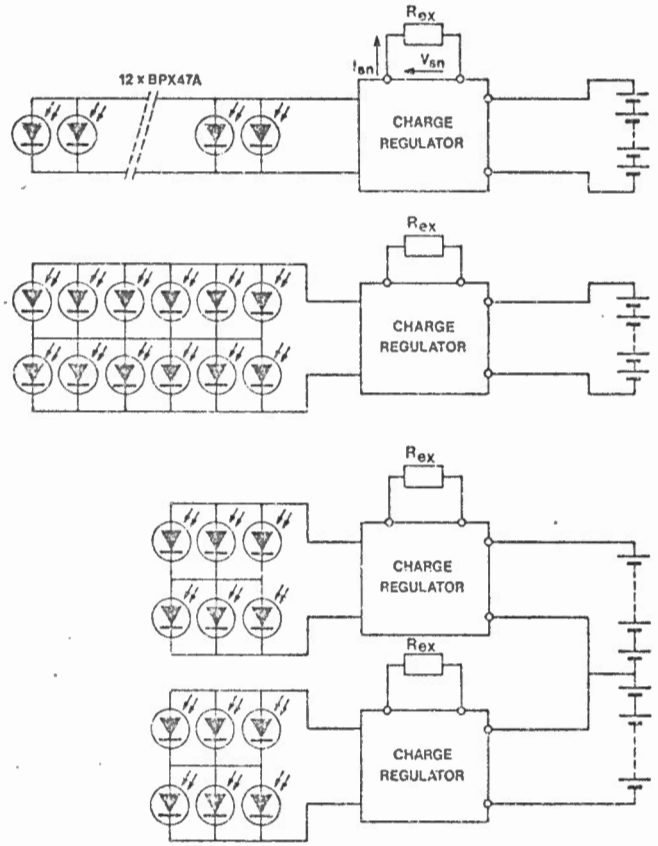

The charge regulator switches off the photovoltaic current if the output voltage exceeds V_{max}. In order to enable the charge regulator to measure the battery voltage at the output terminals the maximum allowed voltage drop in the connecting cable is 0.2 Volts. When higher currents are desired than specified, more solar generators can be connected in parallel. This offers the additional advantage that, with a high battery voltage, the charging current will be switched of step by step.

Solar powerod pump system.

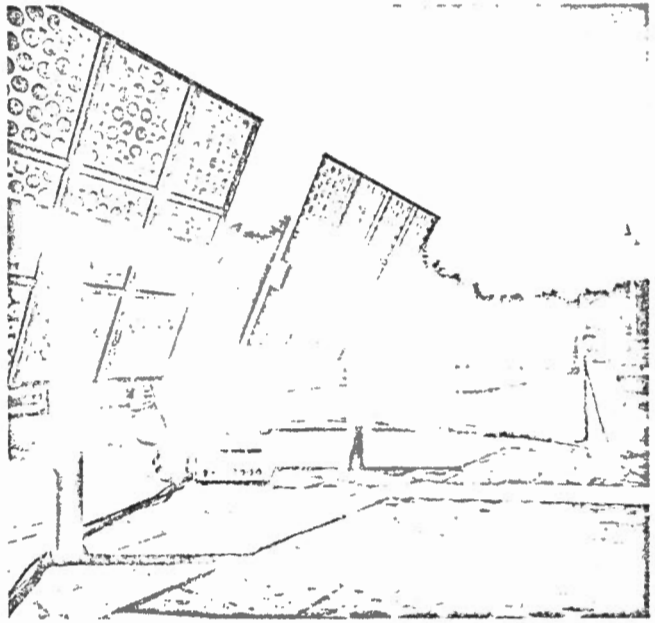

In this application, solar energy is used directly to pump water from a depth of about 20 metres. The electrical energy produced by three or four SG 1247 units is converted to 3-phase AC to power the submersible pump. About 10 m³ of water is produced daily. The converter also provides an optimum energy match between solar generators and the pump in order to make the best use of the energy produced.

Control Unit.

Solar generator with 8 BPX 47A Photovoltaic panels for school for the deaf, Kenya.

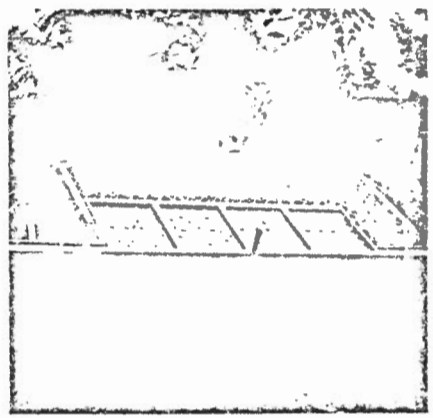

An example of a "tailor-made" solar generator for a special project is shown. * This system uses 8 photovoltaic panels PBX 47A mounted in a saddle-shaped frame. This is the best solution for locations close to the equator. The associated charge regulator provides an almost constant output voltage independent of the output current. Excess energy is dissipated in the unit. Transportable batteries can therefore be used. During sunshine, the unit can be run without batteries. This principle is impracticable for larger systems because of the dissipation.

* Information for special applications can be provided on request.

Philips Electronics Ltd
Energy Systems

PHILIPS

601 Milner Avenue
Scarborough, Ontario
M1B 1M8

May 1, 1978.

Mr. R. Hayman,
Seismological Instrumentation
Laboratory,
Earth Physics Branch,
Energy, Mines and Resources,
1 Observatory Crescent,
Ottawa, Ontario.

Dear Mr. Hayman:

As promised in my letter of April 4th, please find enclosed the detailed computer calculations for your photovoltaic application.

You will see we have picked cities close to the areas that you specified in order that we could use actual weather data.

The format of the printouts is identical for the three locations:-

Printout A is self-explanatory if you use the separate sheet enclosed explaining what each column is.

Other printouts are variations of tilt angle and/or antonomy days.

To summarize -

$17^{o}N$	3 photovoltaic modules at 30 degrees with 6 two volt batteries
$49^{o}N$	5 photovoltaic modules at 90 degrees with 18 two volt batteries
$53^{o}N$	5 photovoltaic modules at 90 degrees with 6 two volt batteries

The batteries that may be used at the ESB Type DD-5-1.

..../2

telephone. (416) 292-5161
telex: 065-25100
065-25103
065-25104

PHILIPS

Should you wish to discuss these further, you might give me a call and as I am in Ottawa approximately once a month we could arrange to meet.

Yours truly,

Frank Snape. Ph.D.,
Manager.

/lw

Encl.

COLUMN 1 = MEASURED GLOBAL ENERGY , PER MONTH, IN KJ
COLUMN 2 = CALCULATED GLOBAL ENERGY , CLEAR SKY, PER MONTH, IN KJ
COLUMN 3 = MEASURED/CALCULATED ENERGIES
COLUMN 4 = CALCULATED ENERGY ON TILTED SURFACE, CLEAR SKY, PER MONTH IN KJ
COLUMN 5 = CHARGE OF TILTED PANEL, CLEAR SKY, PER MONTH, IN AH
COLUMN 6 = CHARGE OF TILTED PANEL, CLOUDY SKY, PER MONTH, IN AH
COLUMN 7 = QUANTITY OF SUN HOURS,CLEAR SKY,PER MONTH
COLUMN 8 = CALCULATED DIRECT RADIATION ON HORIZONTAL SURFACE,CLEAR SKY,PER MONTH IN KJ
COLUMN 9 = CALCULATED DIFFUSE RADIATION ON HORIZONTAL SURFACE,CLEAR SKY,PER MONTH IN KJ
COLUMN 10= CALCULATED DIFFUSE / GLOBAL RADIATION

	1	2	3	4	5	6	7	8	9	10
JAN.	54.5	65.7	0.830	83.4	160.2	133.0	344.9	53.8	11.9	0.161
FEBR.	53.9	67.1	0.804	78.2	149.7	120.3	321.3	55.9	11.2	0.167
MARCH	64.9	82.6	0.784	85.7	163.5	128.5	349.8	69.8	12.8	0.155
APRIL	64.1	84.1	0.761	76.8	146.0	111.1	372.2	71.6	12.5	0.149
MAY	66.8	87.4	0.787	71.3	135.1	106.4	397.0	74.5	12.9	0.146
JUNE	44.1	83.7	0.765	64.6	122.4	93.7	390.0	71.3	12.4	0.148
JULY	67.5	85.9	0.785	68.5	129.8	102.0	399.5	73.2	12.7	0.148
AUG.	67.5	85.8	0.794	75.1	142.6	113.2	368.2	72.4	12.6	0.148
SEPT.	59.0	79.1	0.747	79.4	151.2	112.9	361.7	67.0	12.0	0.152
OCT.	44.6	74.8	0.781	84.9	162.4	126.8	354.0	62.6	12.2	0.163
NOV.	56.4	64.3	0.820	80.6	154.7	126.9	335.5	52.9	11.4	0.178
DEC.	51.9	62.2	0.835	81.4	156.5	130.7	341.0	50.6	11.6	0.187
TOTAL	727.3	921.8	0.789	929.9	1774.2	1405.6	4380.0	775.6	146.2	0.159

LATITUDE	=	17.00	DEGREES	PANEL CURRENT	=	0.68 A AT 1 KW/M**
ALTITUDE	=	10	METERS	PANEL VOLTAGE	=	15 VOLTS
REFLECTION COEFFICIENT EARTH	=	0.20		COST OF PANEL	=	
TILT	=	30	DEGREES	BATTERY CELL VOLTAGE	=	2 VOLTS
MEAN DAILY CHANGE	=	3.85	AH	BATTERY CELL CAPACITY	=	50 AH
ENERGY CORRECTION FACTOR	=	1.00		SELF DISCHARGE BATTERY	=	3 % PER MONTH
SYSTEM POWER	=	4.00	WATTS	EFFICIENCY IN AH	=	90 %
SYSTEM VOLTAGE	=	12	VOLTS	COST OF BATTERY CELL	=	
REQUIRED AUTONOMY	=	10	DAYS	QUANTITY OF PANELS	=	3
				QUANTITY OF BATTERY CELLS	=	12

	REQUIRED CHARGE AH	PRODUCED CHARGE AH	EXCESS CHARGE AH	BATTERY CHARGE AH	BATTERY CHARGE %	AUTONOMY DAYS
JAN.	265	399	134	100	100	11.7
FEBR.	238	361	123	100	100	11.7
MARCH	264	385	121	100	100	11.7
APRIL	255	333	78	100	100	11.7
MAY	264	319	55	100	100	11.7
JUNE	255	281	26	100	100	11.7
JULY	264	306	42	100	100	11.7
AUG.	264	340	76	100	100	11.7
SEPT.	255	339	83	100	100	11.7
OCT.	264	381	117	100	100	11.7
NOV.	255	381	125	100	100	11.7
DEC.	264	392	128	100	100	11.7

AUTONOMY AT THE END OF MONTH

	0	1	2	3	4	5	6
JAN.	20.90	21.63	18.48	16.19	14.47	13.23	12.29
FEBR.	24.00	21.63	18.48	16.19	14.47	13.23	12.29
MARCH	26.06	21.63	18.48	16.19	14.47	13.23	12.29
APRIL	24.99	21.37	18.48	16.19	14.47	13.23	12.29
MAY	21.80	18.95	16.84	15.33	14.21	13.23	12.29
JUNE	16.43	14.27	12.88	12.01	11.41	10.94	10.41
JULY	12.15	10.72	10.10	9.96	9.93	10.00	9.91
AUG.	10.65	10.04	10.27	10.94	11.54	12.22	12.29
SEPT.	10.02	10.23	11.31	12.78	14.01	13.23	12.29
OCT.	11.88	13.01	15.04	16.19	14.47	13.23	12.29
NOV.	14.70	16.75	18.48	16.19	14.47	13.23	12.29
DEC.	17.52	20.52	18.48	16.19	14.47	13.23	12.29
	SEPT.	SEPT.	AUG.	AUG.	AUG.	AUG.	AUG.

BEST CASE CALCULATION
REQUIRED TILT = 30

	REQUIRED CHARGE AH	PRODUCED CHANGE AH	EXCESS CHARGE AH	BATTERY CHARGE AH	BATTERY CHARGE %	AUTONOMY DAYS
JAN.	265	399	134	100	100	11.7
FEBR.	239	361	122	100	100	11.7
MARCH	265	385	120	100	100	11.7
APRIL	256	333	77	100	100	11.7
MAY	265	319	54	100	100	11.7
JUNE	256	281	25	100	100	11.7
JULY	265	306	41	100	100	11.7
AUG.	265	340	75	100	100	11.7
SEPT.	256	339	82	100	100	11.7
OCT.	265	381	116	100	100	11.7
NOV.	256	381	124	100	100	11.7
DEC.	265	392	127	100	100	11.7

LATITUDE	=	17.00	DEGREES	PANEL CURRENT	=	0.68 A AT 1 KW/M**
ALTITUDE	=	10	METERS	PANEL VOLTAGE	=	15 VOLTS
REFLECTION COEFFICIENT EARTH	=	0.20		COST OF PANEL	=	
TILT	=	30	DEGREES	BATTERY CELL VOLTAGE	=	2 VOLTS
MEAN DAILY CHANGE	=	3.85	AH	BATTERY CELL CAPACITY	=	50 AH
ENERGY CORRECTION FACTOR	=	1.00		SELF DISCHARGE BATTERY	=	3 % PER MONTH
SYSTEM POWER	=	4.00	WATTS	EFFICIENCY IN AH	=	90 %
SYSTEM VOLTAGE	=	12	VOLTS	COST OF BATTERY CELL	=	
REQUIRED AUTONOMY	=	10	DAYS	QUANTITY OF PANELS	=	3
				QUANTITY OF BATTERY CELLS	=	12

AUTONOMY AT THE END OF MONTH

	0	1	2	3	4	5	6	7	8	9	10
JAN.	10.41	11.62	8.38	6.04	4.32	3.08	2.19	1.55	1.10	0.78	0.55
FEBR.	13.89	11.62	8.38	6.04	4.32	3.08	2.19	1.55	1.10	0.78	0.55
MARCH	16.13	11.62	8.38	6.04	4.32	3.08	2.19	1.55	1.10	0.78	0.55
APRIL	15.04	11.35	8.38	6.04	4.32	3.08	2.19	1.55	1.10	0.78	0.55
MAY	11.84	8.93	6.76	5.25	4.13	3.08	2.19	1.55	1.10	0.78	0.55
JUNE	6.46	4.24	2.78	1.99	1.41	0.86	0.40	0.06	0.00	0.00	-0.00
JULY	2.16	0.69	0.00	0.00	0.00	-0.00	-0.00	0.00	0.36	0.71	0.55
AUG.	0.65	0.00	0.17	1.05	1.69	2.30	2.19	1.55	1.10	0.78	0.55
SEPT.	0.00	0.18	1.21	2.96	4.25	3.08	2.19	1.55	1.10	0.78	0.55
OCT.	1.84	2.95	4.94	6.04	4.32	3.08	2.19	1.55	1.10	0.78	0.55
NOV.	4.65	6.68	8.38	6.04	4.32	3.08	2.19	1.55	1.10	0.78	0.55
DEC.	7.44	10.44	8.38	6.04	4.32	3.08	2.19	1.55	1.10	0.78	0.55
	SEPT.	AUG.	JULY	AUG.	AUG.	JULY	AUG.	JULY	JUNE	JULY	JUNE

BEST CASE CALCULATION
REQUIRED TILT = 30

	REQUIRED CHARGE AH	PRODUCED CHARGE AH	EXCESS CHARGE AH	BATTERY CHARGE AH	BATTERY CHARGE %	AUTONOMY DAYS
JAN.	263	399	134	50	100	5.9
FEBR.	239	361	122	50	100	5.9
MARCH	265	385	120	50	100	5.9
APRIL	256	333	77	50	100	5.9
MAY	265	319	54	50	100	5.9
JUNE	256	281	25	50	100	5.9
JULY	265	306	41	50	100	5.9
AUG.	265	340	75	50	100	5.9
SEPT.	256	339	82	50	100	5.9
OCT.	265	381	116	50	100	5.9
NOV.	256	381	124	50	100	5.9
DEC.	265	392	127	50	100	5.9

LATITUDE	=	17.00	DEGREES	PANEL CURRENT	=	0.68 A AT 1 KW/M**
ALTITUDE	=	10	METERS	PANEL VOLTAGE	=	15 VOLTS
REFLECTION COEFFICIENT EARTH	=	0.20		COST OF PANEL	=	
TILT	=	30	DEGREES	BATTERY CELL VOLTAGE	=	2 VOLTS
MEAN DAILY CHANGE	=	3.85	AH	BATTERY CELL CAPACITY	=	50 AH
ENERGY CORRECTION FACTOR	=	1.00		SELF DISCHARGE BATTERY	=	3 % PER MONTH
SYSTEM POWER	=	4.00	WATTS	EFFICIENCY IN AH	=	90 %
SYSTEM VOLTAGE	=	12	VOLTS	COST OF BATTERY CELL	=	
REQUIRED AUTONOMY	=	0	DAYS	QUANTITY OF PANELS	=	3
				QUANTITY OF BATTERY CELLS	=	6

Solar-cell technology

Little by little, solar-cell technology is being directed by the federal government toward increasing the nation's energy supplies. While solar-electric, or photovoltaic power systems have a long way to go before they actually compete with fossil-fueled power plants, there are signs indicating that progress is being made:

- Commercial use of photovoltaic power in the field has increased to 500 kW, from 100 kW in 1970.
- The 1978 price of a unit of solar power, a peak watt (W_p), is expected to get down near $13—from $90 in 1970.
- Silicon-fabrication techniques are breaking away from the 20-year-old Czochralski growth process and edging into high-volume and potentially low-cost silicon ribbons and sheets.
- A dozen materials are being studied for their photovoltaic effect; single-crystal silicon still dominates, but polycrystal silicon, gallium arsenide and cadmium sulphide are getting increased attention for special uses.
- Optical concentrators are increasing the effective area of solar arrays by converting more incident energy than would otherwise fall on the cells.
- Computers are helping to configure and optimize complete commercial photovoltaic power systems, according to load, geography, weather and even the cost of money.

The impetus is free energy—a cloudless summer day with the sun shining brightly yields a peak energy distribution of about 1 kW/m², the maximum solar irradiation defined by a peak watt. Just lying in the sunlight, a 2-in. diameter solar cell provides 1/4 W_p, a 3-in. wafer 1/2 W_p, and a 4-in. wafer, 1 W_p.

Each unit cell outputs a fixed voltage, about a half-volt (see box). The cells are normally configured in series-parallel arrays to provide a specific voltage and current capability. Except for the cost involved, there is *no limit* to the number of cells that can be interconnected.

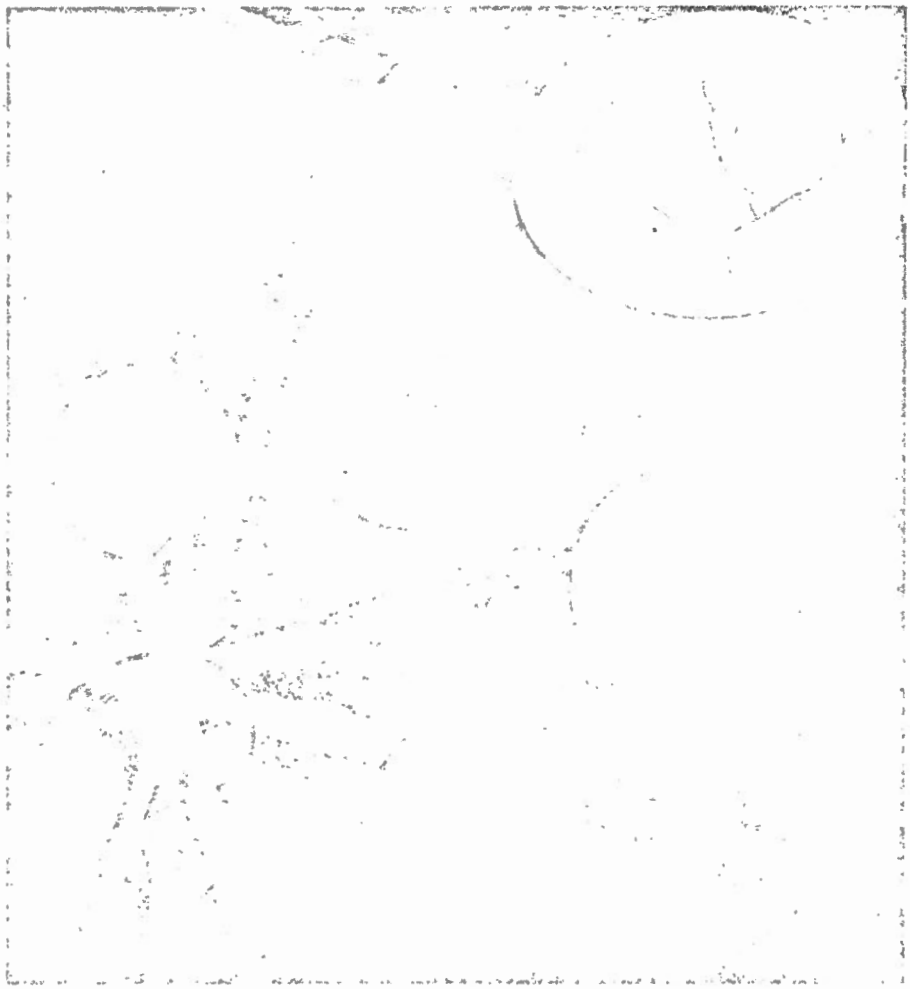

Czochralski-grown silicon crystals with up to a 5-in. diameter are sliced wafer-thin to produce solar cells. After diffusion, the discs are metalized with an electron-collecting grid. It becomes one of the output terminals. (Motorola).

The price volume quandary

But solar-cell technology faces a dilemma. Without high-volume orders, meaningful price reductions can't be realized; without low prices, high volume orders can't be placed. And the 1977 price for a peak watt, $15, is three times what it should be if photovoltaic power is to enjoy widespread use.

For three years the Energy Resources Development Administration (ERDA), now part of the newly created Dept. of Energy, has been funding OEM manufacturers and universities in an over-all solar-electric cost-reduc-

Dick Hackmeister
Western Editor

advances—but slowly

tion program, which relies on the federal government's three existing research facilities. The Jet Propulsion Laboratory in Pasadena, CA, researches and develops raw solar-cell material, fabricating large-area sheets, encapsulating the finished cells, integrating them into modules and testing the completed array. Sandia Laboratories in Albuquerque, NM, designs and evaluates optical concentrators and "total energy" systems, and power-conditioning and storage subsystems, and identifies over-all system tradeoffs. Lewis Research Center in Miami, OH, tests and demonstrates real-life systems in the field. Through Lewis, the largest solar-electric array was installed and set into operation—a 25-kW (W_p) irrigation-water pumping station in Nebraska.

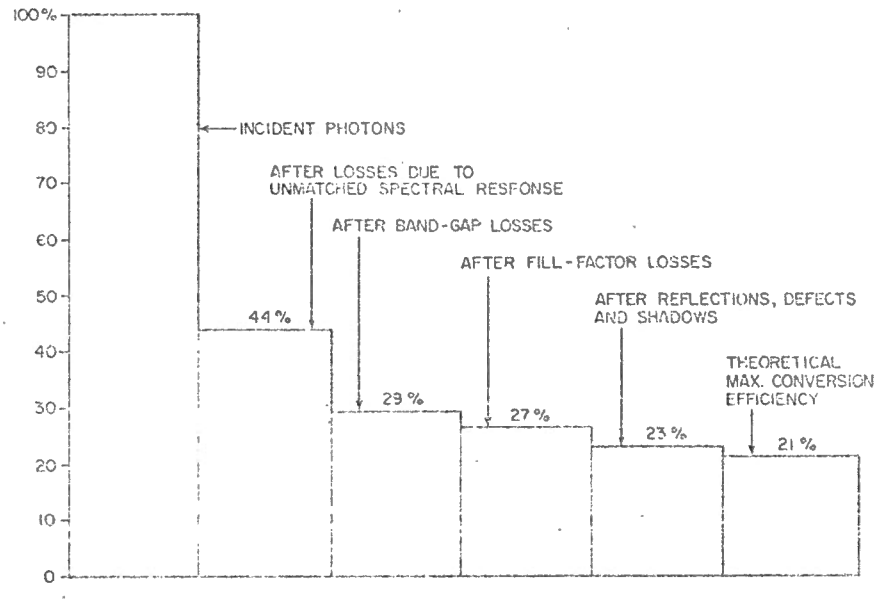

Even the best solar cells won't reach more than 21% conversion efficiency, according to theory. Today's devices range from 8 to 18%.

Introducing SERI

Soon, however, federal solar-energy R&D will be consolidated under the roof of the Solar Energy Research Institute (SERI) in Golden, CO. Created by Congress, SERI is just now getting staffed and organized under the directorship of Dr. Paul Rappaport, recognized as one of the country's leading experts in photovoltaic conversion.

Since petroleum is the most portable energy source around, Rappaport sees its use only for the transportation industry. Stationary facilities will ultimately be powered by the sun, Rappaport predicts. But more efficient solar-cell manufacturing processes are needed before that can happen. Because low-production volume requires a great deal of manual intervention, Rappaport advocates shifting away from the batch-oriented schemes to a continuous flow process that can be automated. "Just sawing a boule of silicon into wafers adds 35 cents to the price of each watt," he notes.

Most of today's commercially avail-

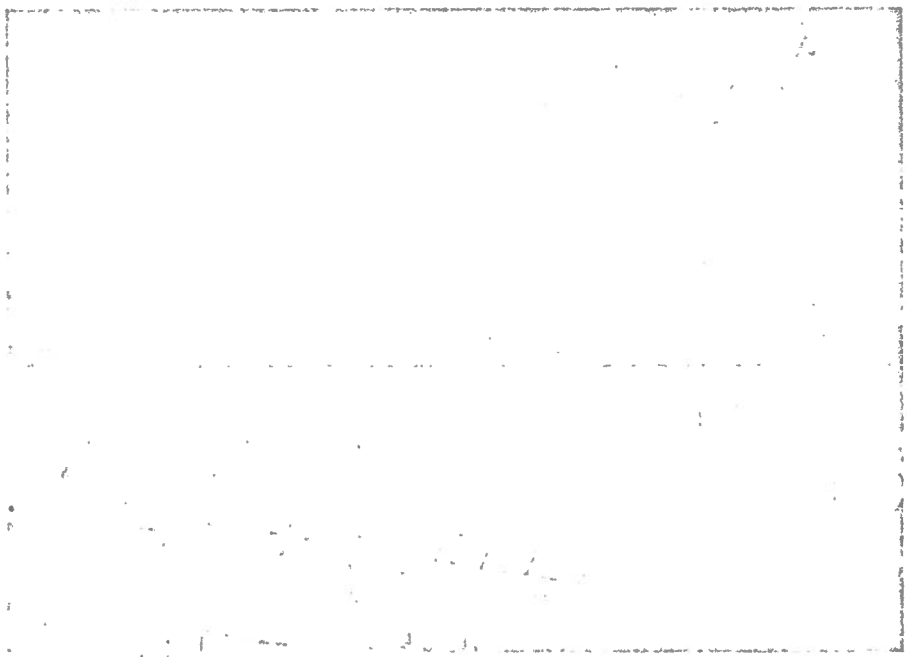

Generating 1000 W_p, this two-axis tracking array uses fresnel lenses to concentrate solar energy 60 times. Lenses are 80% efficient; grooves are turned inward to prevent dirt from accumulating.

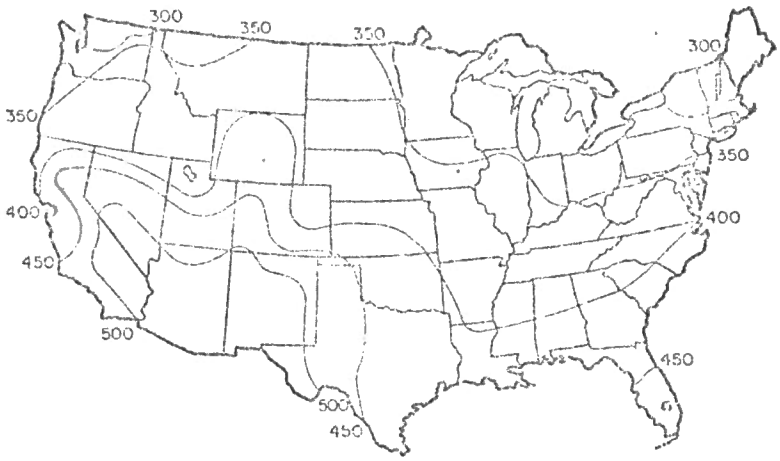

This map shows the total daily energy in Langleys falling on the U.S., in the course of a year (1L=1.162 mWh/cm²).

able solar cells are made by the same process that produces their cousins, discrete transistors and integrated circuits. Round wafers are made by growing a cylindrical ingot, or boule, of high-purity, single-crystal silicon. The Czochralski process, which grows the silicon boule from a small silicon crystal, makes wafers up to 5 in. in diameter (see photo). Slicing the boule like a salami leaves many discs standing on edge. They are then cut away from the common spine. Separated from the spine, each disc of silicon is made into a single, large diode (see box) by the same diffusion process that creates ICs and transistors, except that the wafer surface isn't masked and only a single diffusion step is necessary. (Interestingly, it makes no difference whether the *p* side or the *n* side of the junction faces the sun.)

Finally, an ohmic, current-collecting grid is deposited over the face of the wafer. It becomes one of the solar cell's output terminals—the other terminal is formed by metal deposited on the backside of the cell. Output voltage polarity is determined by the direction of the p-n junction; current flows in the forward direction.

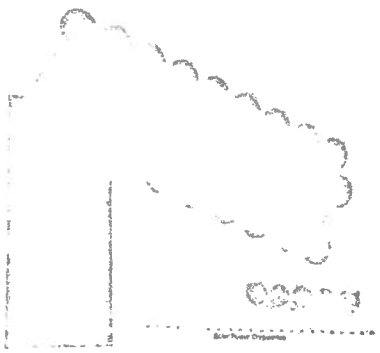

Solar cells are arranged in commercially available modules to fit the application. These units, which are available from Solar Power Corp., North Billerica, MA, generate 25 W_p, 9.2 W_p and 1.4 W_p, respectively.

The ultimate in efficiency

Growing silicon in boules is great for producing quarter-inch IC chips (the wafers are scribed, then cracked into squares). But the process is woefully inappropriate for making carpet-sized sheets of the material to collect and convert sunlight. Several firms are currently under contract to the Jet Propulsion Laboratory to produce large-area silicon, either in ribbons or in sheets. These companies include Mobil-Tyco (Waltham, MA), Motorola (Phoenix, AZ), RCA (Princeton, NJ), Rockwell International (Anaheim, CA), Honeywell (Bloomington, MN), Westinghouse and General Electric (Schenectady, NY).

Other JPL contractors are working to alter the existing batch-manufacturing process with such alternatives as ingot casting and improved sawing or cutting of the boules. These contractors include Texas Instruments (Dallas, TX), Varian (Lexington, MA), Coors (Golden, CO), Crystal Systems (Salem, MA) and Eagle Picher (Miami, OK).

Meanwhile, commercially available solar arrays are beset with problems. For one thing, they are only about 12% efficient—that is, they convert incident sunlight into usable electric power at the rate of 120 W/m². Small-area laboratory devices have reached efficiencies as high as 18%, but theoretically no cell can exceed 21%.

For silicon, unmatched spectral response reduces the available photons to 44% efficiency. The band-gap limit further reduces them to 29%, and fill factor brings the number down to 27%. After surface reflections and defects, the figure is 21%, which still doesn't allow for dirt, metal-mask shadows and I^2R losses.

Geographical location has a profound effect on a solar array's output. Peak watts are generated only during the ideal conditions of summer sun and clear skies. Even then, peak watts occur only at noon. Averaging peak power with cloud cover, night darkness, and the sun's acute angle of incidence in winter cuts the annual amount of usable power down to 25% of the peak in Phoenix, and down to 16% of the peak in Boston (see map).

Temperature takes a toll, too, and a solar array with a supposed 15-V output will droop to 13 V if noontime temperatures hit 110 F (43 C). Evaluation arrays purchased by JPL are spec'd for operation at 150 F (65 C), but that's probably overkill for most OEM applications.

Problems on earth

Properly interconnected and potted, solar cells can be expected to operate indefinitely. In fact, solar cells have

The largest photovoltaic installation yet is this 25-kW_p array at an irrigation-water pumping station in Nebraska.

been used in space for years. And the Jet Propulsion Laboratory not been able to find a measurable degradation or failure yet. But back on earth, a few reliability problems do crop up. The chief culprit, not surprisingly, is the encapsulating, or potting material of a solar-cell module.

Although a module needn't be hermetically sealed, it must be weatherproof and impervious to moisture so that it can withstand day/night temperature cycling. Moisture on the cell's surface degrades the unit's performance rapidly. It causes extra losses by absorption and refraction, and it promotes the growth of organic substances that block valuable sunlight.

Another performance degrader, oddly enough, is the sun, whose ultraviolet rays darken the encapsulant material.

There is even a problem with the most used encapsulant, silicone rubber. Its sticky surface collects dirt. Manufacturers cover the module's face with clear plastic or tempered glass to make the module better able to clean itself: The surface should wash clean in the rain, and snow should slide off.

Cell interconnections within the module can also become failure mechanisms, so multiple, redundant connections must be made to the disc.

Since solar arrays make power while the sun shines but never at night, power conditioning and storage facilities are prime requisites for any commercial solar-electric system.

Automobile-type, lead-acid storage batteries remain the only realistic power buffers. Vendors combine them with solar-cell modules, a shunt regulator, a blocking diode (to prevent shorting out the batteries at night), mounting hardware and cabling to configure a complete OEM solar power generator.

System configuration is called "sizing," which normally includes a computer analysis of the site's latitude, longitude, altitude, mean temp and yearly "in-sol-ation"—which refers to the amount of time the site is in the sun, or "in sol." The unit of measure of insolation is the Langley, which is equal to 1.162 mWh/cm² (see map).

Armed with a description of the power required and the site's solar circumstances, a computer determines the most efficient system for that application: the number of solar modules and their series-parallel connections, the array's compass heading and tilt angle, the number of batteries required and their interconnections, as well as projected system performance on a monthly basis.

This two-axis, three-section tracking concentrator generates 300 W_p, and uses a solar-powered μP and stepping motors to follow the sun. RCA expects this "fly's eye" concentrator to cost \$1/W_p in volume quantities.

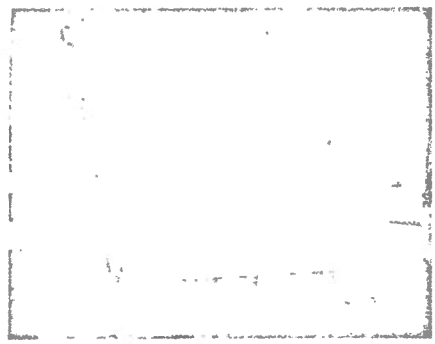

A nontracking, solar concentrator uses high-density strips of cells and parabolic reflectors to generate 100 W_p. (Argonne National Laboratory).

The 'Un-led,' and how it works

Operating, the solar cell is a light-emitting diode working backwards.

A conventional LED, like the type that might be used as a display in your watch, has a depletion layer formed in the semiconductor material by oppositely doped impurities. An external energy source—voltage—excites the electrons to conduct through the depletion layer. Excess energy is given off as photons, which you can see.

A solar cell, too, has a depletion layer formed in the semiconductor material by oppositely doped impurities (the cell is a p-n junction). But it works in reverse. Photons excite the electrons, and the junction develops a voltage.

Working on different sides of the street, a LED doesn't emit a broad range of wavelengths, and a solar cell doesn't absorb a broad range—which accounts for the cell's losses due to imperfect spectral response.

The solar cell and LED do share limitations. The energy band gap ($\Delta \cong 1.5$ eV) limits the amount of energy either one can convert. And because they're less-than-ideal diodes, both the LED and the solar cell suffer reflection losses as well as losses due to electron-hole pairs recombined in impure areas.

Concentrating on the sun

Concentrators can gather and focus more of the sun's energy on available solar cells using parabolas, fresnel and optical lenses. Tests at Sandia show that concentrators can boost the equivalent efficiency of silicon solar cells above 15%, and gallium arsenide cells to almost 20%, they are most effective in the southwestern United States where sunlight is most intense and least diffuse. Both tracking and nontracking concentrators show promise.

Nontracking concentrators effectively multiply the surface area of a solar cell as much as 20 times (20 suns). They use parabolic shapes to collect extra photons and form them into a beam, like that of a flashlight. An array of concentrators and a like number of solar cells are mounted on a rack that looks like a backyard swing. The rack tilts the array at the best angle for the site's latitude, and is adjusted seasonally.

Beyond a concentration ratio of 20 suns or so, the optical alignment of sun, lens and cells becomes too critical for a fixed-frame array—because of the earth's rotation. The sun must be tracked.

The tracking speeds involved are slow enough for stepping motors to move the frame of a tracking concentrator—it's all under μP control. Together, the stepping motors and the μP consume only a small fraction of the energy they help collect.

The highest concentration ratio to date is in RCA's "fly's eye" (see photo). With a concentration ratio of 300 suns, the tracking must be very accurate: the unit updates its position 30 times a minute.

THE BELL SYSTEM
TECHNICAL JOURNAL

VOLUME XXXVI MAY 1957 NUMBER 3

Radio Propagation Fundamentals*

By KENNETH BULLINGTON

(Manuscript received June 21, 1956)

The engineering of radio systems requires an estimate of the power loss between the transmitter and the receiver. Such estimates are affected by many factors, including reflections, fading, refraction in the atmosphere, and diffraction over the earth's surface.

In this paper, radio transmission theory and experiment in all frequency bands of current interest are summarized. Ground wave and sky wave transmission are included, and both line of sight and beyond horizon transmission are considered. The principal emphasis is placed on quantitative charts that are useful for engineering purposes.

I. INTRODUCTION

The power radiated from a transmitting antenna is ordinarily spread over a relatively large area. As a result the power available at most receiving antennas is only a small fraction of the radiated power. This ratio of radiated power to received power is called the radio transmission loss and its magnitude in some cases may be as large as 10^{15} to 10^{20} (150 to 200 decibels).

The transmission loss between the transmitting and receiving antennas determines whether the received signal will be useful. Each radio

* This paper has been prepared for use in a proposed "Antenna Handbook" to be published by McGraw-Hill.

N.B.

system has a maximum allowable transmission loss which, if exceeded, results in either poor quality or poor reliability. Reasonably accurate predictions of transmission loss can be made on paths that approximate the ideals of either free space or plane earth. On many paths of interest, however, the path geometry or atmospheric conditions differ so much from the basic assumptions that absolute accuracy cannot be expected; nevertheless, worthwhile results can be obtained by using two or more different methods of analysis to "box in" the answer.

The basic concept in estimating radio transmission loss is the loss expected in free space; that is, in a region free of all objects that might absorb or reflect radio energy. This concept is essentially the inverse square law in optics applied to radio transmission. For a one wavelength separation between nondirective (isotropic) antennas, the free space loss is 22 db and it increases by 6 db each time the distance is doubled. The free space transmission ratio at a distance d is given by:

$$\frac{P_r}{P_t} = \left(\frac{\lambda}{4\pi d}\right)^2 g_t g_r \tag{1a}$$

where:

P_r = received power
P_t = radiated power
} measured in same units

λ = wavelength in same units as d

g_t (or g_r) = power gain of transmitting (or receiving) antenna

The power gain of an ideal isotropic antenna that radiates power uniformly in all directions is unity by definition. A small doublet whose over-all physical length is short compared with one-half wavelength has a gain of $g = 1.5$ (1.76 decibels) and a one-half wave dipole has a gain of 2.15 decibels in the direction of maximum radiation. A nomogram for the free space transmission loss between isotropic antennas is given in Fig. 1.

When antenna dimensions are large compared with the wavelength, a more convenient form of the free space ratio is[1]

$$\frac{P_r}{P_t} = \frac{A_t A_r}{(\lambda d)^2} \tag{1b}$$

where $A_{t,r}$ = effective area of transmitting or receiving antennas.

Another form of expressing free space transmission is the concept of

e transmission loss which, if exceeded,
poor reliability. Reasonably accurate
n be made on paths that approximate
lane earth. On many paths of interest,
tmospheric conditions differ so much
bsolute accuracy cannot be expected;
an be obtained by using two or more
ox in" the answer.

ng radio transmission loss is the loss
a region free of all objects that might
his concept is essentially the inverse
radio transmission. For a one wave-
rective (isotropic) antennas, the free
es by 6 db each time the distance is
sion ratio at a distance d is given by:

$$\left(\frac{\lambda}{4\pi d}\right)^2 g_t g_r \qquad \text{(1a)}$$

measured in same units

ne units as d

nsmitting (or receiving) antenna

pic antenna that radiates power uni-
y definition. A small doublet whos
npared with one-half wavelength ha
nd a one-half wave dipole has a gai
naximum radiation. A nomogram fo
tween isotropic antennas is given in

arge compared with the wavelength.
space ratio is[1]

$$\frac{A_t A_r}{(\lambda d)^2} \qquad \text{(1b}$$

mitting or receiving antennas.
space transmission is the concept o

the free space field intensity E_0 which is given by:

$$E_0 = \frac{\sqrt{30 P_t g_t}}{d} \text{ volts per meter} \qquad (2)$$

where d is in meters and P_t in watts.

The use of the field intensity concept is frequently more convenient than the transmission loss concept at frequencies below about 30 mc,

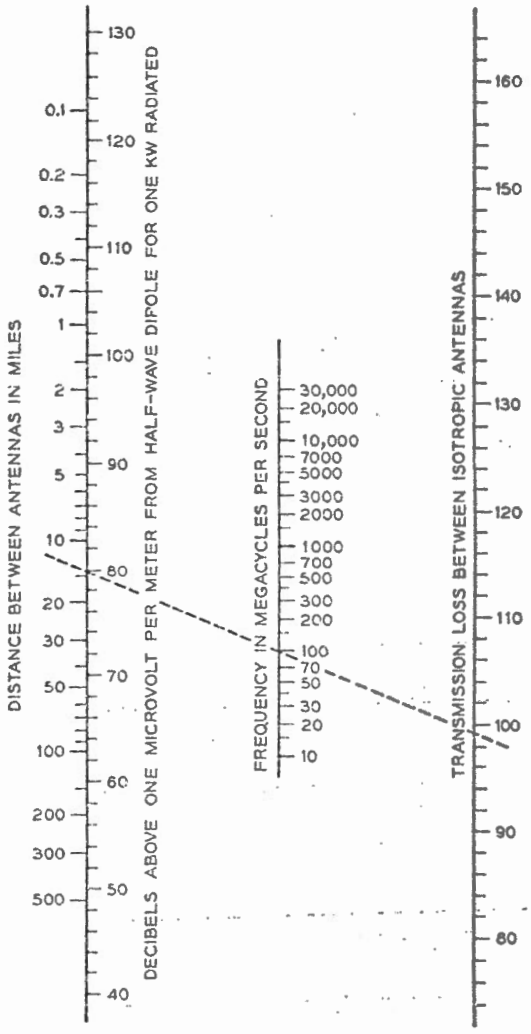

FIG. 1 — Free space transmission.

where external noise is generally controlling and where antenna dimensions and heights are comparable to or less than a wavelength. The free-space field intensity is independent of frequency and its magnitude for one kilowatt radiated from a half-wave dipole is shown on the left hand scale on Fig. 1.

The concept of free space transmission assumes that the atmosphere is perfectly uniform and nonabsorbing and that the earth is either infinitely far away or its reflection coefficient is negligible. In practice, the modifying effects of the earth, the atmosphere and the ionosphere need to be considered. Both theoretical and experimental values for these effects are described in the following sections.

II. Transmission within Line of Sight

The presence of the ground modifies the generation and the propagation of radio waves so that the received power or field intensity is ordinarily less than would be expected in free space.[2] The effect of plane earth on the propagation of radio waves is given by

$$\frac{E}{E_0} = \underbrace{1}_{\text{Direct Wave}} + \underbrace{Re^{j\Delta}}_{\text{Reflected Wave}} + \underbrace{(1-R)Ae^{j\Delta}}_{\text{"Surface Wave"}} + \underbrace{\cdots}_{\text{Induction Field and Secondary Effects of the Ground}} \qquad (3)$$

where

R = reflection coefficient of the ground

A = "surface wave" attenuation factor

$\Delta = \dfrac{4\pi h_1 h_2}{\lambda d}$

$h_{1,2}$ = antenna heights measured in same units as the wavelength and distance

The parameters R and A vary with both polarization and the electrical constants of the ground. In addition, the term "surface wave" has led to considerable confusion since it has been used in the literature to stand for entirely different concepts. These factors are discussed more completely in Section IV. However, the important point to note in this section is that considerable simplification is possible in most practical cases, and that the variations with polarization and ground constants

controlling and where antenna dimen-
to or less than a wavelength. The fre-
nt of frequency and its magnitude for
-wave dipole is shown on the left hand

mission assumes that the atmosphere is
ng and that the earth is either infinitely
t is negligible. In practice, the modify
osphere and the ionosphere need to b
experimental values for these effect-
tions.

F SIGHT

odifies the generation and the propaga
eceived power or field intensity is or
cted in free space.[2] The effect of plan
waves is given by

Induction Field
and Secondary
d ace Effects of the
Wave" Ground

$$+ (1 - R)Ae^{j\Delta} + \cdots \qquad (3$$

the ground

tion factor

ed in same units as the wavelength

ith both polarization and the electr
ion, the term "surface wave" has
t has been used in the literature
pts. These factors are discussed m
r, the important point to note in t
lification is possible in most pract
th polarization and ground consta

and the confusion about the surface wave can often be neglected. For near grazing paths, R is approximately equal to -1 and the factor A can be neglected as long as both antennas are elevated more than a wavelength above the ground (or more than 5–10 wavelengths above sea water). Under these conditions the effect of the earth is independent of polarization and ground constants and (3) reduces to

$$\left|\frac{E}{E_0}\right| = \sqrt{\frac{P_r}{P_o}} = 2 \sin \frac{\Delta}{2} = 2 \sin \frac{2\pi h_1 h_2}{\lambda d} \qquad (4)$$

where P_0 is the received power expected in free space.

The above expression is the sum of the direct and ground reflected rays and shows the lobe structure of the signal as it oscillates around the free space value. In most radio applications (except air to ground) the principal interest is in the lower part of the first lobe; that is, where $\Delta/2 < \pi/4$. In this case, $\sin \Delta/2 \approx \Delta/2$ and the transmission loss over plane earth is given by:

$$\frac{P_r}{P_t} = \left(\frac{\lambda}{4\pi d}\right)^2 \left(\frac{4\pi h_1 h_2}{\lambda d}\right)^2 g_t g_r$$
$$= \left(\frac{h_1 h_2}{d^2}\right)^2 g_t g_r \qquad (5)$$

It will be noted that this relation is independent of frequency and it is shown in decibels in Fig. 2 for isotropic antennas. Fig. 2 is not valid when the indicated transmission loss is less than the free space loss shown in Fig. 1, because this means that Δ is too large for this approximation.

Although the transmission loss shown in (5) and in Fig. 2 has been derived from optical concepts that are not strictly valid for antenna heights less than a few wavelengths, approximate results can be obtained for lower heights by using h_1 (or h_2) as the larger of either the actual antenna height or the minimum effective antenna height shown in Fig. 1. The concept of minimum effective antenna height is discussed further in Section IV. The error that can result from the use of this artifice does not exceed ±3 db and occurs where the actual antenna height is approximately equal to the minimum effective antenna height.

The sine function in (4) shows that the received field intensity oscillates around the free space value as the antenna heights are increased. The first maximum occurs when the difference between the direct and ground reflected waves is a half wavelength. The signal maxima have a magnitude $1 + |R|$ and the signal minima have a magnitude of $1 - |R|$. Frequently the amount of clearance (or obstruction) is described in terms of Fresnel zones. All points from which a wave could be reflected

with a path difference of one-half wavelength form the boundary of the first Fresnel zone; similarly, the boundary of the n^{th} Fresnel zone consists of all points from which the path difference is $n/2$ wavelengths. The n^{th} Fresnel zone clearance H_n at any distance d_1 is given by:

$$H_n = \sqrt{\frac{n\lambda d_1(d - d_1)}{d}} \tag{6}$$

Although the reflection coefficient is very nearly equal to -1 for

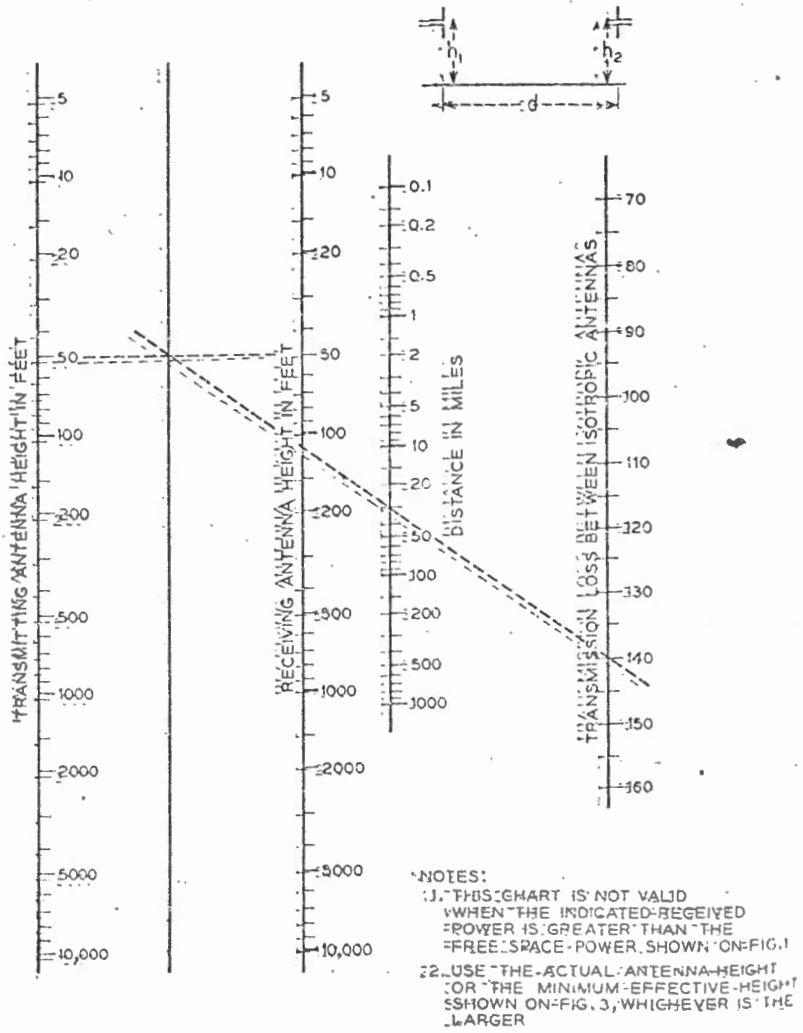

FIG. 2 — Transmission loss over plane earth.

half wavelength form the boundary of the
he boundary of the n^{th} Fresnel zone con-
the path difference is $n/2$ wavelengths.
e H_n at any distance d_1 is given by:

$$\sqrt{\frac{n\lambda d_1(d-d_1)}{d}} \tag{6}$$

fficient is very nearly equal to -1 for

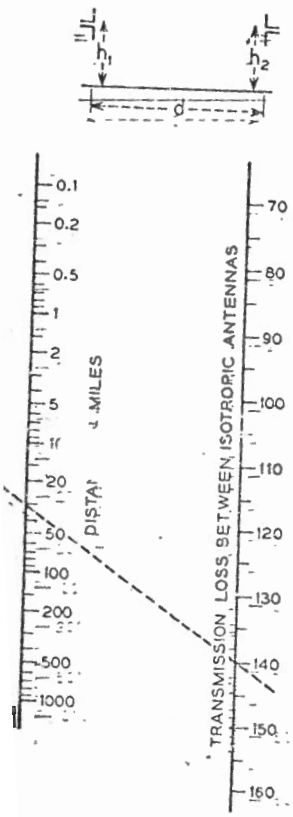

NOTES:
1. THIS CHART IS NOT VALID WHEN THE INDICATED RECEIVED POWER IS GREATER THAN THE FREE SPACE POWER SHOWN ON FIG. 1
2. USE THE ACTUAL ANTENNA HEIGHT OR THE MINIMUM EFFECTIVE HEIGHT SHOWN ON FIG. 3, WHICHEVER IS THE LARGER

oss over plane earth.

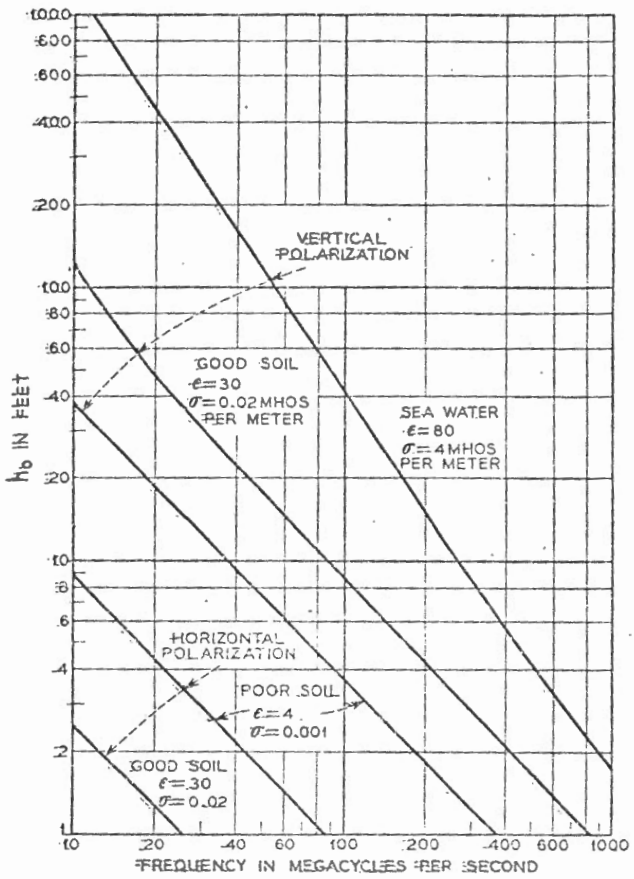

FIG. 3—Minimum effective antenna height.

grazing angles over smooth surfaces, its magnitude may be less than unity when the terrain is rough. The classical Rayleigh criterion of roughness indicates that specular reflection occurs when the phase deviations are less than about $\pm(\pi/2)$ and that the reflection coefficient will be substantially less than unity when the phase deviations are greater than $\pm(\pi/2)$. In most cases this theoretical boundary between specular and diffuse reflection occurs when the variations in terrain exceed $\frac{1}{8}$ to $\frac{1}{4}$ of the first Fresnel zone clearance. Experimental results with microwave transmission have shown that most practical paths are "rough" and ordinarily have a reflection coefficient in the range of 0.2–0.4. In addition, experience has shown that the reflection coefficient is a statistical problem and cannot be predicted accurately from the path profile.[3]

Fading Phenomena

Variations in signal level with time are caused by changing atmospheric conditions. The severity of the fading usually increases as either the frequency or path length increases. Fading cannot be predicted accurately but it is important to distinguish between two general types: (1) inverse bending and (2) multipath effects. The latter includes the fading caused by interference between direct and ground reflected waves as well as interference between two or more separate paths in the atmosphere. Ordinarily, fading is a temporary diversion of energy to some other than the desired location; fading caused by absorption of energy is discussed in a later paragraph.

The path of a radio wave is not a straight line except for the ideal case of a uniform atmosphere. The transmission path may be bent up or down depending on atmospheric conditions. This bending may either increase or decrease the effective path clearance and inverse bending may have the effect of transforming a line of sight path into an obstructed one. This type of fading may last for several hours. The frequency of its occurrence and its depth can be reduced by increasing the path clearance, particularly in the middle of the path.

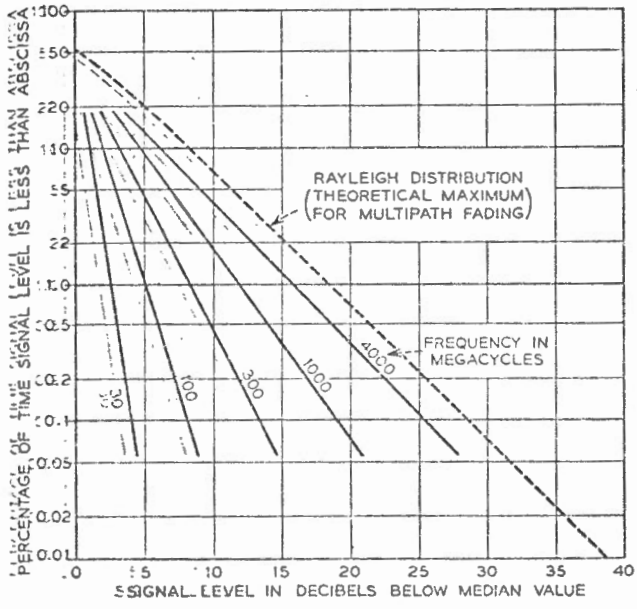

FIG. 4 — Typical fading characteristics in the worst month on 30 to 40 mile line-of-sight paths with 50 to 100 foot clearance.

n time are caused by changing atmos-
of the fading usually increases as either
reases. Fading cannot be predicted ac-
distinguish between two general types:
ltipath effects. The latter includes the
ween direct and ground reflected waves
vo or more separate paths in the atmos-
mporary diversion of energy to some
fading caused by absorption of energy

ot a straight line except for the ideal
e transmission path may be bent up or
conditions. This bending may either
e path clearance and inverse bending
-g a line of sight path into an obstructed
for several hours. The frequency of its
reduced by increasing the path clear-
-f the

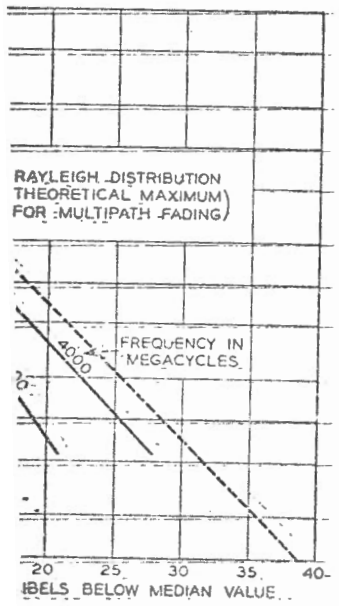

es in the worst month on 30 to 40 mile
earance.

Severe fading may occur over water or on other smooth paths because the phase difference between the direct and reflected rays varies with atmospheric conditions. The result is that the two rays sometimes add and sometimes tend to cancel. This type of fading can be minimized, if the terrain permits, by locating one end of the circuit high while the other end is very low. In this way the point of reflection is placed near the low antenna and the phase difference between direct and reflected rays is kept relatively steady.

Most of the fading that occurs on "rough" paths with adequate clearance is the result of interference between two or more rays traveling slightly different routes in the atmosphere. This multipath type of fading is relatively independent of path clearance and its extreme condition approaches the Rayleigh distribution. In the Rayleigh distribution, the probability that the instantaneous value of the field is greater than the value R is $\exp[-(R/R_0)]$, where R_0 is the rms value.

Representative values of fading on a path with adequate clearance are shown on Fig. 4. After the multipath fading has reached the Rayleigh distribution, a further increase in either distance or frequency increases the number of fades of a given depth but decreases the duration so that the product is the constant indicated by the Rayleigh distribution.

Miscellaneous Effects

The remainder of this Section describes some miscellaneous effects of line of sight transmission that may be important at frequencies above about 1,000 mc. These effects include variation in angles of arrival, maximum useful antenna gain, useful bandwidth, the use of frequency or space diversity, and atmospheric absorption.

On line of sight paths with adequate clearance some components of the signal may arrive with variations in angle of arrival of as much as $\frac{1}{2}°$ to $\frac{3}{4}°$ in the vertical plane, but the variations in the horizontal plane are less than 0.1°.[4, 5] Consequently, if antennas with beamwidths less than about 0.5° are used, there may occasionally be some loss in received signal because most of the incoming energy arrives outside the antenna beamwidth. Signal variations due to this effect are usually small compared with the multipath fading.

Multipath fading is selective fading and it limits both the maximum useful bandwidth and the frequency separation needed for adequate frequency diversity. For 40-db antennas on a 30-mile path the fading on frequencies separated by 100–200 mc is essentially uncorrelated regardless of the absolute frequency. With less directive antennas, uncorrelated fading can occur at frequencies separated by less than 100 mc.[6, 7]

Larger antennas (more narrow beamwidths) will decrease the fast multipath fading and widen the frequency separation between uncorrelated fading but at the risk of increasing the long term fading associated with the variations in the angle of arrival.

Optimum space diversity, when ground reflections are controlling, requires that the separation between antennas be sufficient to place one antenna on a field intensity maximum while the other is in a field intensity minimum. In practice, the best spacing is usually not known because the principal fading is caused by multipath variations in the atmosphere. However, adequate diversity can usually be achieved with a vertical separation of 100–200 wavelengths.

At frequencies above 5,000–10,000 mc, the presence of rain, snow, or fog introduces an absorption in the atmosphere which depends on the amount of moisture and on the frequency. During a rain of cloud burst proportions the attenuation at 10,000 mc may reach 5 db per mile and at 25,000 mc it may be in excess of 25 db per mile.[8] In addition to the effect of rainfall some selective absorption may result from the oxygen and water vapor in the atmosphere. The first absorption peak due to water vapor occurs at about 24,000 mc and the first absorption peak for oxygen occurs at about 60,000 mc.

III. TROPOSPHERIC TRANSMISSION BEYOND LINE OF SIGHT

A basic characteristic of electromagnetic waves is that the energy is propagated in a direction perpendicular to the surface of uniform phase. Radio waves travel in a straight line only as long as the phase front is plane and is infinite in extent.

Energy can be transmitted beyond the horizon by three principal methods: reflection, refraction and diffraction. Reflection and refraction are associated with either sudden or gradual changes in the direction of the phase front, while diffraction is an edge effect that occurs because the phase surface is not infinite. When the resulting phase front at the receiving antenna is irregular in either amplitude or position, the distinctions between reflection, refraction, and diffraction tend to break down. In this case the energy is said to be scattered. Scattering is frequently pictured as a result of irregular reflections although irregular refraction plus diffraction may be equally important.

The following paragraphs describe first the theories of refraction and of diffraction over a smooth sphere and a knife edge. This is followed by empirical data derived from experimental results on the transmission to points far beyond the horizon, on the effects of hills and trees, and on fading phenomena.

nwidths) will decrease the fast multi-
ncy separation between uncorrelated
the long term fading associated with
al.

ground reflections are controlling,
n antennas be sufficient to place one
num while the other is in a field in-
best spacing is usually not known be-
ed by multipath variations in the
versity can usually be achieved with
velengths.

00 mc, the presence of rain, snow, or
e atmosphere which depends on the
quency. During a rain of cloud burst
00 mc may reach 5 db per mile and
25 db per mile.[8] In addition to the
orption may result from the oxygen
e. The first absorption peak due to
mc and the first absorption peak for

EYOND LINE OF SIGHT

agnetic waves is that the energy is
ular to the surface of uniform phase.
ie only as long as the phase front is

ond the horizon by three principal
diffraction. Reflection and refrac-
den or gradual changes in the direc-
action is an edge effect that occurs
nite. When the resulting phase front
in either amplitude or position, the
action, and diffraction tend to break
d to be scattered. Scattering is fre-
gular reflections although irregular
qually important.

e first the theories of refraction and
nd a knife edge. This is followed by
ental results on the transmission to
he effects of hills and trees, and on

Refraction

The dielectric constant of the atmosphere normally decreases gradually with increasing altitude. The result is that the velocity of transmission increases with the height above the ground and, on the average, the radio energy is bent or refracted toward the earth. As long as the change in dielectric constant is linear with height, the net effect of refraction is the same as if the radio waves continued to travel in a straight line but over an earth whose modified radius is:

$$ka = \frac{a}{1 + \frac{a}{2}\frac{d\epsilon}{dh}} \tag{7}$$

where

a = true radius of earth

$\frac{d\epsilon}{dh}$ = rate of change of dielectric constant with height

Under certain atmospheric conditions the dielectric constant may increase ($0 < k < 1$) over a reasonable height, thereby causing the radio waves in this region to bend away from the earth. This is the cause of the inverse bending type of fading mentioned in the preceding section. It is sometimes called substandard refraction. Since the earth's radius is about 2.1×10^7 feet, a decrease in dielectric constant of only 2.4×10^{-8} per foot of height results in a value of $k = \frac{4}{3}$, which is commonly assumed to be a good average value.[9] When the dielectric constant decreases about four times as rapidly (or by about 10^{-7} per foot of height), the value of $k = \infty$. Under such a condition, as far as radio propagation is concerned, the earth can then be considered flat, since any ray that starts parallel to the earth will remain parallel.

When the dielectric constant decreases more rapidly than 10^{-7} per foot of height, radio waves that are radiated parallel to, or at an angle above the earth's surface, may be bent downward sufficiently to be reflected from the earth. After reflection the ray is again bent toward the earth, and the path of a typical ray is similar to the path of a bouncing tennis ball. The radio energy appears to be trapped in a duct or waveguide between the earth and the maximum height of the radio path. This phenomenon is variously known as trapping, duct transmission, anomalous propagation, or guided propagation.[10, 11] It will be noted that in this case the path of a typical guided wave is similar in form to the path of sky waves, which are lower-frequency waves trapped between the

earth and the ionosphere. However, there is little or no similarity between the virtual heights, the critical frequencies, or the causes of refraction in the two cases.

Duct transmission is important because it can cause long distance interference with another station operating on the same frequency; however, it does not occur often enough nor can its occurrence be predicted with enough accuracy to make it useful for radio services requiring high reliability.

Diffraction Over a Smooth Spherical Earth and Ridges

Radio waves are also transmitted around the earth by the phenomenon of diffraction. Diffraction is a fundamental property of wave motion, and in optics it is the correction to apply to geometrical optics (ray theory) to obtain the more accurate wave optics. In other words, all shadows are somewhat "fuzzy" on the edges and the transition from "light" to "dark" areas is gradual, rather than infinitely sharp. Our common experience is that light travels in straight lines and that shadows are sharp, but this is only because the diffraction effects for these very short wavelengths are too small to be noticed without the aid of special laboratory equipment. The order of magnitude of the diffraction at radio frequencies may be obtained by recalling that a 1,000-mc radio wave has about the same wavelength as a 1,000-cycle sound wave in air, so that these two types of waves may be expected to bend around absorbing obstacles with approximately equal facility.

The effect of diffraction around the earth's curvature is to make possible transmission beyond the line-of-sight. The magnitude of the loss caused by the obstruction increases as either the distance or the frequency is increased and it depends to some extent on the antenna height.[12] The loss resulting from the curvature of the earth is indicated by Fig. 5 as long as neither antenna is higher than the limiting value shown at the top of the chart. This loss is in addition to the transmission loss over plane earth obtained from Fig. 2.

When either antenna is as much as twice as high as the limiting value shown on Fig. 5, this method of correcting for the curvature of the earth indicates a loss that is too great by about 2 db, with the error increasing as the antenna height increases. An alternate method of determining the effect of the earth's curvature is given by Fig. 6. The latter method is approximately correct for any antenna height, but it is theoretically limited in distance to points at or beyond the line-of-sight, assuming that the curved earth is the only obstruction. Fig. 6 gives the loss relative to free-space transmission (and hence is used with Fig. 1) as a func-

er, there is little or no similarity be-
tical frequencies, or the causes of re-

t because it can cause long distance
operating on the same frequency;
nough nor can its occurrence be pre-
ake it useful for radio services requir-

l Earth and Ridges

l around the earth by the phenomenon
damental property of wave motion,
to apply to geometrical optics (ray
ate wave optics. In other words, all
the edges and the transition from
l, rather than infinitely sharp. Our
avels in straight lines and that shad-
ause the diffraction effects for these
all to be noticed without the aid of
order agnitude of the diffraction
ed by recalling that a 1,000-mc radio
gth as a 1,000-cycle sound wave in
es may be expected to bend around
tely equal facility.
e earth's curvature is to make possi-
f-sight. The magnitude of the loss
s as either the distance or the fre-
ls to some extent on the antenna
curvature of the earth is indicated
a is higher than the limiting value
oss is in addition to the transmission
Fig. 2.
s twice as high as the limiting value
ecting for the curvature of the earth
bout 2 db, with the error increasing
lternate method of determining the
en by Fig. 6. The latter method is
ana height, but it is theoretically
beyond the line-of-sight, assuming
truction. Fig. 6 gives the loss rela-
ence is used with Fig. 1) as a func-

tion of three distances: d_1 is the distance to the horizon from the lower antenna, d_2 is the distance to the horizon from the higher antenna, and d_3 is the distance beyond the line-of-sight. In other words, the total distance between antennas, $d = d_1 + d_2 + d_3$. The distance to the horizon over smooth earth is given by:

$$d_{1,2} = \sqrt{2kah_{1,2}} \qquad (8)$$

where $h_{1,2}$ is the appropriate antenna height and ka is the effective earth's radius.

The preceding discussion assumes that the earth is a perfectly smooth sphere and the results are critically dependent on a smooth surface and a uniform atmosphere. The modification in these results caused by the

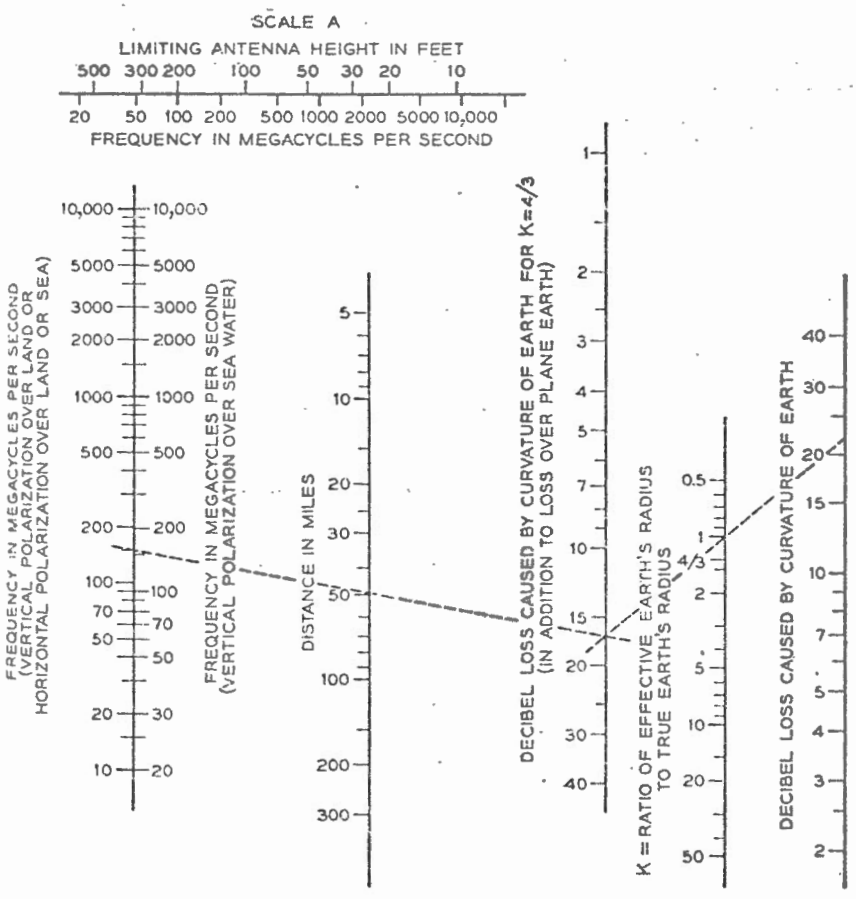

FIG. 5 — Diffraction loss around a perfect sphere.

presence of hills, trees, and buildings is difficult or impossible to compute, but the order of magnitude of these effects may be obtained from a consideration of the other extreme case, which is propagation over a perfectly absorbing knife edge.

The diffraction of plane waves over a knife edge or screen causes a shadow loss whose magnitude is shown on Fig. 7. The height of the obstruction H is measured from the line joining the two antennas to the top of the ridge. It will be noted that the shadow loss approaches 6 db

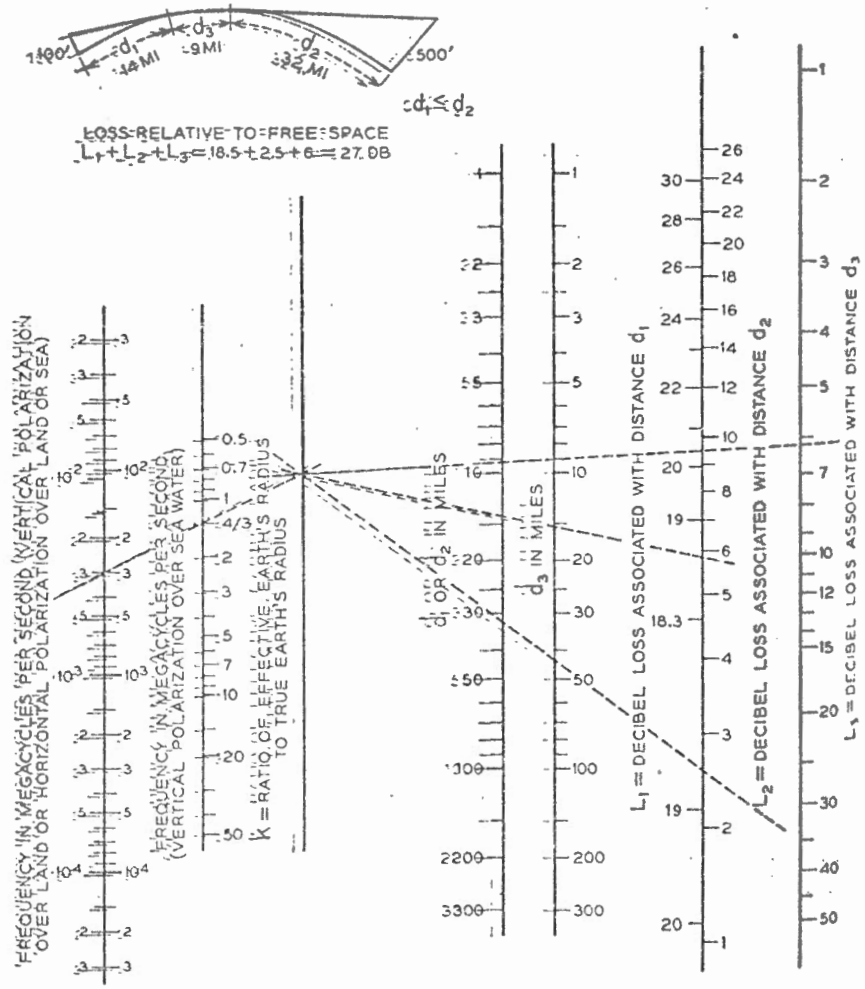

FIG. 6.—Diffraction loss relative to free-space transmission at all locations beyond line-of-sight over a smooth sphere.

s is difficult or impossible to compute,
e effects may be obtained from a con-
se, which is propagation over a per-

over a knife edge or screen causes a
own on Fig. 7. The height of the ob-
line joining the two antennas to the
hat the shadow loss approaches 6 db

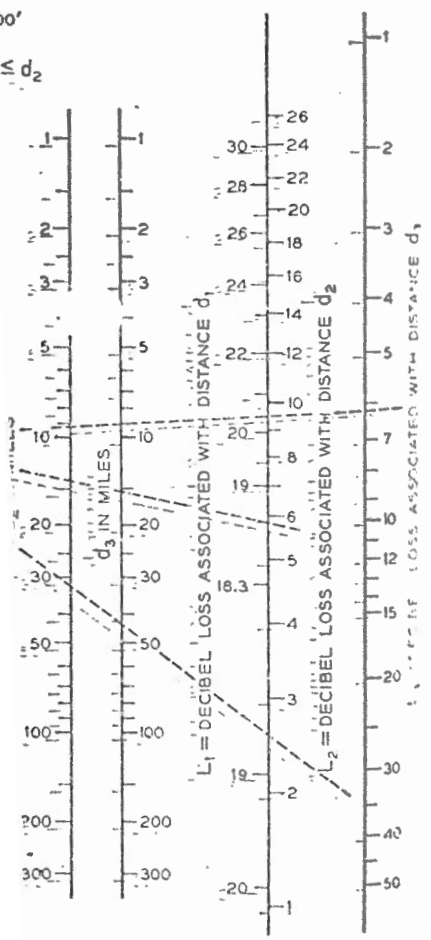

ee space transmission at all locatio

as H approaches 0 (grazing incidence), and that it increases with increasing positive values of H. When the direct ray clears the obstruction, H is negative, and the shadow loss approaches 0 db in an oscillatory manner as the clearance is increased. In other words, a substantial clearance is required over line-of-sight paths in order to obtain "free-space" transmission. The knife edge diffraction calculation is substantially independent of polarization as long as the distance from the edge is more than a few wavelengths.

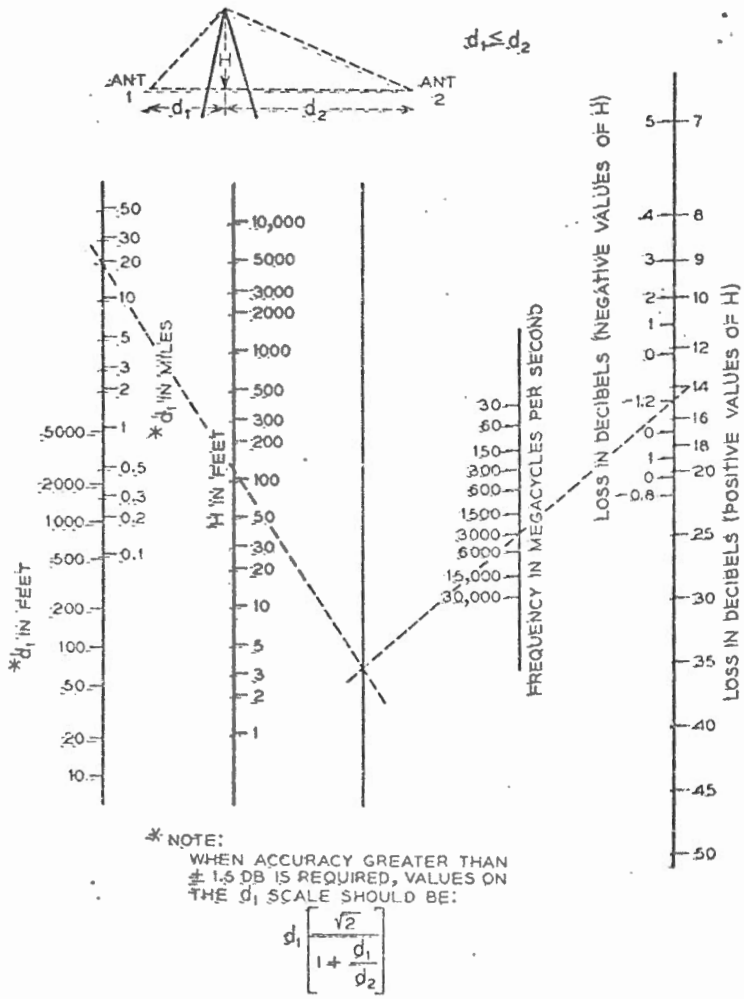

FIG. 7 — Knife-edge diffraction loss relative to free space.

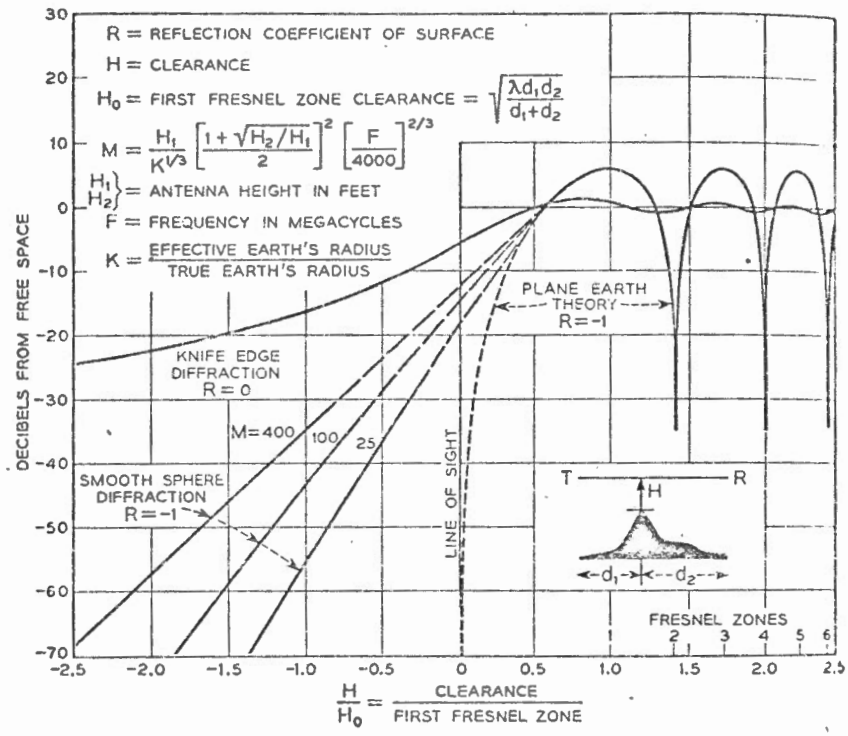

FIG. 8 — Transmission loss versus clearance.

At grazing incidence, the expected loss over a ridge is 6 db (Fig. 7) while over a smooth spherical earth Fig. 6 indicates a loss of about 20 db. More accurate results in the vicinity of the horizon can be obtained by expressing radio transmission in terms of path clearance measured in Fresnel zones as shown in Fig. 8. In this representation the plane earth theory and the ridge diffraction can be represented by single lines; but the smooth sphere theory requires a family of curves with a parameter M that depends primarily on antenna heights and frequency. The big difference in the losses predicted by diffraction around a perfect sphere and by diffraction over a knife edge indicates that diffraction losses depend critically on the assumed type of profile. A suitable solution for the intermediate problem of diffraction over a rough earth has not yet been obtained.

Experimental Data Far Beyond the Horizon

Most of the experimental data at points far beyond the horizon fall in between the theoretical curves for diffraction over a smooth sphere

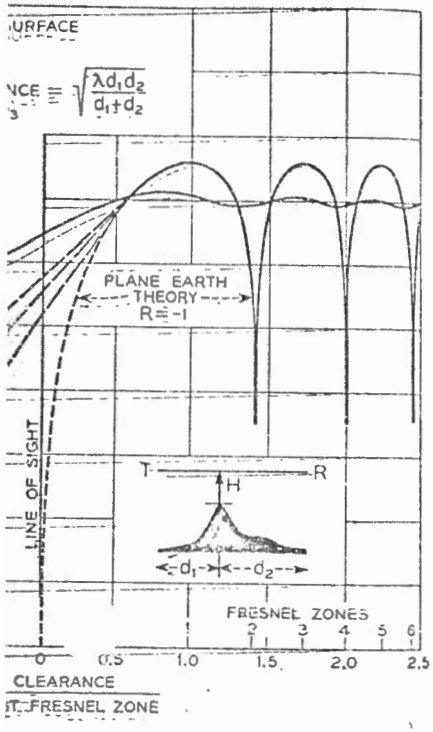

n loss versus clearance.

ed loss over a ridge is 6 db (Fig. 7) n Fig. 6 indicates a loss of about 20 inity of the horizon can be obtained n terms of path clearance measured 8. In this representation the plane on can be represented by single lines; res a family of curves with a param- antenna heights and frequency. The ed by diffraction around a perfect nife edge indicates that diffraction med type of profile. A suitable solu- f diffraction over a rough earth has

Horizon

t points far beyond the horizon fall or diffraction over a smooth sphere

and for diffraction over a knife edge obstruction. Various theories have been advanced to explain these effects but none has been reduced to a simple form for every day use.[13] The explanation most commonly accepted is that energy is reflected or scattered from turbulent air masses in the volume of air that is enclosed by the intersection of the beamwidths of the transmitting and receiving antennas.[14]

The variation in the long term median signals with distance has been derived from experimental results and is shown in Fig. 9 for two frequencies.[15] The ordinate is in db below the signal that would have been expected at the same distance in free space with the same power and the same antennas. The strongest signals are obtained by pointing the antennas at the horizon along the great circle route. The values shown on Fig. 9 are essentially annual averages taken from a large number of paths, and substantial variations are to be expected with terrain, climate, and season as well as from day to day fading.

Antenna sites with sufficient clearance so that the horizon is several miles away will, on the average, provide a higher median signal (less loss) than shown on Fig. 9. Conversely, sites for which the antenna must be pointed upward to clear the horizon will ordinarily result in appreciably more loss than shown on Fig. 9. In many cases the effects of path length and angles to the horizon can be combined by plotting the experimental results as a function of the angle between the lines drawn tangent to the horizon from the transmitting and receiving sites.[16]

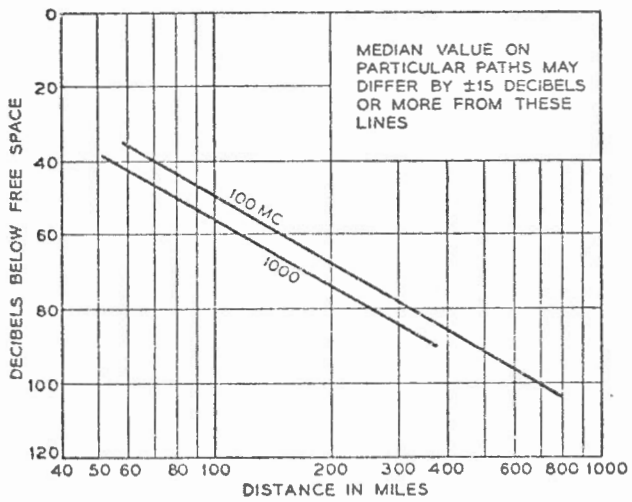

Fig. 9 — Beyond-horizon transmission — median signal level versus distance.

When the path profile consists of a single sharp obstruction that can be seen from both terminals, the signal level may approach the value predicted by the knife edge diffraction theory.[17] While several interesting and unusual cases have been recorded, the knife edge or "obstacle gain" theory is not applicable to the typical but only to the exceptional paths.

As in the case of line-of-sight transmission the fading of radio signals beyond the horizon can be divided into fast fading and slow fading. The fast fading is caused by multipath transmission in the atmosphere, and for a given size antenna, the rate of fading increases as either the frequency or the distance is increased. This type of fading is much faster than the maximum fast fading observed on line of sight paths, but the two are similar in principle. The magnitude of the fades is described by the Rayleigh distribution.

Slow fading means variations in average signal level over a period of hours or days and it is greater on beyond horizon paths than on line-of-sight paths. This type of fading is almost independent of frequency and seems to be associated with changes in the average refraction of the atmosphere. At distances of 150 to 200 miles the variations in hourly median value around the annual median seem to follow a normal probability law in db with a standard deviation of about 8 db. Typical fading distributions are shown on Fig. 10.

The median signal levels are higher in warm humid climates than in cold dry climates and seasonal variations of as much as ±10 db or more from the annual median have been observed.[18]

Since the scattered signals arrive with considerable phase irregularities in the plane of the receiving antenna, narrow-beamed (high gain) antennas do not yield power outputs proportional to their theoretical area gains. This effect has sometimes been called loss in antenna gain, but it is a propagation effect and not an antenna effect. On 150 to 200 miles this loss in received power may amount to one or two db for a 40 db gain antenna, and perhaps six to eight db for a 50 db antenna. These extra losses vary with time but the variations seem to be uncorrelated with the actual signal level.

The bandwidth that can be used on a single radio carrier is frequently limited by the selective fading caused by multipath or echo effects. Echoes are not troublesome as long as the echo time delays are very short compared with one cycle of the highest baseband frequency. The probability of long delayed echoes can be reduced (and the rate of fast fading can be decreased) by the use of narrow beam antennas both within and beyond the horizon.[19, 20] Useful bandwidths of several mega-

single sharp obstruction that can
al level may approach the value
a theory.[17] While several interest-
rded, the knife edge or "obstacle
ypical but only to the exceptional

nission the fading of radio signals
o fast fading and slow fading. The
nsmission in the atmosphere, and
fading increases as either the fre-
This type of fading is much faster
ed on line of sight paths, but the
nitude of the fades is described by

erage signal level over a period of
ond horizon paths than on line-of-
ost independent of frequency and
in the average refraction of the
200 miles the variations in hourly
an seem to follow a normal proba-
tion out 8 db. Typical fading

r in warm humid climates than in
ons of as much as ±10 db or more
oserved.[18]
th considerable phase irregularities
narrow-beamed (high gain) anten-
portional to their theoretical area
called loss in antenna gain, but it
ntenna effect. On 150 to 200 miles
ount to one or two db for a 40 db
ght db for a 50 db antenna. These
variations seem to be uncorrelated

a single radio carrier is frequently
sed by multipath or echo effects.
as the echo time delays are very
e highest baseband frequency. The
an be reduced (and the rate of fast
se of narrow beam antennas both
Useful bandwidths of several mega-

cycles appear to be feasible with the antennas that are needed to provide adequate signal-to-noise margins. Successful tests of television and of multichannel telephone transmission have been reported on a 188-mile path at 5,000 mc.[21]

The effects of fast fading can be reduced substantially by the use of either frequency or space diversity. The frequency or space separation required for diversity varies with time and with the degree of correlation that can be tolerated. A horizontal (or vertical) separation of about 100 wavelengths is ordinarily adequate for space diversity on 100- to 200-mile paths. The corresponding figure for the required frequency separation for adequate diversity seems likely to be more than 20 mc.

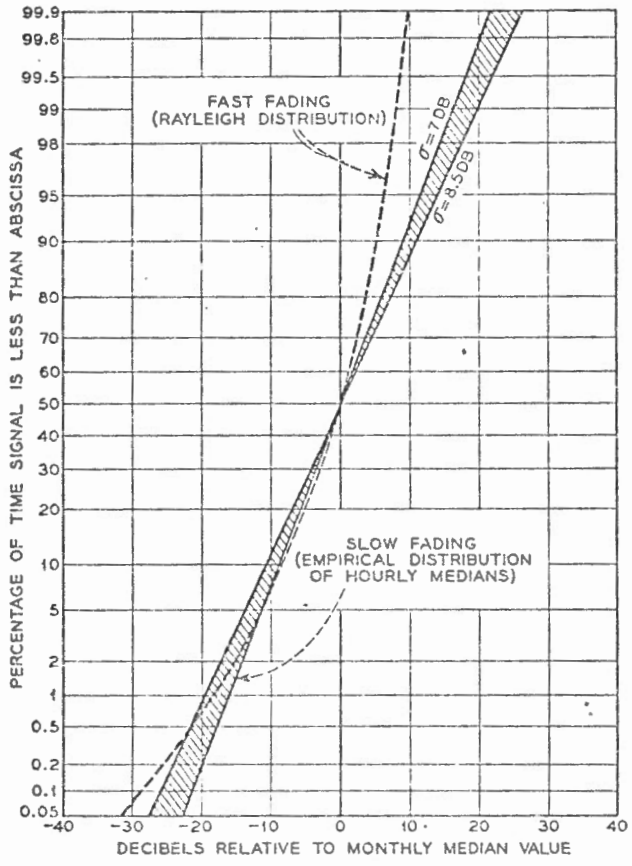

FIG. 10 — Typical fading characteristics at points far beyond the horizon.

Effects of Nearby Hills — Particularly on Short Paths

The experimental results on the effects of hills indicate that the shadow losses increase with the frequency and with the roughness of the terrain.[22]

An empirical summary of the available data is shown on Fig. 11. The roughness of the terrain is represented by the height H shown on the profile at the top of the chart. This height is the difference in elevation between the bottom of the valley and the elevation necessary to obtain line of sight from the transmitting antenna. The right hand scale in Fig. 11 indicates the additional loss above that expected over plane earth. Both the median loss and the difference between the median and the 10 per cent values are shown. For example, with variations in terrain of 500 feet, the estimated median shadow loss at 450 mc is about 20 db and the

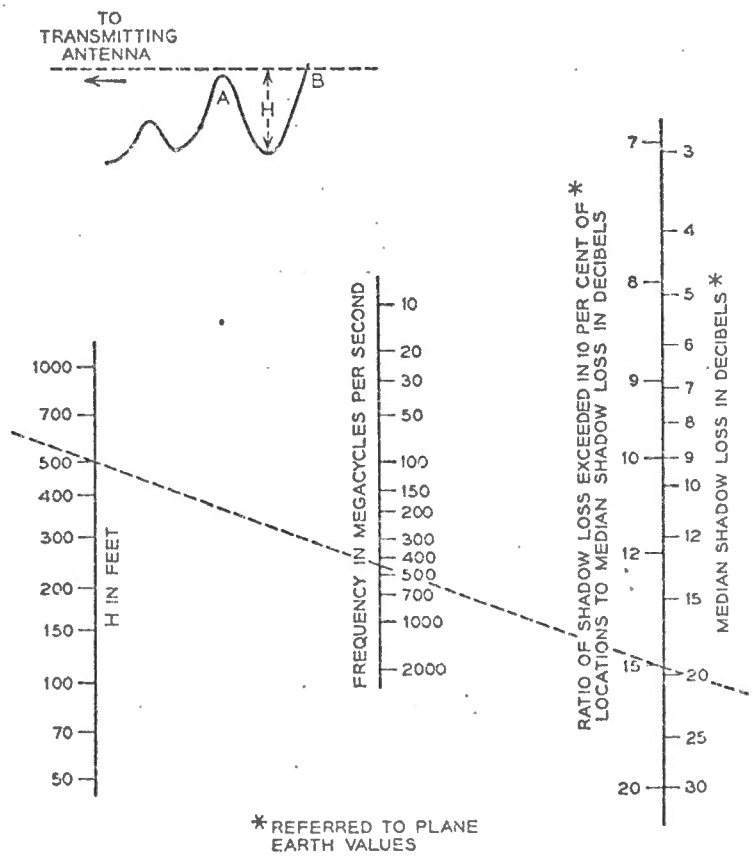

FIG. 11 — Estimated distribution of shadow losses.

y on Short Paths

ects of hills indicate that the shadow
d with the roughness of the terrain.[22]
lable data is shown on Fig. 11. The
ted by the height H shown on the
height is the difference in elevation
d the elevation necessary to obtain
ntenna. The right hand scale in Fig.
ve that expected over plane earth.
nce between the median and the 10
ple, with variations in terrain of 500
ss at 450 mc is about 20 db and the

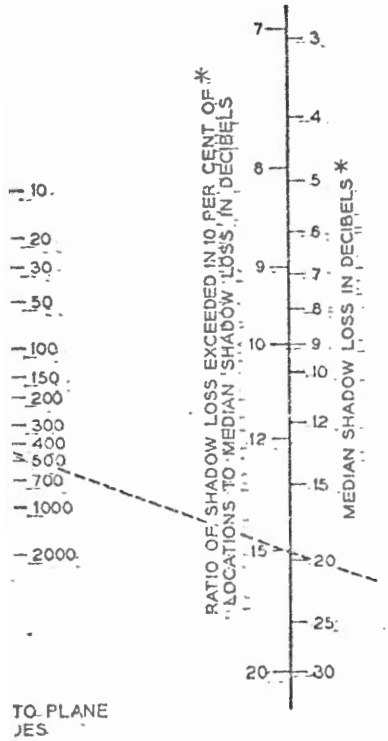

bution of shadow losses.

shadow loss exceeded in only 10 per cent of the possible locations between points A and B is about $20 + 15 = 35$ db. It will be recognized that this analysis is based on large-scale variations in field intensity, and does not include the standing wave effects which sometimes cause the field intensity to vary considerably within a few feet.

Effects of Buildings and Trees

The shadow losses resulting from buildings and trees follow somewhat different laws from those caused by hills. Buildings may be more transparent to radio waves than the solid earth, and there is ordinarily much more back scatter in the city than in the open country. Both of these factors tend to reduce the shadow losses caused by the buildings but, on the other hand, the angles of diffraction over or around the buildings are usually greater than for natural terrain. In other words, the artificial canyons caused by buildings are considerably narrower than natural valleys, and this factor tends to increase the loss resulting from the presence of buildings. The available quantitative data on the effects of buildings are confined primarily to New York City. These data indicate that in the range of 40 to 450 mc there is no significant change with frequency, or at least the variation with frequency is somewhat less than that noted in the case of hills.[23] The median field intensity at street level for random locations in Manhattan (New York City) is about 25 db below the corresponding plane earth value. The corresponding values for the 10 per cent and 90 per cent points are about 15 and 35 db, respectively.

Typical values of attenuation through a brick wall, are from 2 to 5 db at 30 mc and 10 to 40 db at 3,000 mc, depending on whether the wall is dry or wet. Consequently most buildings are rather opaque at frequencies of the order of thousands of megacycles.

When an antenna is surrounded by moderately thick trees and below tree-top level, the average loss at 30 mc resulting from the trees is usually 2 or 3 db for vertical polarization and is negligible with horizontal polarization. However, large and rapid variations in the received field intensity may exist within a small area, resulting from the standing-wave pattern set up by reflections from trees located at a distance of several wavelengths from the antenna. Consequently, several near-by locations should be investigated for best results. At 100 mc the average loss from surrounding trees may be 5 to 10 db for vertical polarization and 2 or 3 db for horizontal polarization. The tree losses continue to increase as the frequency increases, and above 300 to 500 mc they tend to be independent of the type of polarization. Above 1,000 mc, trees that are thick

enough to block vision are roughly equivalent to a solid obstruction of the same over-all size.

IV. MEDIUM AND LOW FREQUENCY GROUND WAVE TRANSMISSION

Wherever the antenna heights are small compared with the wavelength, the received field intensity is ordinarily stronger with vertical polarization than with horizontal and is stronger over sea water than over poor soil. In these cases the "surface wave" term in (3) cannot be neglected. This use of the term "surface wave" follows Norton's usage and is not equivalent to the Sommerfeld or Zenneck "surface waves."

The parameter A is the plane earth attenuation factor for antennas at ground level. It depends upon the frequency, ground constants, and type of polarization. It is never greater than unity and decreases with increasing distance and frequency, as indicated by the following approximate equation:[24, 25]

$$A \approx \frac{-1}{1 + j\frac{2\pi d}{\lambda}(\sin\theta + z)^2} \tag{9}$$

where

$z = \dfrac{\sqrt{\epsilon_0 - \cos^2\theta}}{\epsilon_0}$ for vertical polarization

$z = \sqrt{\epsilon_0 - \cos^2\theta}$ for horizontal polarization

$\epsilon_0 = \epsilon - j60\sigma\lambda$

θ = angle between reflected ray and the ground

= 0 for antennas at ground level

ϵ = dielectric constant of the ground relative to unity in free space

σ = conductivity of the ground in mhos per meter

λ = wavelength in meters

In terms of these same parameters the reflection coefficient of the ground is given by[26]

$$R = \frac{\sin\theta - z}{\sin\theta + z} \tag{10}$$

When $\theta \ll |z|$ the reflection coefficient approaches -1; when $\theta \gg |z|$

equivalent to a solid obstruction of

GROUND WAVE TRANSMISSION

are small compared with the wave-
is ordinarily stronger with vertical
and is stronger over sea water than
surface wave" term in (3) cannot be
urface wave" follows Norton's usage
erfeld or Zenneck "surface waves."
arth attenuation factor for antennas
he frequency, ground constants, and
eater than unity and decreases with
as indicated by the following approxi-

$$\frac{-1}{\frac{2\pi d}{\lambda}(\quad + z)^2} \tag{9}$$

olarization

al polarization

and the ground

evel

ground relative to unity in free space

in mhos per meter

eters the reflection coefficient of the

$$\frac{\sin\theta - z}{\sin\theta + z} \tag{10}$$

icient approaches -1; when $\theta \gg |$

(which can happen only with vertical polarization) the reflection coefficient approaches $+1$. The angle for which the reflection coefficient is a minimum is called the pseudo-Brewster angle and it occurs for $\sin\theta = |z|$.

For antennas approaching ground level the first two terms in (3) cancel each other (h_1 and h_2 approach zero and R approaches -1) and the magnitude of the third term becomes

$$|(1 - R)A| \approx \frac{2}{\frac{2\pi d}{\lambda} z^2} = \frac{4\pi h_0^2}{\lambda d} \tag{11}$$

where h_0 = minimum effective antenna height shown in Fig. 3

$$= \left|\frac{\lambda}{2\pi z}\right|$$

The surface wave term arises because the earth is not a perfect reflector. Some energy is transmitted into the ground and sets up ground currents, which are distorted relative to what would have been the case in an ideal perfectly reflecting surface. The surface wave is defined as the vertical electric field for vertical polarization, or the horizontal electric field for horizontal polarization, that is associated with the extra components of the ground currents caused by lack of perfect reflection. Another component of the electric field associated with the ground currents is in the direction of propagation. It accounts for the success of the wave antenna at lower frequencies, but it is always smaller in magnitude than the surface wave as defined above. The components of the electric vector in three mutually perpendicular co-ordinates are given by Norton.[27]

In addition to the effect of the earth on the propagation of radio waves, the presence of the ground may also affect the impedance of low antennas and thereby may have an effect on the generation and reception of radio waves.[28] As the antenna height varies, the impedance oscillates around the free space value, but the variations in impedance are usually unimportant as long as the center of the antenna is more than a quarter-wavelength above the ground. For vertical grounded antennas (such as are used in standard AM broadcasting) the impedance is doubled and the net effect is that the maximum field intensity is 3 db above the free space value instead of 6 db as indicated in (4) for elevated antennas.

Typical values of the field intensity to be expected from a grounded quarter-wave vertical antenna are shown in Fig. 12 for transmission over poor soil and in Fig. 13 for transmission over sea-water. These charts in-

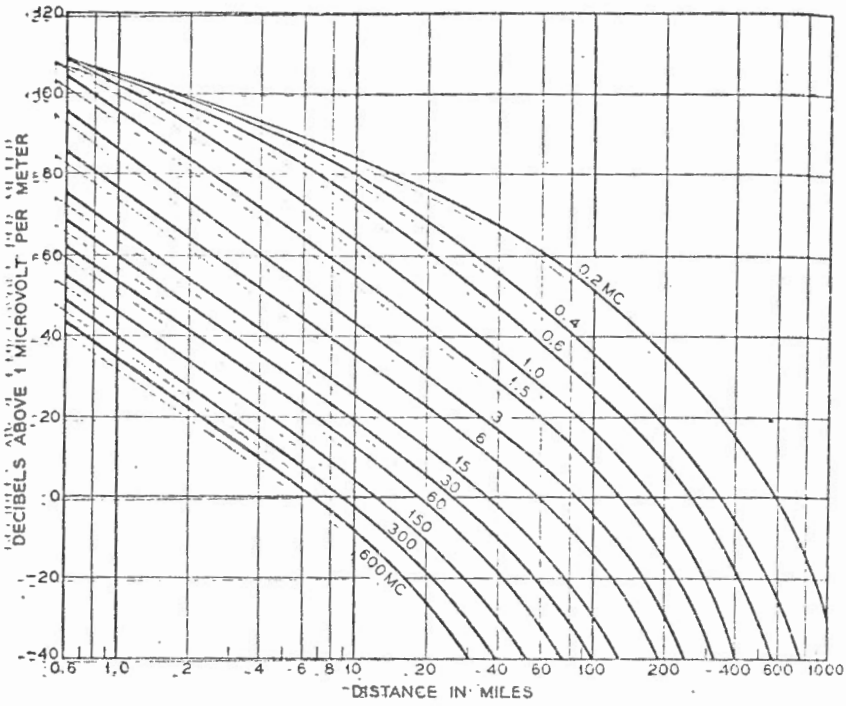

FIG. 12—Field intensity for vertical polarization over poor soil for 1-kw radiated power from a grounded whip antenna.

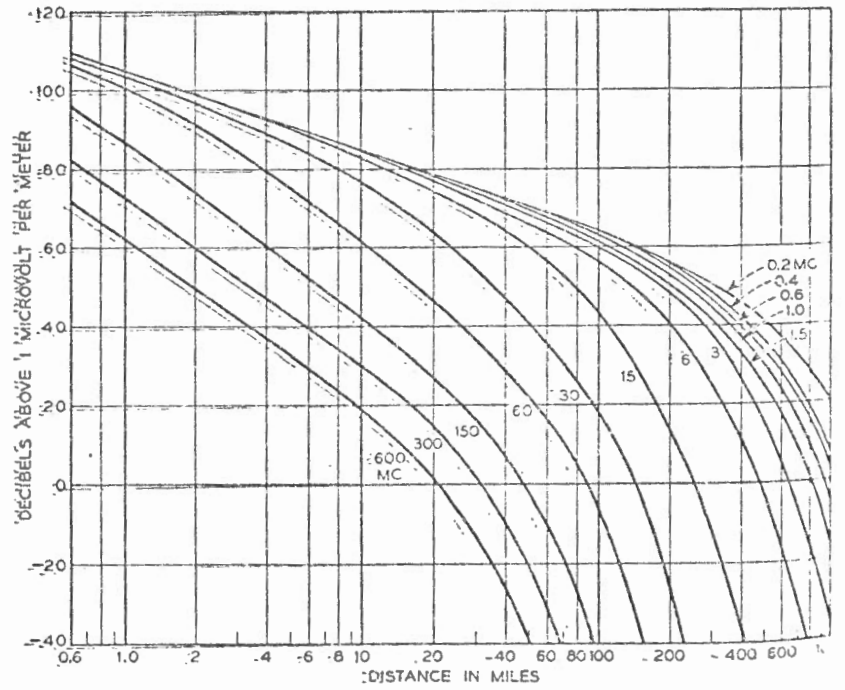

FIG. 13—Field intensity for vertical polarization over sea water for 1 kw radiated power from a grounded whip antenna.

clude the effe
spherical earth
spheric effect
tained by ra
and Fig. 15 fo

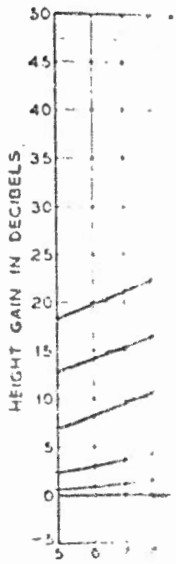

FIG. 11

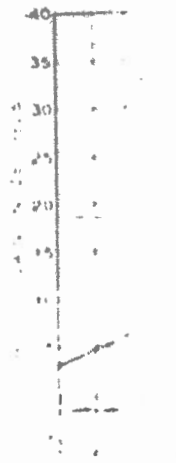

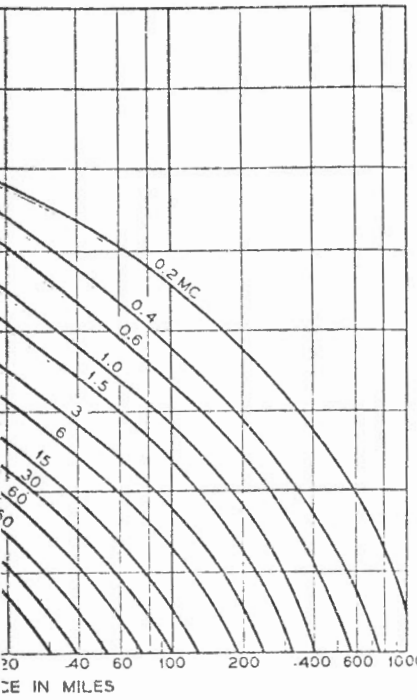

cal p ation over poor soil for 1-kw
anten

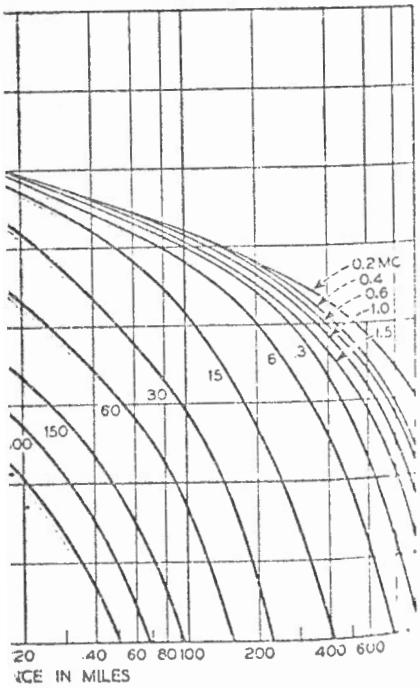

al po ition over sea water for 1
nteun

516

clude the effect of diffraction and average refraction around a smooth spherical earth as discussed in Section III, but do not include the ionospheric effects described in the next Section. The increase in signal obtained by raising either antenna height is shown in Fig. 14 for poor soil and Fig. 15 for sea water.

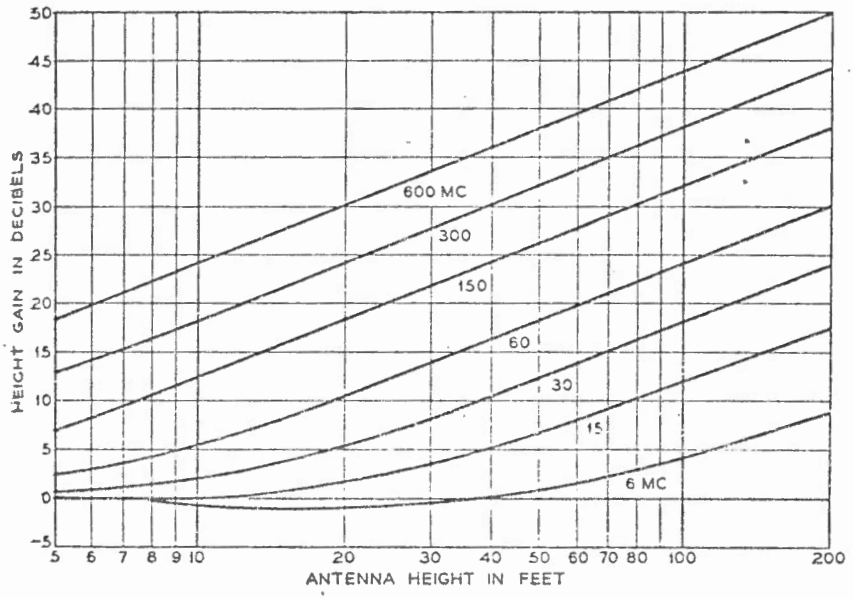

FIG. 14 — Antenna height gain factor for vertical polarization over poor soil.

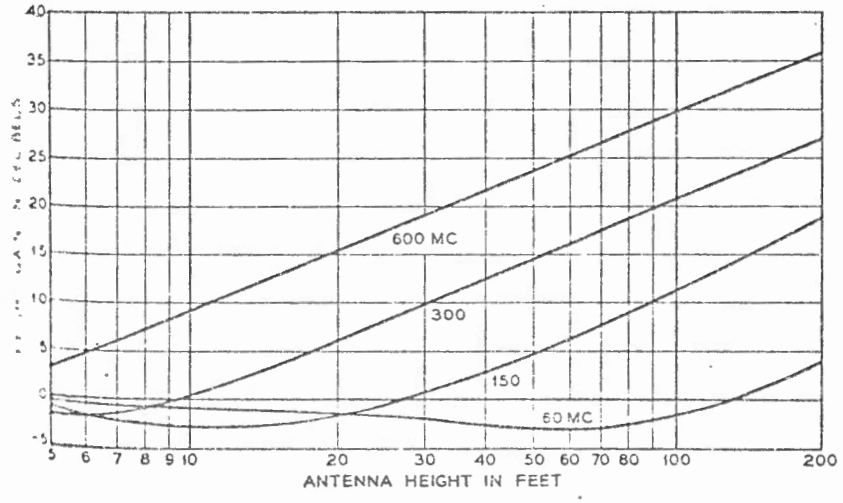

FIG. 15 — Antenna height gain factor for vertical polarization over sea water.

V. IONOSPHERIC TRANSMISSION

In addition to the tropospheric or ground wave transmission discussed in the preceding sections, useful radio energy at frequencies below about 25 to 100 mc may be returned to the earth by reflection from the ionosphere, which consists of several ionized layers located 50 to 200 miles above the earth. The relatively high density of ions and free electrons in this region provides an effective index of refraction of less than one, and the resulting transmission path is similar to that in the well known optical phenomenon of total internal reflection. The mechanism is generally spoken of as reflection from certain virtual heights.[29] Polarization is not maintained in ionospheric transmission and the choice depends on the antenna design that is most efficient at the desired elevation angles.

Regular Ionospheric Transmission

The ionosphere consists of three or more distinct layers. This does not mean that the space between layers is free of ionization but rather that the curve of ion density versus height has several distinct peaks. The *E*, *F*1, and *F*2 layers are present during the daytime but the F_1 and F_2 combine to form a single layer at night. A lower layer called the *D* layer is also present during the day, but its principal effect is to absorb rather than reflect.

Information about the nature of the inosphere has been obtained by transmitting pulsed radio signals directly overhead and by recording the signal intensity and the time delay of the echoes returned from these layers. At night all frequencies below the critical frequency f_c are returned to earth with an average signal intensity that is about 3 to 6 db below the free space signal that would be expected for the round trip distance. At frequencies higher than the critical frequency the signal intensity is very weak or undetectable. Typical values of the critical frequency for Washington, D. C., are shown in Fig. 16.

During the daytime, the critical frequency is increased 2 to 3 times over the corresponding nighttime value. This apparent increase in the useful frequency range for ionospheric transmission is largely offset by the heavy daytime absorption which reaches a maximum in the 1 to 2 mc range. This absorption is caused by interaction between the free electrons and the earth's magnetic field. The absence of appreciable absorption at night indicates that most of the free electrons disappear when the sun goes down. Charged particles traveling in a magnetic field have a resonant or gyromagnetic frequency, and for electrons in the earth's magnetic field, of about 0.5 gauss, this resonance occurs at about 1 1

r ground wave transmission discussed
dio energy at frequencies below about
he earth by reflection from the iono-
onized layers located 50 to 200 miles
h density of ions and free electrons in
dex of refraction of less than one, and
milar to that in the well known optical
ection. The mechanism is generally
virtual heights.[29] Polarization is not
ssion and the choice depends on the
it at the desired elevation angles.

or more distinct layers. This does not
s is free of ionization but rather that
ight has several distinct peaks. The
uring the daytime but the F_1 and F_2
ight. A lower layer called the D layer
its principal effect is to absorb rather

of the ionosphere has been obtained
ls directly overhead and by record-
ne delay of the echoes returned from
es below the critical frequency f_c are
signal intensity that is about 3 to 6
it would be expected for the round
than the critical frequency the signal
able. Typical values of the critical
re shown in Fig. 16.
frequency is increased 2 to 3 times
alue. This apparent increase in the
eric transmission is largely offset by
h reaches a maximum in the 1 to 2-
by interaction between the free elec-
. The absence of appreciable absorp
of the free electrons disappear when
es traveling in a magnetic field have
ncy, and for electrons in the earth's
this resonance occurs at about 1.4

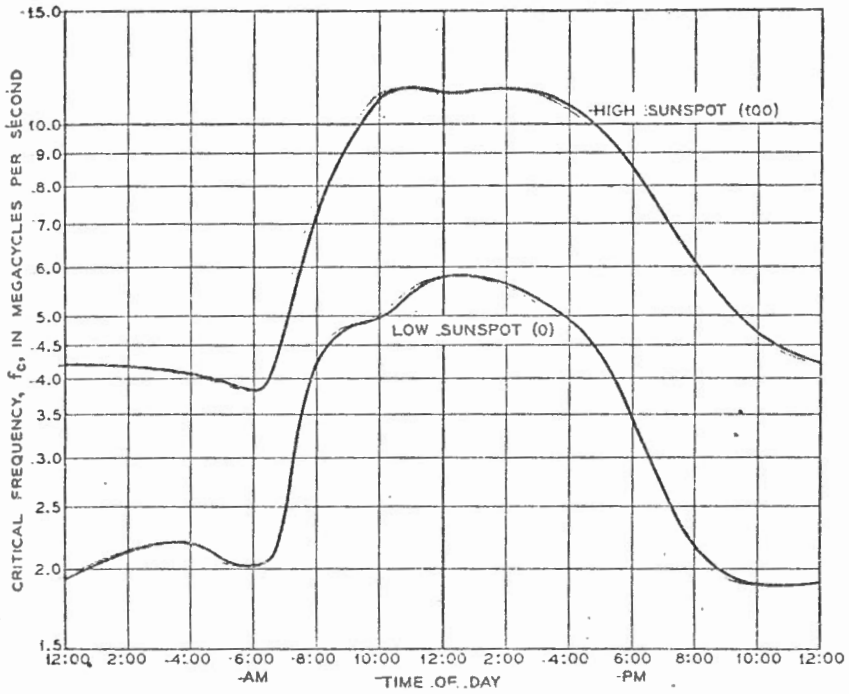

FIG. 16 — Typical diurnal variation of critical frequency for January at latitude 40 degrees.

me. The magnitude of the absorption varies with the angle of the sun above the horizon and is a maximum about noon. The approximate midday absorption is shown on Fig. 17 in terms of db per 100 miles of path length. (On short paths this length is the actual path traveled, not the distance along the earth's surface.)

Long distance transmission requires that the signal be reflected from the ionosphere at a small angle instead of the perpendicular incidence used in obtaining the critical frequency. For angles other than directly overhead an assumption which seems to be borne out in practice is that the highest frequency for which essentially free space transmission is obtained is $f_c/\sin \alpha$, where α is the angle between the radio ray and ionospheric layer. This limiting frequency is greater than the critical frequency and is called the maximum usable frequency which is usually abbreviated muf. The curved geometry limits the distance that can be obtained with one-hop transmission to about 2,500 miles and the muf at the longer distances does not exceed 3 to 3.5 times the critical frequency.

The difference between day and night effects means that most sky-

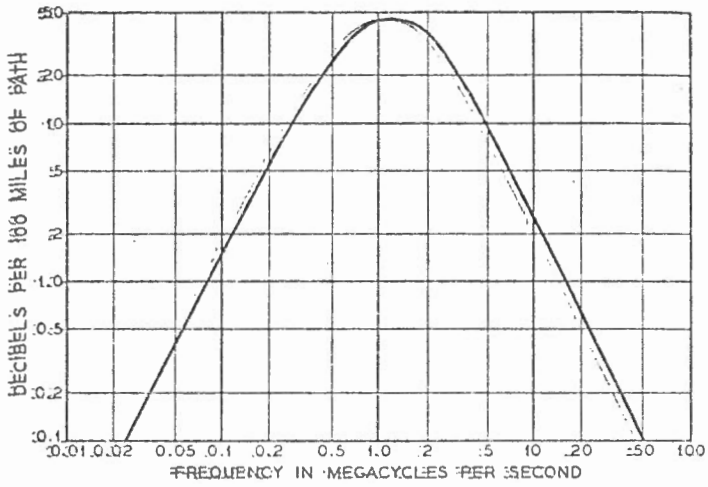

FIG. 17 — Typical values of midday ionospheric absorption.

wave paths require at least two frequencies. A relatively low frequency is needed to get under the nighttime muf and a higher frequency is needed that is below the daytime muf but above the region of high absorption. This lower limit depends on the available signal-to-noise margin and is commonly called the lowest useful high frequency.

Frequencies most suitable for transmission of 1000 miles or more will ordinarily not be reflected at the high angles needed for much shorter distances. As a result the range of skywave transmission ordinarily does not overlap the range of groundwave transmission, and the intermediate region is called the skip zone because the signal is too weak to be useful. At frequencies of a few megacycles the groundwave and skywave ranges may overlap with the result that severe fading occurs when the two signals are comparable in amplitude.

In addition to the diurnal variations in frequency and in absorption there are systematic changes with season, latitude, and with the nominally eleven-year sunspot cycle. Random changes in the critical frequency of about ±15 per cent from the monthly median value are also to be expected from day to day.

The F layer is the principal contributor to transmission beyond 1,000 to 1,500 miles and typical values of the maximum usable frequency can be summarized as follows: The median nighttime critical frequency for F layer transmission at the latitude at Washington, D. C., is about 2 mc in the month of June during a period of low sunspot activity. All frequencies below about 2 mc are strongly reflected to earth while the higher

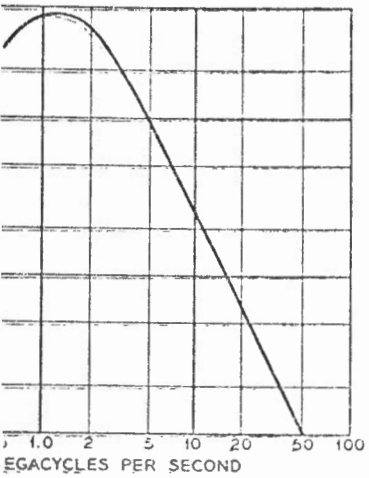

midday ionospheric absorption.

equencies. A relatively low frequency
time muf and a higher frequency is
e mu above the region of high
nds on the available signal-to-noise
e lowest useful high frequency.
ansmission of 1000 miles or more will
high angles needed for much shorter
skywave transmission ordinarily does
re transmission, and the intermediate
se the signal is too weak to be useful.
the groundwave and skywave ranges
severe fading occurs when the two
e.

ions in frequency and in absorption
season, latitude, and with the nom-
random changes in the critical fre-
the monthly median value are also

butor to transmission beyond 1,000 to
e maximum usable frequency can be
nighttime critical frequency for F
t Washington, D. C., is about 2 mc
od of low sunspot activity. All fre
gly reflected to earth while the high-

frequencies are either greatly attenuated or are lost in outer space. The approximate maximum usable frequency for other conditions is greater than 2 mc by the ratios shown in Table I.

TABLE I

Variation With	Multiplying factor
(1) Time of Day	
Midnight	1 (Reference)
Early Afternoon—June	2
December	3
(2) Path Length	
Less than 200 Miles	1 (Reference)
Approx. 1000 Miles	2
More than 2500 Miles	3.5
(3) Sunspot Cycle	
Minimum	1 (Reference)
For one year in five—June	1.5
December	2
For one year in fifty—June	2
December	3

When all of the above variations add "in phase," transmission for distances of 2,500 miles or more is possible at frequencies up to 40 to 60 mc. For example, using the table, 2,500-mile transmission on an early December afternoon in one year out of five can be expected on a frequency of about 42 mc, which is $3 \times 3.5 \times 2 = 21$ times the reference critical frequency of 2 mc. Peaks of the sunspot cycle occurred in 1937 and in 1947–1948 so another peak is expected in 1958–1959.

The maximum usable frequency also varies with the geomagnetic latitude but, as a first approximation, the above values are typical of continental U. S. Forecasts of the muf to be expected throughout the world are issued monthly by the National Bureau of Standards.[30, 31] These estimates include the diurnal, seasonal, and sunspot effects.

Another type of absorption, over and above the usual daytime absorption, occurs both day and night on transmission paths that travel through the auroral zone. The auroral zones are centered on the north and south magnetic poles at about the same distance as the Arctic Circle is from the geographical north pole. During periods of magnetic storms these auroral zones expand over an area much larger than normal and thereby disrupt communication by introducing unexpected absorption. These conditions of poor transmission can last for hours and sometimes even for days. These periods of increased absorption are more common in the polar regions than in the temperate zones or the tropics because of the proximity of the auroral zone and are frequently called HF "blackouts." During a "blackout," the signal level is decreased considerably

but the signal does not drop out completely. It appears possible that the outage time normally associated with HF transmission could be greatly reduced by the use of transmitter power and antenna size comparable to that needed in the ionospheric scatter method described below.

In addition to the auroral-zone absorption, there are shorter periods of severe absorption over the entire hemisphere facing the sun. These erratic and unpredictable effects which seem to be associated with eruptions on the sun are called sudden ionospheric disturbances (SID's) or the Dellinger effect.

The preceding information is based primarily on F layer transmission. The E layer is located closer to the earth than the F layer and the maximum transmission distance for a single reflection is about 1,200 miles.

Reflections from the E layer sometimes occur at frequencies above about 20 mc but are erratic in both time and space. This phenomenon has been explained by assuming that the E layer contains clouds of ionization that are variable in size, density, and location. The maximum frequency returned to earth may at times be as high as 70 or 80 mc.[32] The high values are more likely to occur during the summer, and during the minimum of the sunspot cycle.

Rapid multipath fading exists on ionospheric circuits and is superimposed on the longer term variations discussed above. The amplitude of the fast fading follows the Rayleigh distribution and echo delays up to several milliseconds are observed. These delays are 10^4 to 10^5 times as long as for tropospheric transmission. As a result of these relatively long delays uncorrelated selective fading can occur within a few hundred cycles. This produces the distortion on voice circuits that is characteristic of "short wave" transmission.

Ionospheric Scatter

The maximum usable frequency used in conventional skywave transmission is defined as the highest frequency returned to earth for which the average transmission is within a few db of free space. As the frequency increases above the muf the signal level decreases rapidly but does not drop out completely. Although the signal level is low, reliable transmission can be obtained at frequencies up to 50 mc or higher and to distances up to at least 1,200 to 1,500 miles.[33] In this case the signal is 80 to 100 db below the free-space value and its satisfactory use requires much higher power and larger antennas than are ordinarily used in ionospheric transmission. The approximate variation in median signal level with frequency is shown in Fig. 18.

Ionospheric scatter is apparently the result of reflections from many

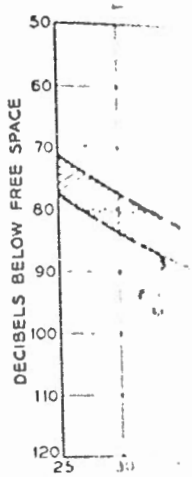

FIG. 18 M

patches of ioniza
important in
has not been cl

In common
a Rayleigh di
tive to the long
sporadic E tra
probability law

Ionospheric
channels but th
fading that is ch

VI. NOISE LEVE

The usefulne
ceiver. This
first circuit

Atmospheri
few megacycl
above 200 to
depends on th
static, man
The the
of the elec

mpletely. It appears possible that the
ith IIF transmission could be greatly
power and antenna size comparable
catter method described below.
absorption, there are shorter periods
ire hemisphere facing the sun. These
hich seem to be associated with erup-
ı ionospheric disturbances (SID's) or

sed primarily on F layer transmission.
earth than the F layer and the maxi-
single reflection is about 1,200 miles.
ometimes occur at frequencies above
.h time and space. This phenomenon
that the E layer contains clouds of
density, and location. The maximum
at times be as high as 70 or 80 mc.[32]
occur during the summer, and during

on ionospheric circuits and is super-
ions discussed above. The amplitude
eigh ibution and echo delays up
d. These delays are 10^4 to 10^5 times as
sion. As a result of these relatively
ading can occur within a few hundred
ı on voice circuits that is characteris-

used in conventional skywave trans-
equency returned to earth for which
ı a few db of free space. As the fre-
he signal level decreases rapidly but
ıough the signal level is low, reliable
equencies up to 50 mc or higher and
) 1,500 miles.[33] In this case the signal
ıce value and its satisfactory use r
er antennas than are ordinarily used
proximate variation in median signa
ig. 18.
the result of reflections from many

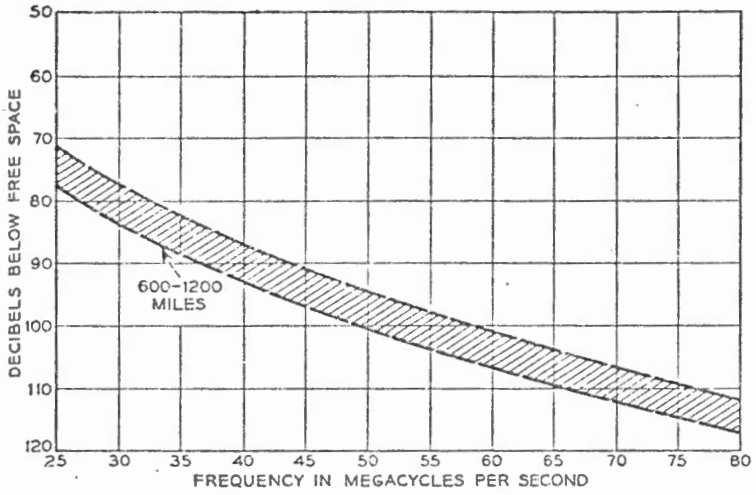

FIG. 18 — Median signal levels for ionospheric scatter transmission.

patches of ionization in the *E* layer. It is suspected that meteors are important in establishing and in maintaining this ionization but this has not been clearly determined.

In common with other types of transmission, the fast fading follows a Rayleigh distribution. The distribution of hourly median values relative to the long term median (after the high signals resulting from sporadic *E* transmission have been removed) is approximately a normal probability law with a standard deviation of about 6 to 8 db.

Ionospheric scatter transmission is suitable for several telegraph channels but the useful bandwidth is limited by the severe selective fading that is characteristic of all ionospheric transmission.

VI. NOISE LEVELS

The usefulness of a radio signal is limited by the "noise" in the receiver. This noise may be either unwanted external interference or the first circuit noise in the receiver itself.

Atmospheric static is ordinarily controlling at frequencies below a few megacycles while set noise is the primary limitation at frequencies above 200 to 500 mc. In the 10- to 200-mc band the controlling factor depends on the location, time of day, etc. and may be either atmospheric static, man made noise, cosmic noise, or set noise.

The theoretical minimum circuit noise caused by the thermal agitation of the electrons at usual atmospheric temperatures is 204 db below one

watt per cycle of bandwidth; that is, the thermal noise power, in db is $-204 + 10 \log$ (bandwidth). The first circuit or set noise is usually higher than the theoretical minimum by a factor known as the noise figure. For example, the set noise in a receiver with a 6-kc noise bandwidth and an 8-db noise figure is 158 db below 1 watt, which is equivalent to 0.12 microvolts across 100 ohms. Variations in thermal noise and set noise follow the Rayleigh distribution, but the quantitative reference is usually the rms value (63.2 per cent point), which is 1.6 db higher than the median value shown on Figs. 4 and 10. Momentary thermal noise peaks more than 10 to 12 db above the median value occur for a small percentage of the time.

Atmospheric static is caused by lightning and other natural electrical disturbances, and is propagated over the earth by ionospheric transmission. Static levels are generally stronger at night than in the daytime. Atmospheric static is more noticeable in the warm tropical areas where the storms are most frequent than it is in the colder northern regions which are far removed from the lightning storms.

Typical average values of noise in a 6-kc band are shown on Fig. 19. The atmospheric static data are rough yearly averages for a latitude of 40°. Typical summer averages are a few db higher than the value on Fig. 19 and the corresponding winter values are a few db lower. The average noise levels in the tropics may be as much as 15 db higher than

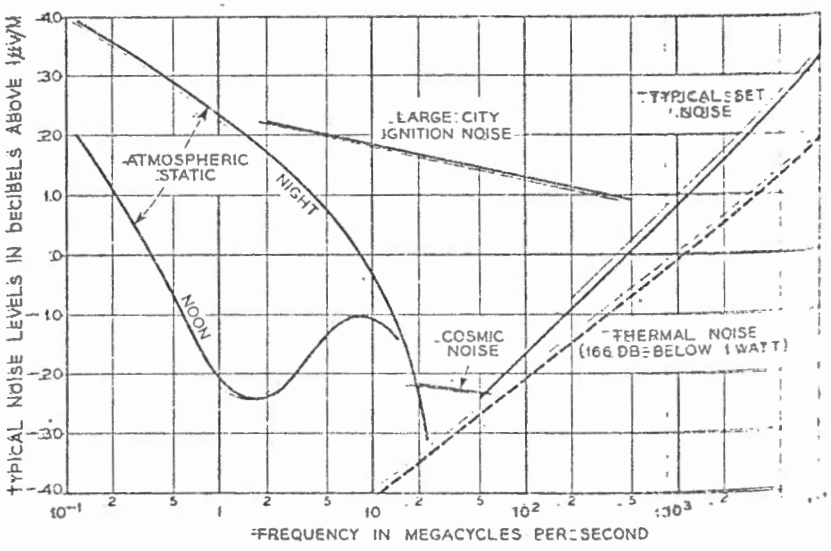

FIG. 19 — Typical average noise level in a 6-kc band.

, is, the thermal noise power, in dbw
'he first circuit or set noise is usually
ıum by a factor known as the noise
in a receiver with a 6-kc noise band-
,58 db below 1 watt, which is equiva-
ohms. Variations in thermal noise and
bution, but the quantitative reference
r cent point), which is 1.6 db higher
Figs. 4 and 10. Momentary thermal
ɔ above the median value occur for a

lightning and other natural electrical
over the earth by ionospheric trans-
y stronger at night than in the day-
noticeable in the warm tropical areas
ent than it is in the colder northern
m the lightning storms.
in a band are shown on Fig. 19.
rough yearly averages for a latitude
are a few db higher than the value on
inter values are a few db lower. The
may be as much as 15 db higher than

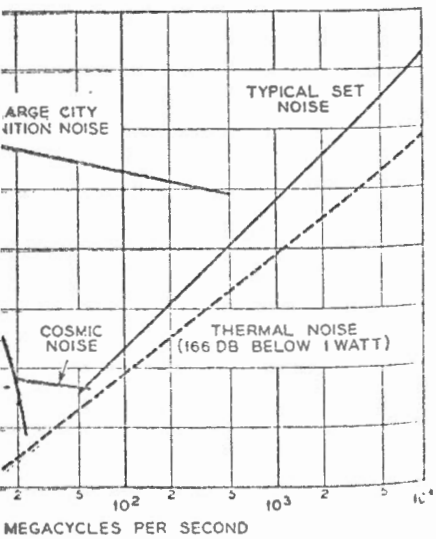

ge noise level in a 6-kc band.

for latitudes of 40° while in the Arctic region the noise may be 15 to 25 db lower. The corresponding values for other bandwidths can be obtained by adding 10 db for each 10-fold increase in bandwidth. More complete estimates of atmospheric noise on a world wide basis are given in the National Bureau of Standards Bulletin 462.[29] These noise data are based on measurements with a time constant of 100 to 200 milliseconds. Noise peaks, as measured on a cathode ray tube, may be considerably higher.

The man made noise shown on Fig. 19 is caused primarily by operation of electric switches, ignition noise, etc., and may be a controlling factor at frequencies below 200 to 400 mc. Since radio transmission in this frequency range is primarily tropospheric (ground wave), man made noise can be relatively unimportant beyond 10 to 20 miles from the source. In rural areas, the controlling factor can be either set noise or cosmic noise.

Cosmic and solar noise is a thermal type interference of extra-terrestial origin.[34] Its practical importance as a limitation on communication circuits seems to be in the 20- to 80-mc range. Cosmic noise has been found at much higher frequencies but its magnitude is not significantly above set noise. On the other hand, noise from the sun increases as the frequency increases and may become the controlling noise source when high gain antennas are used. The rapidly expanding science of radio astronomy is investigating the variations in both time and frequency of these extra-terrestial sources of radio energy.

References

1. H. T. Friis, A Note on a Simple Transmission Formula Proc. I.R.E., 34, pp. 254–256, May, 1946.
2. K. Bullington, Radio Propagation at Frequencies Above 30 Megacycles, Proc. I.R.E., 35, pp. 1122–1136; Oct., 1947.
3. K. Bullington, Reflection Coefficients of Irregular Terrain, Proc. I.R.E., 42, pp. 1258–1262; Aug., 1954.
4. W. M. Sharpless, Measurements of the Angle of Arrival of Microwaves, Proc. I.R.E., 34, pp. 837–845, Nov., 1946.
5. A. B. Crawford and W. M. Sharpless, Further Observations of the Angle of Arrival of Microwaves, Proc. I.R.E., 34, pp. 845–848, Nov., 1946.
6. A. B. Crawford and W. C. Jakes, Selective Fading of Microwaves, B.S.T.J., 31, pp. 68–90; January, 1952.
7. R. L. Kaylor, A Statistical Study of Selective Fading of Super High Frequency Radio Signals, B.S.T.J., 32, pp. 1187–1202, Sept., 1953.
8. H. E. Bussey, Microwave Attenuation Statistics Estimated from Rainfall and Water Vapor Statistics, Proc. I.R.E., 38, pp. 781–785, July, 1950.
9. J. C. Schelleng, C. R. Burrows, E. B. Ferrell, Ultra-Short Wave Propagation, B.S.T.J., 12, pp. 125–161, April, 1933.
10. MIT Radiation Laboratory Series, L. N. Ridenour, Editor-in-Chief, Volume 13, Propagation of Short Radio Waves, D. E. Kerr, Editor, 1951, McGraw-Hill.

11. Summary Technical Report of the Committee on Propagation, National Defense Research Committee. Volume 1, Historical and Technical survey. Volume 2, Wave Propagation Experiments. Volume 3, Propagation of Radio Waves. Stephen S. Attwood, editor, Washington, D.C., 1946.
12. C. W. Burrows and M. C. Gray, The Effect of the Earth's Curvature on Ground Wave Propagation, Proc. I.R.E., **29**, pp. 16–24, Jan., 1941.
13. K. Bullington Characteristics of Beyond-Horizon Radio Transmission, Proc. I.R.E., **43**, p. 1175; Oct., 1955.
14. W. E. Gordon, Radio Scattering in The Troposphere, Proc. I.R.E., **43**, p. 23, Jan., 1955.
15. K. Bullington, Radio Transmission Beyond the Horizon in the 40- to 4,000 MC Band, Proc. I.R.E., **41**, pp. 132–135, Jan., 1953.
16. K. A. Norton, P. L. Rice and L. E. Vogler, The Use of Angular Distance in Estimating Transmission Loss and Fading Range for Propagation Through a Turbulent Atmosphere Over Irregular Terrain, Proc. I.R.E., **43**, pp. 1488–1526, Oct., 1955.
17. F. H. Dickson, J. J. Egli, J. W. Herbstreit, and G. S. Wickizer, Large Reductions of VHF Transmission Loss and Fading by Presence of Mountain Obstacle in Beyond Line-Of-Sight Paths, Proc. I.R.E., **41**, pp. 967–9, Aug., 1953.
18. K. Bullington, W. J. Inkster and A. L. Durkee, Results of Propagation Tests at 505 MC and 4090 MC on Beyond-Horizon Paths, Proc. I.R.E., **43**, pp. 1306–1316, Oct., 1955.
19. Same as 13.
20. H. G. Booker and J. T. deBettencourt, Theory of Radio Transmission by Tropospheric Scattering Using Very Narrow Beams, Proc. I.R.E., **43**, pp. 281–290, March, 1955.
21. W. H. Tidd, Demonstration of Bandwidth Capabilities of Beyond-Horizon Tropospheric Radio Propagation, Proc. I.R.E., **43**, pp. 1297–1299, October, 1955.
22. K. Bullington, Radio Propagation Variations at VHF and UHF, Proc. I.R.E., **38**, pp. 27–32, Jan., 1950.
23. W. R. Young, Comparison of Mobile Radio Transmission at 150, 450, 900 and 3700 MC, B.S.T.J., **31**, pp. 1068–1085, Nov., 1952.
24. K. A. Norton, The Physical Reality of Space and Surface Waves in the Radiation Field of Radio Antennas, Proc. I.R.E., **25**, pp. 1192–1202, Sept., 1937.
25. Same as 2.
26. C. R. Burrows, Radio Propagation Over Plane Earth-Field Strength Curves, B.S.T.J., **16**, pp. 45–75, Jan., 1937.
27. K. A. Norton, The Propagation of Radio Waves Over the Surface of the Earth and in the Upper Atmosphere, Part II, Proc. I.R.E., **25**, pp. 1203–1236, Sept., 1937.
28. Same as 26.
29. National Bureau of Standards Circular 462, Ionospheric Radio Propagation, Superintendent of Documents, U.S. Govt. Printing Office, Washington 25, D.C.
30. National Bureau of Standards, CRPL Series D, Basic Radio Propagation Predictions, issued monthly by U.S. Govt. Printing Office.
31. National Bureau of Standards Circular 465, Instructions for Use of Basic Radio Propagation Predictions, Superintendent of Documents, U.S. Govt Printing Office, Washington, D.C.
32. E. W. Allen, Very-High Frequency and Ultra-High Frequency Signal Ranges as Limited by Noise and Co-channel Interference, Proc. I.R.E., **35**, pp. 128–136, Feb., 1947.
33. D. K. Bailey, R. Bateman and R. C. Kirby, Radio Transmission at VHF by Scattering and Other Processes in the Lower Ionosphere, Proc. I.R.E., **43**, pp. 1181–1230, Oct., 1955.
34. J. W. Herbstreit, Advances in Electronics, **1**, Academic Press, Inc., pp. 367–380, 1948.